CHAPTER 4:
CONCRETE-STEEL BOND MODEL

4.1 Introduction

The utility of reinforced concrete as a structural material is derived from the combination of concrete that is strong and relatively durable in compression with reinforcing steel that is strong and ductile in tension. Maintaining composite action requires transfer of load between the concrete and steel. This load transfer is referred to as bond and is idealized as a continuous stress field that develops in the vicinity of the steel-concrete interface. For reinforced concrete structures subjected to moderate loading, the bond stress capacity of the system exceeds the demand and there is relatively little movement between the reinforcing steel and the surrounding concrete. However, for systems subjected to severe loading, localized bond demand may exceed capacity, resulting in localized damage and significant movement between the reinforcing steel and the surrounding concrete. For reinforced concrete beam-column bridge connections subjected to earthquake loading, the force transfer and anchorage mechanisms within the vicinity of the joint typically result in severe localized bond demand. Laboratory testing of representative beam-column connections subjected to simulated earthquake loading indicates that the global response of these components may be determined by the local bond response [e.g., Paulay *et al.*, 1978; Ehsani and Wight, 1984; Leon and Jirsa, 1986; Leon, 1990; Cheung *et al.*, 1993; Pantazopoulou and Bonacci, 1994; Sritharan *et al*., 1998, and Lowes and Moehle, 1999]. Thus, analysis and prediction of the behavior of reinforced concrete beam-column joint sub-assemblages requires explicit modeling of the bond between concrete and steel.

For this investigation a model is developed to characterize the response of a volume of bond zone material subjected to severe reversed cyclic loading. The proposed model defines bond to be a multi-dimensional phenomenon with load and deformation fields rep-

resented in a local, two-dimensional coordinate system that is aligned parallel to the axis of the reinforcing steel. Bond response is determined by a variety of parameters including concrete and steel material and mechanical properties and load history. The model is implemented within the framework of the finite element method, and a non-local modeling technique is used to incorporate dependence of the bond response on the stress, strain and damage state of the concrete and steel in the vicinity of the concrete-steel interface. The proposed model is verified through comparison with experimental data.

The following sections present the concrete-to-steel bond model developed for use in finite element analysis of reinforced concrete beam-column connections. Section 4.2 presents the experimental data considered in establishing the mechanisms of bond response, developing models to represent these mechanisms and in calibrating the global model. Section 4.3 presents several bond models that are typical of those proposed in previous investigations. Section 4.4 discusses the model implemented in this study. Section 4.5 presents a comparison of observed and computed behavior for reinforcing steel anchored in plain and reinforced concrete sections and subjected to variable load histories.

4.2 Bond Behavior Characterized Through Experimental Investigation

Data from previous investigations of the bond phenomenon support development of a model to characterize behavior. In evaluating these data it is necessary to consider first the scale at which bond response is to be represented. At the scale of interest to this study, bond response may be characterized as a combination of several simplified mechanisms. The fundamental action of these mechanisms is quantified on the basis of data from previous experimental investigations. Data collected from experimental investigation of bond zone and reinforced concrete component responses are used to verify the proposed model.

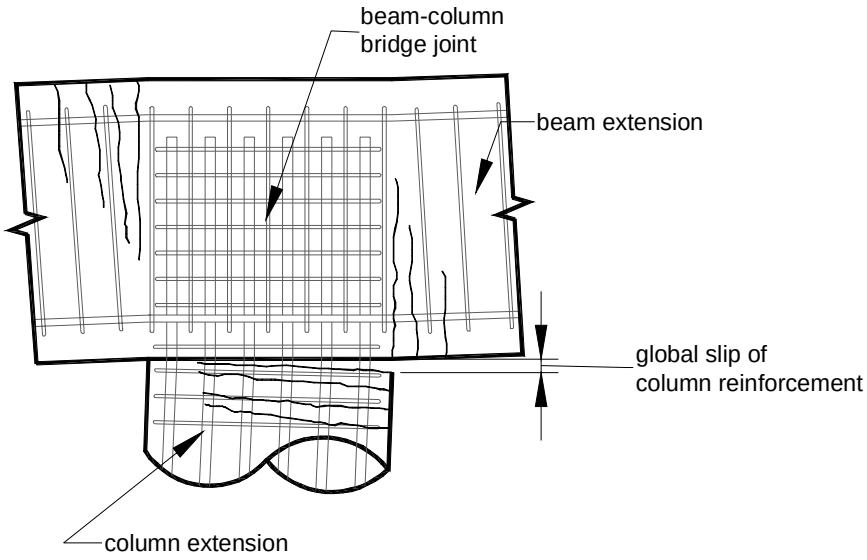

(a) Global Bond Response - Scale of the Structural Elements

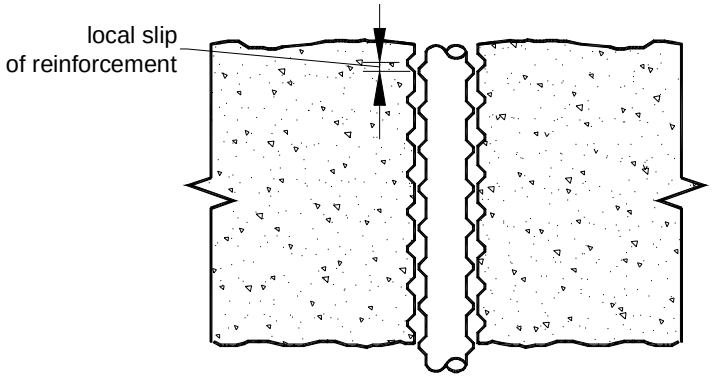

(b) Local Bond Response - Scale of the Reinforcement

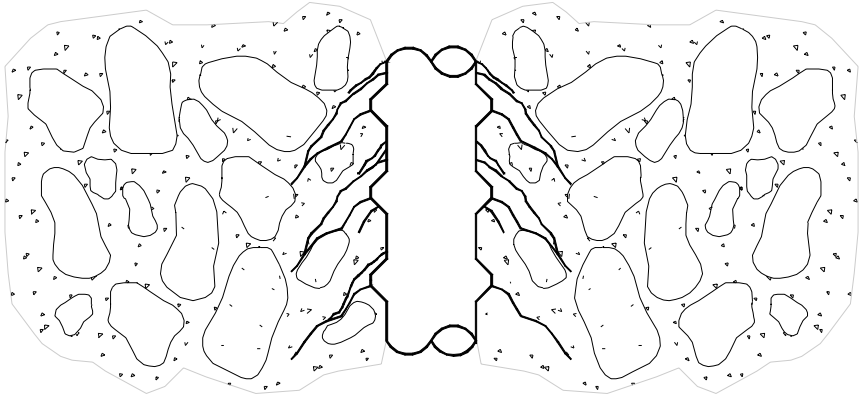

(c) Bond Response - Scale of the Reinforcement Lugs

Figure 4.1: Scale of Bond Response

4.2.1 Scale of the Investigation, Characterization and Model Development

Bond response may be investigated, characterized and analytically modeled at three different scales. These scales typically are defined by the dimensions of the structural element, the reinforcing bar and the lugs on the bar (Figure 4.1). A model developed to represent bond at a particular scale requires a unique set of data and is appropriate for combination with a unique set of material models. In the current investigation, bond is represented at the scale of the reinforcing bar.

Development of a bond model at the scale of the structural element is not appropriate for the current investigation. The current study requires an objective bond model that characterizes local bond-zone behavior for use within the framework of the finite element method. Modeling bond response at the scale of the structural element implies development of a model that characterizes the effect of bond-zone response on global beam, column or connection response. Typically, such models are appropriate for representing bond response only for one particular structural element (i.e., bridge column reinforcing bars confined by a specific volume of spiral reinforcement and anchored in a spread footing, bridge column reinforcement confined by spiral reinforcement and anchored in a beam-column connection or building beam longitudinal reinforcement confined by transverse hoop reinforcement anchored in a square beam-column connection). This system dependence is introduced because in collecting experimental data at the scale of the structural element it is impossible to isolate completely bond response from the flexural, shear and torsional response of the elements. Additionally, it is impossible to define exactly the bond zone state during a test. Thus, the model that is developed is necessarily both an explicit and an implicit function of the element design parameters. In addition to producing a bond model that is not generally applicable, model development at the scale of the structural element typically does not facilitate implementation within the framework of a continuum

finite element model. At this scale, bond data often includes cumulative information such as total bar slip at the interface between two structural elements or total bond stress transfer over a relatively large anchorage zone. Thus, assumptions about the bond stress distribution and slip distribution over the entire bond zone are required to introduce these data into a continuum finite element model. These assumptions may compromise both the generality and objectivity of the global model.

Bond response can be considered at the scale of the lugs on the reinforcing bar. At this scale, the response is determined by the material properties of the concrete mortar and aggregate, the deformation pattern of the steel reinforcing bar, load transfer between concrete mortar and aggregate and the rate of energy dissipation through fracture and crushing of the concrete mortar and aggregate. However, data defining the material properties of the mortar, aggregate and boundary zone materials for reinforced concrete laboratory specimens used in previous bond investigations are limited. The development of an analytical model of the system at this scale is complicated further by the need to account explicitly for the inhomogeniety of the concrete, the deformation pattern on the reinforcing steel and as the discrete crack pattern in the vicinity of the bar. Implementation of a lug-scale model in the global finite element model requires introduction of either sophisticated meshing or solution algorithms or both. Special meshing algorithms are required because the level of mesh refinement required for explicit representation of the bond zone is not appropriate for modeling the entire sub-assemblage as this level of mesh reinforcement both invalidates the assumption of a homogeneous concrete material and leads to a problem that is to large to be computationally feasible. A solution algorithm for facilitating implementation of a lug-scale bond zone model is generalized sub-structuring technique. However, sub-structuring greatly complicates the solution algorithm for non-linear problems, does not eliminate the need to introduce material inhomogenity and requires

introduction of some assumption about behavior at the interface between the bond zone and the remainder of the system. Introduction of a lug-scale model increases tremendously the complexity and computational demand of the model. However, it is not clear that this is accompanied by improved accuracy in characterization of global model response. Thus, lug-scale modeling is not considered to be the most appropriate scale for modeling bond response in the current investigation

For this investigation, bond response is defined at the scale of the reinforcing bar. At this scale, the bond zone is represented as a homogenous continuum. Experimental investigation typically employs specimens that are sufficiently large that the system may be consider to be composed of homogenous concrete, steel and bond-zone continua. However, these systems typically have sufficiently small anchorage lengths that development of local bond-slip models on the basis of average data is appropriate. Experimental data from numerous previous investigations of this type are available and define both the fundamental bond response as well as variation in this response as a function of specific characteristics of the bond zone state. At this scale, the bond zone state may be characterized by concrete and steel material properties (e.g., concrete compressive strength, concrete tensile strength, concrete fracture energy or steel yield strength) that are well defined by standardized tests. Finally, bond zone representation at this scale enables essentially direct implementation of the model into a global finite element model, with the result that the global model is of viable complexity and computational demand.

4.2.2 Denomination of Bond Response Quantities

Bond develops in a reinforced concrete element through the action of several mechanisms in the vicinity of the concrete-steel interface. At the scale of the reinforcing steel, the bond response may be defined by continuous stress and deformation fields. Figure 4.2 shows the idealized system. Activation of bond mechanisms results in the development of

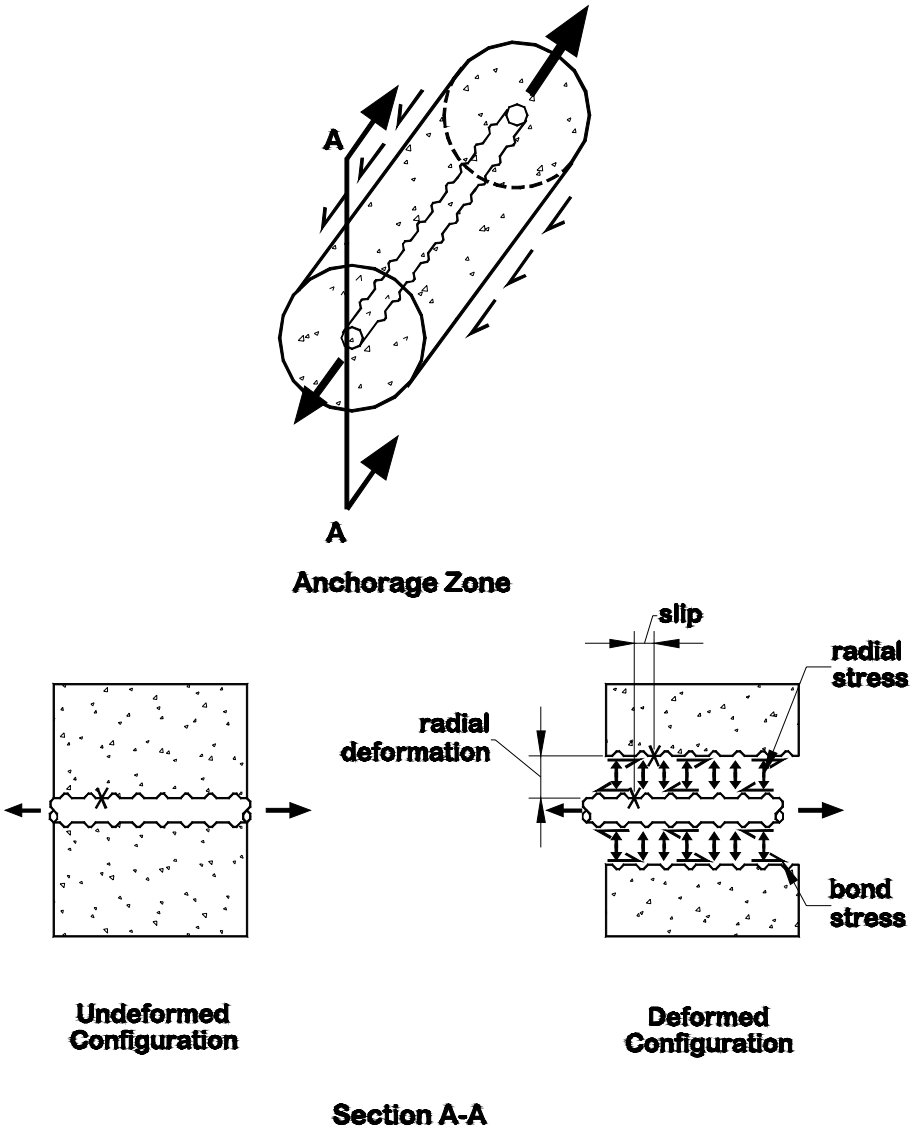

Figure 4.2: Denomination of Bond Response Quantities

bond stress in the direction parallel to the axis of a reinforcing bar and *radial stress* in the direction perpendicular to the bar axis. This complete stress field does not satisfy equilibrium of a general three-dimensional homogenous bond zone continuum, unless the bond zone is represented as a finite-length, zero-width body. On the basis of this volumetric definition, bond stress and radial stress represent a complete and admissible stress field. A deformation field that is compatible with the proposed stress field comprises *slip*, dis-

placement between concrete and steel that is parallel to the axis of the reinforcing steel, and *radial deformation*, relative displacement that is perpendicular to the axis of the bar.

4.2.3 Experimental Investigation of Bond Zone Response

Experimental investigation is required to identify the mechanisms of bond response and the parameters that determine this response. Past research suggests that the microscopic, lug-scale behavior of the material in the vicinity of the concrete-steel interface is defined by complex stress, strain and damage fields and that variation in these fields is a function of highly localized system parameters [*e.g.* Lutz and Gergely, 1967; Goto, 1971]. Investigation and characterization of bond response at the scale of the reinforcing steel provides a smoothed representation of the microscopic response and limits the experimental data required for model development and calibration. However, because an average response is considered, an appropriate experimental investigation provides data that define the response of a well defined bond zone and that define all system parameters including the material stress, strain and deformation fields that determine the observed bond response.

To simplify investigation of bond, many experimental programs use specimens in which a single reinforcing bar is embedded with a short anchorage length in a concrete block that has transverse reinforcing details that are a simplified representation of an actual system. This short anchorage length provides a well-defined bond zone length and supports the assumption of uniform stress and deformation fields in the zone. Additionally, the short anchorage length limits variation along the bond zone of the system parameters, such as confining pressure, concrete damage and steel strain, that determine response.

While the use of short anchorage length facilitates some aspects of the investigation, this limits the total load applied to the steel reinforcement and thus the steel strain demand.

To consider the effect of bar yielding on bond response, an experimental investigation must use longer anchorage lengths or apply loads at both exposed ends of the bar as shown in Figure 4.2. In this case, appropriate methods must be defined for determination of local stress and deformation fields. Also, appropriate methods for determination of the local system fields that determine response, such as concrete confining pressure and concrete damage, are necessary.

Regardless of anchorage length, a typical experimental test set-up includes a single reinforcing bar anchorage in a plane or reinforced concrete block (Figure 4.3). Many experimental investigations of bond do not fully consider or define all the parameters that determine response. Typically neglected parameters include the concrete stress state in the vicinity of the anchorage bar as controlled by the specimen reactions and/or passive confinement provided by transverse reinforcement. For the current investigation, in some cases neglected system parameters are estimated to allow for use of a particular data set, in other cases the entire experimental test specimen is analyzed using the currently proposed model and data are used in model verification.

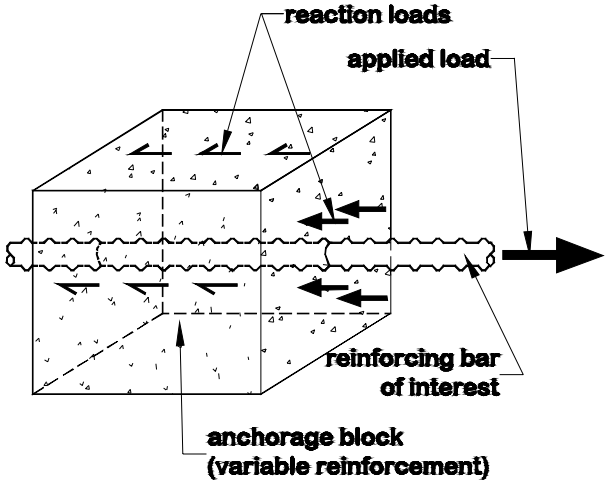

Figure 4.3: Typical Experimental Test Specimen for Investigation of Bond Response

4.2.4 Investigation of Bond Response Mechanisms

Early investigations of concrete-to-steel bond for deformed reinforcing bars focussed on identification of the mechanisms of bond response. Evaluation of the results of these investigations contribute to identification of the dominant response mechanisms included in the bond zone model.

4.2.4.1 Investigation of Bond Response Mechanisms for Deformed Reinforcement

An experimental investigation presented by Rehm [1958] was one of the first investigations of the bond response of deformed reinforcing steel. This experimental test program considered the response of a prototype specimen for which a plain reinforcing bar is machined to create a single concrete key (concrete between the lugs on a deformed bar). The machined bar was anchored in a plain concrete block and subjected to monotonically increasing tensile loading to failure. Sufficient concrete cover over the reinforcement was provided such that failure resulted from pull-out of the steel bar (pull-out failure) rather than the formation and unrestrained propagation of cracks in the concrete along the length of the bar (splitting-type failure). A pull-out bond failure is likely for a system in which the reinforcement is anchored with either moderate concrete cover or a moderate volume of transverse reinforcement, or both. A similar test program completed by Lutz *et al.* [1966] used steel bars machined to create a single lug. For these series of tests, the face angle of the lugs on the reinforcing bar varied from 30 to 105 degrees. Both Lutz *et al.* [1966] and Rhem [1958] note that the response of specimens with lug face angles greater that 40 degrees was approximately the same and thus apparently independent of lug face angle. The authors conclude that for these specimens slip initially is due to concrete crushing in front of the lug. Lutz *et al.* [1966] notes that the concrete in the vicinity of the bar and extending in front of the lugs a distance equal to 5 to 7 times the height of the lugs is crushed under moderate bond demand and that a zone of crushed concrete extending in

front of the lugs a distance of at most twice the height of the lugs moves with the reinforcing bar as slip occurs. Lutz *et al.* [1966] note similar damage patterns.

While these investigations do not consider all of the key parameters that control bond response, the data collected from these test programs do provide understanding of the force, deformation and damage patterns associated with bond response, and thereby contribute to the characterization of the concrete-steel interface. The observed patterns of crushed concrete indicate the importance of mechanical interaction between concrete and reinforcement lugs in transferring load between concrete and reinforcing steel. The progressive crushing of concrete in front of the lugs suggest that the global bond-slip response likely has a history dependence that is comparable to that of plain concrete subjected to uniaxial compressive loading. Additionally, compaction of crushed concrete in front of the lugs and movement of this concrete with the reinforcing steel suggests that under moderate bond loading an effective concrete-steel interface is formed with approximately the same orientation for reinforcement with lug face angles in excess of 40 degrees. The results of these investigations suggest also that this effective interface is invariant at relatively high slip levels.

4.2.4.2 Comprehensive Evaluation of Bond Response for Deformed Reinforcement

An investigation of bond response presented by Lutz and Gergely [1967] provides a comprehensive evaluation of the mechanisms of bond response for systems with deformed reinforcement. This investigation is supported by the experimental and analytical investigations of a number of researchers [Broms, 1955; Rehm, 1958; Watstein and Mathey, 1959, and Lutz *et al.*, 1966]. Lutz and Gergley conclude that load transfer between concrete and steel occurs through the action of three mechanisms: chemical adhesion, friction and mechanical interaction of the lugs of the deformed reinforcement bearing on the surrounding concrete. For deformed reinforcement, mechanical interaction is the dominant

mechanism of response. Drawing on the experimental data provided by Rhem [1958] and Lutz *et al.* [1966], the authors propose that slip between the reinforcement and concrete results initially from crushing of concrete in front of the reinforcement lugs and, at increased levels of slip, from splitting of concrete due to the wedging action of the lugs bearing on the concrete. Lutz and Gergely propose that regardless of the face angle of the lugs on the reinforcement, crushed concrete forms a wedge in front of the lug resulting in a effective lug face angle of approximately 30 to 40 degrees. Once this wedge forms, slip results predominately from splitting due to wedge action of the effective lug face bearing on the surrounding concrete.

This study clearly identifies the dominant modes of bond response that must be incorporated into the model developed for this investigation. Specifically the model must account for bond developed through mechanical interaction and through friction. The study reinforces the fact that the concrete-steel interface is a zone of compacted crushed concrete that forms a wedge with a face angle of 30 to 40 degrees in front of the lugs on the reinforcing bar. Additionally, identification of this interface suggests that the dominant mode of bond force transfer likely is bearing on this interface, since compacted crushed concrete would not be expected to transfer substantial load through shear.

4.2.4.3 Bond-Zone Damage Patterns

Goto [1971] provides additional understanding of the wedging action of reinforcing lugs acting against concrete. This experimental investigation focused on characterizing the concrete damage associated with tensile bond stress. The prototype specimen consists of a single, deformed reinforcing bar embedded in a plain concrete prism. The reinforcing bar has a diameter of 19 mm (0.75 inches) and the concrete prism dimensions are 100 mm by 100 mm by 1 m (4 in. by 4 in. by 40 in.). Both exposed ends of the bar are loaded in tension to a maximum load that approaches, but does not reach, the yield strength of the rein-

forcing steel. This prototype specimen is representative of a reinforcing bar in the tension zone of a reinforced concrete frame element subjected to flexural loading. Ink is injected into the open concrete cracks under maximum bar load. The specimens are then unloaded, sawed in half lengthwise and the prism crack patterns, highlighted by the ink, are examined. From this series of tests, Goto concludes that radial bond cracks form at an angle of inclination with respect to the axis of the bar of between 45 and 80 degrees with many forming at an angle of approximately 60 degrees. Assuming that bond force is transferred primarily through bearing and that the radial cracks are parallel to the orientation of the normal force acting at the concrete-steel interface, this orientation of the radial crack indicates an angle of inclination of 30 degrees for the contact surface on which load transfer occurs. Additionally, Goto notes that at higher steel stresses longitudinal cracks (parallel to the axis of the reinforcing bar) propagate from the concrete-steel interface to the surface of the concrete prism. The action of reinforcement lugs or compressed concrete wedges bearing against the concrete volume in the vicinity of the reinforcing bar results in the development of tensile hoop stresses around the bar. When concrete tensile capacity is exceeded, longitudinal cracks form. Goto concludes that the deformation of radially cracked concrete at the concrete-steel interface may also contribute to the development of longitudinal cracks.

The Goto study advances bond model development through characterization of load transfer at the concrete-steel interface. Goto notes that initial cracking consists of radial cracks that initiate at the interface and propagate towards the surface with an average angle of inclination of approximately 60 degrees. This level of damage is associated with minimal slip, thus it is unlikely that significant frictional forces are developed between the concrete and reinforcing steel. If it is assumed that load transfer is through bearing, the existence of cracks oriented at an angle of 60 degrees implies a bearing surface oriented at

an angle of 30 degrees and a ratio of bond force to radial force transfer of $1/\sqrt{3}$. The development of radial force at the concrete-steel interface results in the development of tensile hoop stresses in the concrete surrounding the reinforcing bar and the development of longitudinal cracks that initiate at the interface and propagate outward. This is consistent with the observed damage patterns. However, Goto indicates that longitudinal cracks are observed at the surface of the prism at a bond demand of between 970 psi and 1900 psi ($15\sqrt{f_c}$ and $29\sqrt{f_c}$ psi for f_c in psi and $39\sqrt{f_c}$ to $76\sqrt{f_c}$ for f_c in kPa). Since initiation of longitudinal cracks necessarily corresponds to a concrete tensile stress equal to the cracking stress of 400 psi (2.7 MPa), the observed cracking implies a ratio of radial to bond stress of between 0.4 and 0.2 if it is assumed that surface exposure of longitudinal cracks corresponds to initiation of these cracks at the interface under an elastic load distribution or between 1.6 and 0.84 if it is assumed that surface exposure of longitudinal crack corresponds to concrete loaded to tensile strength.

4.2.4.4 Bond Strength

A study presented by Tepfers [1979] was one of the first investigations to focus on prediction of bond strength for deformed reinforcement. Tepfers was the first to propose an analytical model in which the concrete surrounding a single reinforcing bar is characterized as a thick-walled cylinder subjected to internal shear and pressure. In this analogy the internal shear and pressure correspond respectively to the bond and radial stresses developed at the concrete-steel interface. Thus, it follows that the radial force transfer at the concrete-steel interface determines the tensile hoop stress developed in the concrete surrounding the bar and thus the critical load. Tepfers proposes that bond strength is determined by the capacity of the concrete surrounding the reinforcing bars to carry the hoop stresses. Three modes of system failure are proposed: elastic, partially cracked-elastic and plastic. The elastic mode of failure describes a system in which the concrete surrounding

the reinforcing bar exhibits a linearly-elastic material response and bond strength corresponds to the concrete carrying a peak tensile stress equal to the concrete tensile strength. The partially cracked-elastic mode of failure defines a system in which radial cracks initiate in the concrete at the concrete-steel interface but do not propagate to the surface of the specimen. The cracked concrete is assumed to have no tensile strength and bond strength corresponds to the uncracked concrete carrying a maximum stress equal to the tensile strength. The plastic failure mode describes a system in which all of the concrete surrounding the anchored bar is assumed to carry a tensile hoop stress equal to the concrete tensile strength. To verify the analytical model and determine which of the three failure modes is most appropriate for characterizing the response of real systems, Tepfers conducts an experimental investigation in which bond strength is determined for reinforcing bars embedded in concrete blocks with an embedment length of $3d_b$ and a minimum clear cover varying from approximately $1d_b$ to $6d_b$. Here the concrete blocks have a thickness of $3d_b$ and the tensile load applied to the bar is reacted as compression on the face of the concrete block in the vicinity of the bar. Because of the specimen and the load configuration, bond failure results from splitting of the concrete cover surrounding the bar rather than bar pull-out. This failure mode is representative of in-situ elements in which reinforcement is anchored with minimal concrete cover in a region with a minimal volume of transverse reinforcement. Tepfers assumes that the resultant force at the concrete-steel interface is orientated at an angle of 45 degrees with respect to the axis of the reinforcing bar. Results of the experimental investigation indicate that the bond strength of the actual system falls between that predicted assuming a partially cracked mode of response and that predicted assuming a fully plastic mode of response. Similar conclusions can be drawn from evaluation of data provided by Tilantera and Rechardt [1977] who completed an experimental investigation similar to that of Tepfers.

The data presented by Tepfers support the proposition that bond strength is determined by the hoop stresses developed in the surrounding concrete. The data also support the conclusion that the partially cracked elastic model proposed by Tepfers results in a lower bound bond strength. However, the observed bond strength falls between that predicted by the proposed partially cracked and plastic modes of bond failure; thus, neither model provides a true representation of the system. The most likely explanation for the discrepancy between the predicted and observed bond strengths is that an appropriate model for concrete uniaxial tensile stress-strain response includes diminishing post-peak concrete tensile strength. Such a model would provide a system strength falling between that of the two proposed models. Additionally, the unsymmetric specimen configuration necessarily produces an unsymmetric stress state under maximum loading and likely results in higher bond stress transfer along the portion of the bond zone circumference that has substantial concrete cover. Finally, a reduced angle of inclination for the force resultant at the concrete-steel interface could account for bond strength in excess of that predicted by the partially cracked elastic model. It is important to note the tremendous scatter of the experimental data that suggests there may be some issues associated with the test program that are not fully addressed. Scatter in the data may be due to the fact that the thin specimens (to provide short anchorage lengths) likely result in an inhomogenous, and therefore variable, concrete mixture in the vicinity of the critical region. Scatter likely is not due to variation in concrete mix design that might result in variable concrete fracture energy as data for both normal weight and light weight concrete both show similar distributions.

4.2.4.5 Behavior Characteristics Identified through Experimental Investigation of the Bond Response of Deformed Reinforcement

Several conclusions about bond response can be made on the basis of the data provide by the previously discussed investigations. The data presented by Rehm, Lutz, Gergeley and Tepfers suggest that bond is developed through both mechanical interaction and friction between the reinforcing steel and surrounding concrete. At low slip levels mechanical interaction dominates the response, and friction is more significant at large slip levels. The data presented by these researchers support the proposition that mechanical interaction occurs on an effective concrete-steel interface that is oriented at an angle with respect to the axis of the reinforcing steel bar and that bearing forces on this effective interface result in the development of both bond and radial stresses (Figure 4.4). Finally these investigations indicate that bond strength is determined by the tensile strength of the concrete; while, bond-slip response is determined by the tensile and compressive concrete response.

The results of these investigation indicate that mechanical interaction develops through bearing on the surrounding concrete of an effective reinforcement lug that is composed of crushed concrete that becomes compacted in front of the actual lugs on the steel reinforcement. Data from the previously discussed investigations indicate that this effective lug forms a concrete-steel interface that is oriented at between 30 and 45+ degrees with respect to the axis of the reinforcing bar. The data characterizing the damage patterns in the vicinity of a reinforcing bar as presented by Rehm and Lutz suggest that the crushed concrete forms an effective concrete-steel interface that is oriented at an angle of approximately 30 degrees. The relatively shallow orientation of this interface is supported by Goto who observed the formation of radial cracks at the concrete-steel interface oriented at approximately 60 degrees with respect to the axis of the reinforcing bar. Here it is

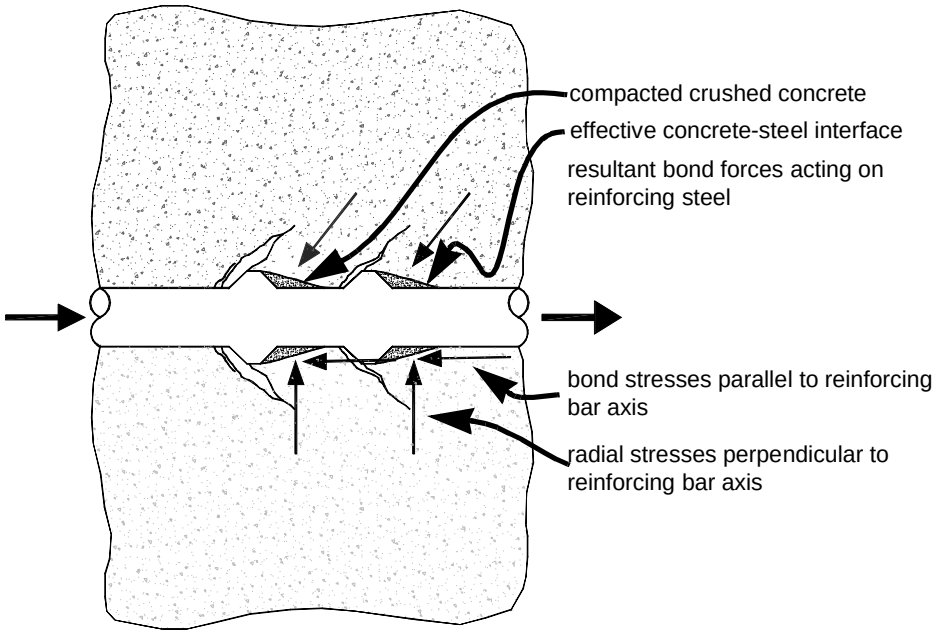

Figure 4.4: Idealization of the Bond Zone

assumed, as previously discussed, that the effective angle of the concrete-steel interface is perpendicular to the orientation of radial cracks. The results of the bond study conducted by Tepfers may be interpreted as supporting an effective concrete-steel interface oriented at an angle in excess of 45 degrees with respect to the bar axis; however, other interpretation of the Tepfers study are plausible, so this interpretation may be discounted. Finally, it is necessary to note that the damage pattern observed by Lutz and Rhem suggest that the orientation of the effective concrete-steel interface is not established immediately but may be considered relatively invariant at moderate to high slip levels.

The results of these studies also suggest that ultimate bond strength is determined by concrete tensile strength. The investigations by Rehm and Lutz and Gergely indicate that initial softening of bond response is due to crushing of concrete in front of the steel lugs. However, for these investigations sufficient concrete cover is provided over the anchored

bar to promote a pull-out type failure characterized by the shearing-off of the concrete lugs. This shear failure likely occurs when concrete principal tension stress exceeds tensile capacity. For the Goto and Tepfers studies, bond failure resulted from the formation, opening and propagation of tensile cracks in the concrete.

4.2.5 Investigation of the Bond Stress Versus Slip Response

Experimental investigation of the bond stress versus slip response has been extensive. System and material parameters for individual investigations vary widely, and as a result, experimental data provided by these investigations vary. However, as a whole this body of data defines the fundamental characteristics of the bond-slip response. A few well defined experimental investigations identify data for refined representation of bond response.

4.2.5.1 Characterization of Bond Response through Evaluation of Specimens with Long Anchorage Lengths

A study presented by Viwathanatepa [1979a, 1979c] is one of the first investigations of the load-deformation response of anchored deformed reinforcement. This investigation considers the bond response of beam longitudinal reinforcement anchored in well-confined interior beam-column building joints. Figure 4.5 shows the prototype specimen and load configuration for this test program. The prototype specimen for this study consists of a single deformed reinforcing bar, Grade 60 with 1 inch (25 mm) nominal diameter, anchored with a 15 inch (380 mm) development length in a reinforced anchorage block with longitudinal reinforcement (perpendicular to the anchored bar and representative of column longitudinal reinforcement) and transverse reinforcement (parallel to the anchored bar and representative of column transverse reinforcement) having volumetric ratios of 0.02 and 0.008, respectively. Load is applied either as tension on one protruding end of the

bar or as tension and compression on opposite ends of the bar. Load is reacted through frictional forces on the surface of the specimen and through bearing of embedded anchors at a prescribed distance from the longitudinal bar. The complete test program presented by Viwathanatepa comprises seventeen specimens; individual specimens vary from the prototype by bar diameter, anchorage length, longitudinal and transverse steel volume, load pattern and slip history. Figure 4.6 shows the experimentally observed bar stress versus slip relationship for a typical specimen subjected to tension and compression loading at opposite ends of the bar. Here bar stress is defined by the load applied at each end of the bar, and slip is defined by the relative movement of a protruding end of the bar with respect to the corresponding face of the concrete block.

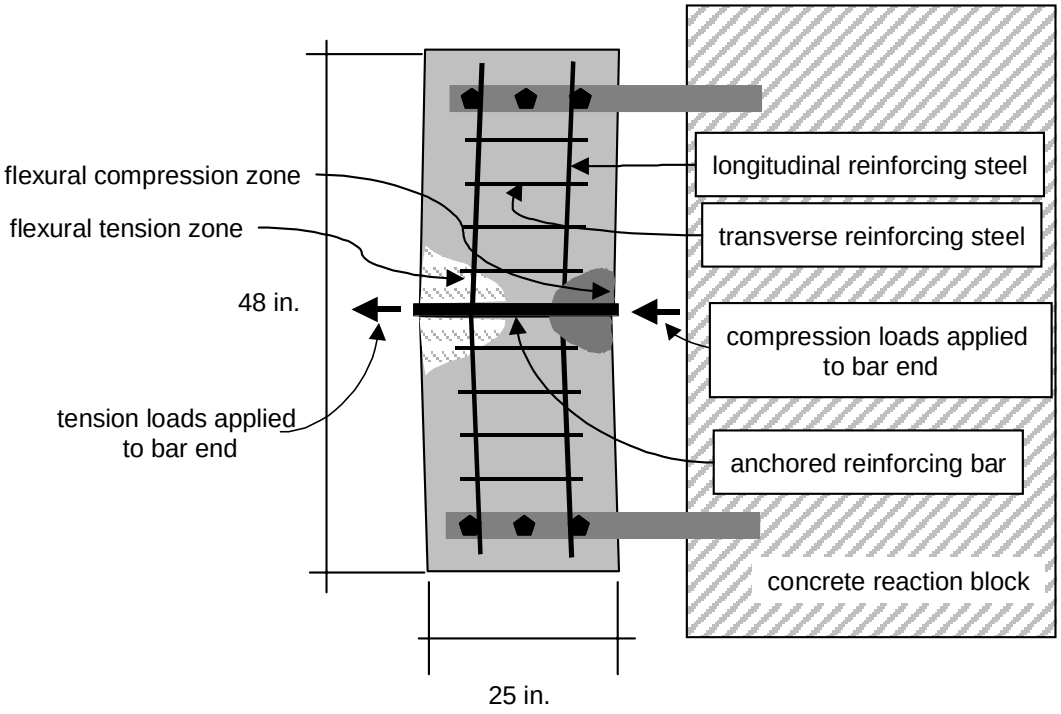

Figure 4.5: Prototype Specimen and Applied Loading for the Viwathanatepa [1979a] Experimental Bond Investigation

In addition to global system response, Viwathanatepa [1979a, 1979c] also provides data that contribute to characterization of local bond behavior. Figure 4.7 shows the local bond stress versus slip histories at points along the embedded length of the bar for the

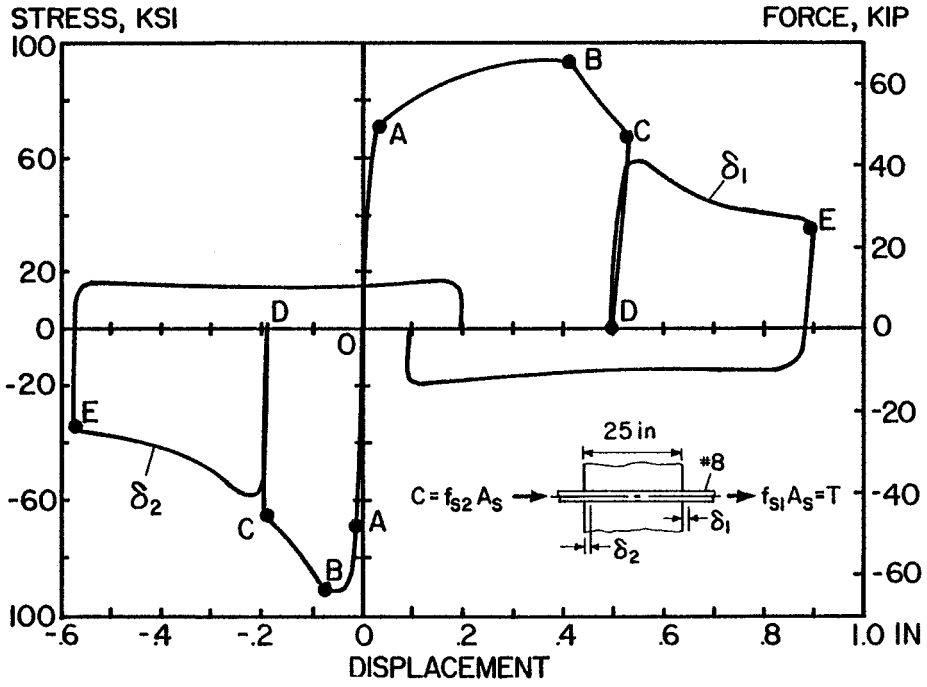

Figure 4.6: Bar Stress versus Bar Slip (Figure 4.11 from Viwathanatepa [1979])

specimen with a 25 inch (1400 mm) anchorage length. Here local bond stress is computed from the steel strains measured at two locations along the bar and the experimentally-observed monotonic steel stress-strain history; the bond stress field is then adjusted to represent a smooth distribution along the anchorage length. These data show that under monotonically increasing load the bond-slip response is initially relatively stiff with reduced stiffness as the peak bond capacity is approached. Once bond capacity is achieved, increased slip demand results in reduced capacity until, at an extreme slip level, only minimal bond capacity is maintained.

The data presented in Figure 4.7 show the effect of concrete stress and damage state and steel stress state on bond response. The load-reaction configuration used by Viwathanatepa results in the concrete block carrying a flexural load such that the concrete at the 'push-end' carries compression in the direction perpendicular to the axis of the reinforcing bar while the concrete at the 'pull-end' carries tension in excess of the concrete tensile

strength. Further, because of the relatively long development lengths, the anchored steel reinforcement at both the compression and tension ends of the bar carries stress that approach the ultimate strength of the steel. The effect of these composite material parameters on bond response is evident in the increased bond strength at the compression end of the bar versus the tension end (Figure 4.7). Since these data show the affect of multiple system parameters on bond response, this information appropriately is used to verify model response rather than to calibrate the model.

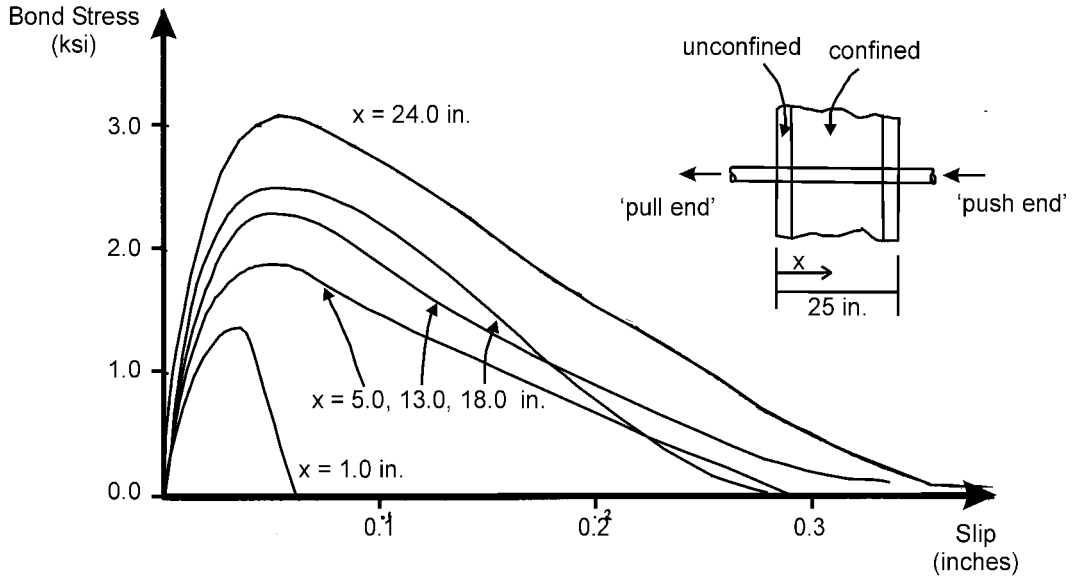

Figure 4.7: Local Bond Stress Versus Slip History Along Length of Embedded Bar [Data from Viwathanatepa, 1979c]

The Viwathanatepa study also provides information about cyclic bond response. Figure 4.8 shows the bar stress versus slip relationship at a location near the 'pull end' of the bar for a typical specimen subjected to reversed cyclic loading. In this series of tests the tensile load and compression load applied to opposite ends of the bar are equal. Thus, the bar stress can be converted to an average bond stress along the anchored length; here the maximum bar stress of 69 ksi (480 MPa) corresponds to a maximum average bond stress of 1400 psi (9.5 MPa). These data show that upon a slip reversal, there is a rapid loss in bond capacity until a moderate resistance to slip in the reversal direction is achieved. This

moderate bond capacity likely results from friction developed as the bar slips against the surrounding concrete. Once the slip in the reversal direction is such that additional slip is resisted by undamaged concrete, bond capacity increases. However, peak bond capacity achieved under reversed cyclic loading is less than that observed under monotonic loading. The data define specimen response on the basis of average bond strength; however, data in Figure 4.6 show local bond strength to be a function of the concrete and steel material stress states. Thus, while these data provided qualitative information about cyclic bond response, they are appropriate for use in model verification rather than calibration.

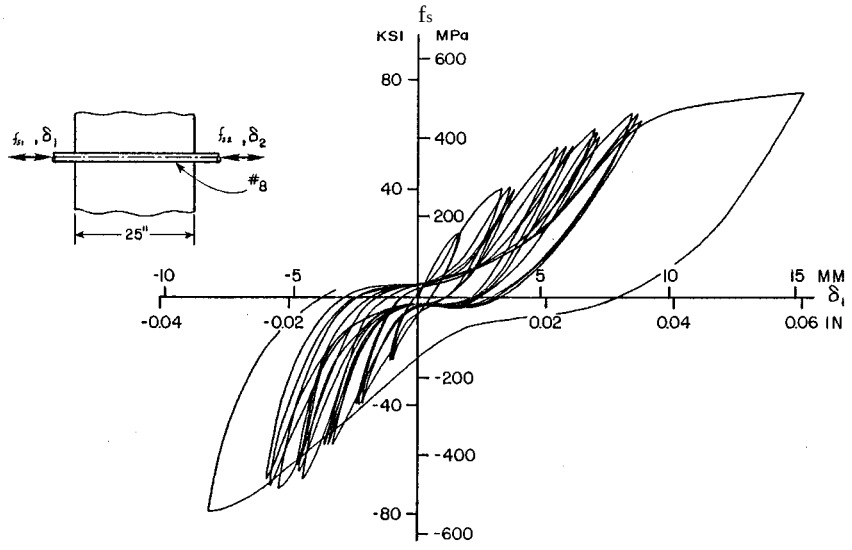

Figure 4.8: Bar Stress at 'Pull End' Versus Slip History for a Typical Specimen Subjected to Reversed Cyclic Loading (Figure 7.29 from Viwathanatepa [1979])

Finally, the data provided by Viwathanatepa offer insight into the effect of bar size. Test results for specimens with nominal bar sizes ranging from No. 6 to No. 10 (bar diameters ranging from 0.75 inches to 1.25 inches (19 mm to 31 mm)) indicate that bond capacity decreases slightly with increasing bar size. The monotonic bond capacity of the specimen with No. 10 bar is 85 percent of that of the specimen with No. 6 reinforcement. Similar results are observed for specimens subjected to reversed cyclic loading.

4.2.5.2 Characterization of Bond Response through Evaluation of Specimens with Short Anchorage Lengths

Eligehausen *et al.* [1983] provide the results of an extensive investigation of bond response under variable system parameters and variable load histories. Like the Viwathanatepa study, this experimental investigation focusses on characterizing the bond-slip response of beam longitudinal reinforcement anchored in the beam-column joint of a building. For this study the prototype specimen (Figure 4.9) consists of a single, deformed reinforcing bar anchored with an embedment length of $5d_b$ in a concrete block that has reinforcing details representative of a beam-column joint with longitudinal (perpendicular to the axis of the anchored bar) and transverse (parallel to the axis of the anchored bar) steel reinforcement ratios each equal to 0.008. One protruding end of the bar is subjected to load under displacement control while slip is measured as the movement of the unloaded end of the bar with respect to the concrete anchorage block. The load applied to the bar is reacted as a compressive force on one of the faces of the concrete block. Because the compressive reactions are relatively close to the reinforcing bar, the load-reaction configuration does not represent well the load distribution observed in an actual beam-column connection. However, the anchorage block is sufficiently large and the bond zone is a sufficient distance from the face of the anchorage block, that the distribution of concrete stress parallel to the direction of the reinforcement likely does not affect significantly the observed response. Because of the relatively short anchorage lengths, it is reasonable to assume that bond response and system parameters are uniform along the anchorage length. Additionally because of the limited anchorage length, steel remains elastic, eliminating steel yielding as a parameter of the investigation.

The data provided by Eligehausen *et al.* [1983] contribute to characterization of the bond-slip response for deformed reinforcement subjected to monotonic and cyclic load

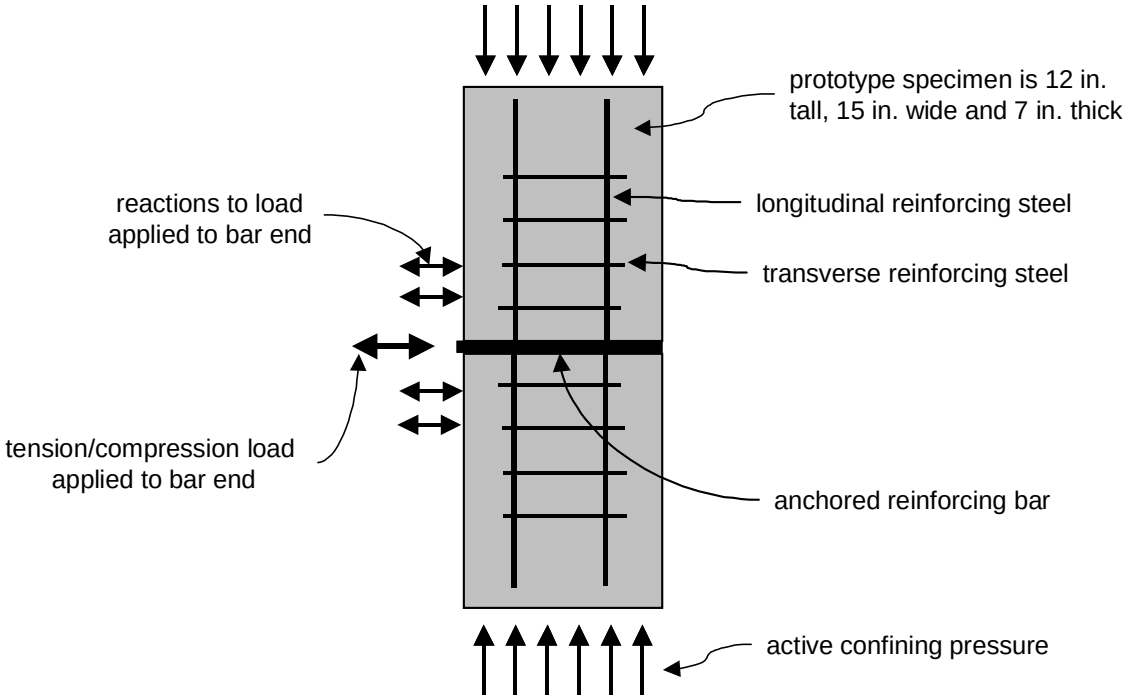

Figure 4.9: Prototype Specimen and Loading for the Experimental Bond Investigation Presented by Eligehausen *et al.* [1983]

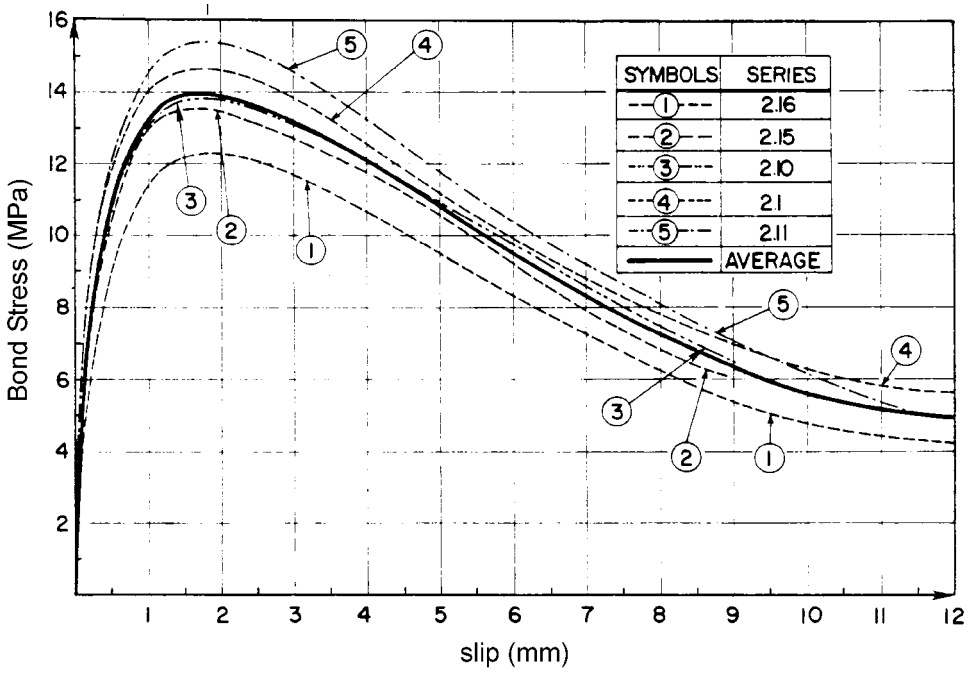

Figure 4.10: Typical Bond Stress Versus Slip Response for Monotonic Load History (Figure 4.8 from Eligehausen *et al.* [1983])

histories. Figure 4.10 shows the range of bond-slip histories for single reinforcing bars with a nominal diameter of 25 mm (1.0 inch) anchored in a block of concrete with compressive strength of approximately 30 MPa (4400 psi) and subjected to monotonically increasing tensile loading. The maximum bond strength and bond-slip response observed in this investigation are similar to those observed by Viwathanatepa (Figure 4.7). The study completed by Eligehausen includes an extensive investigation of the effect of load history on bond response. Data defining the response of 22 specimens characterize bond response for load histories including monotonic tension and compression, reversed cyclic loading to a single maximum slip level, cyclic loading in tension only to a prescribed maximum slip level, reversed cyclic loading to increasing maximum absolute slip levels. The results of the cyclic tests are presented in several forms. Figures 4.11 and 4.12 show bond stress versus slip for identically designed specimens subject to different cyclic slip histories. These data show a response similar to that observed by Viwathanatepa [1979a, 1979c]. Here slip reversal is accompanied by rapid unloading and followed by development of a moderate bond resistance in the direction of the slip reversal. Once slip levels are such that bond forces are transferred to undamaged concrete, bond strength and stiffness increase. The bond capacity achieved in the unload direction may not reach the monotonic bond capacity. Figure 4.11 shows data for an anchored bar subjected to reversed cyclic loading to a prescribed maximum slip that is less than that associated with maximum bond strength. For this load case, deterioration of bond strength from the monotonic response curve is not substantial. Figure 4.12 shows data for an anchored bar subjected to loading to a prescribed slip level in excess of that corresponding to peak capacity. These data and the results of a number of similar tests indicate that cyclic loading to slip levels in excess of that corresponding to peak load results in significant loss of bond capacity under multiple cycles and reduces, from the observed monotonic response his-

tory, the bond capacity achieved at increased levels of slip. Figure 4.13 presents the results of all of the reversed cyclic bond tests and shows the reduction in peak bond capacity as a function of number of cycles and the peak slip demand. These data are appropriate for model development and calibration.

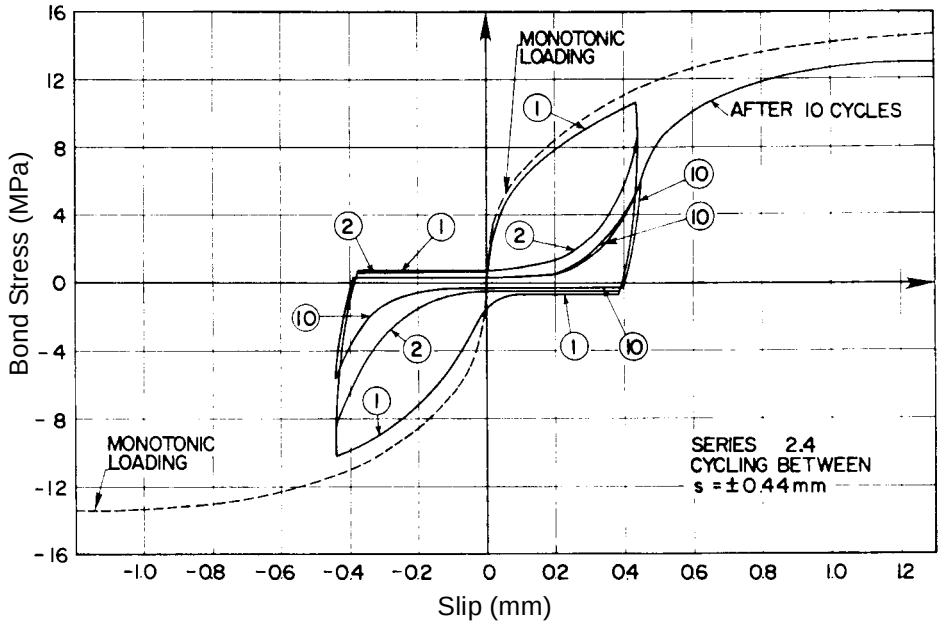

Figure 4.11: Bond Stress Versus Slip for Reinforcement Subjected to Reversed Cyclic Loading to a Maximum Absolute Slip of 0.44 mm (Figure 4.25a from Eligehausen *et al.* [1983])

In addition to characterizing the monotonic and cyclic bond response, the results presented by the Eligehausen study provide numerical data that define the effect on the bond-slip response of concrete strength and bar size. These data are appropriate for model development and calibration. Results of this investigation indicate that bond strength is proportional to the square root of the concrete compressive strength. The results of this investigation also indicate that bar size has a moderate effect on bond capacity; the investigators propose that the bond capacity of No. 6 (nominal bar diameter of 0.75 in. (19 mm)) reinforcement be defined 10 percent higher than that of No. 8 (nominal diameter of 1.0 in. (25 mm)) reinforcement and the bond capacity of No. 10 (nominal diameter of 1.25 in. (31 mm)) reinforcement be defined 10 percent lower than that of No. 8 reinforcement.

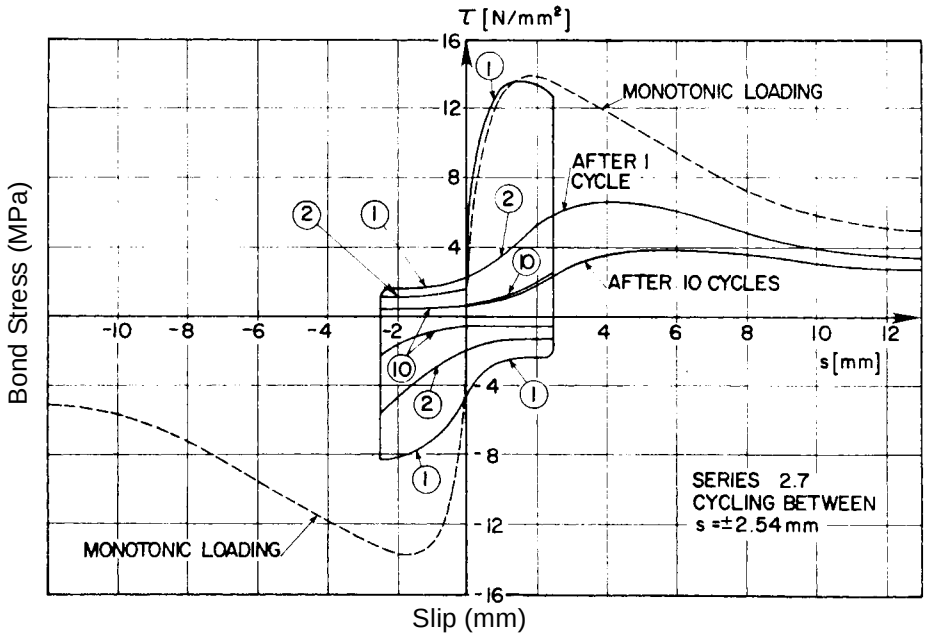

Figure 4.12: Bond Stress Versus Slip for Reinforcement Subjected to Reversed Cyclic Loading to a Maximum Absolute Slip of 2.54 mm (Figure 4.28 from Eligehausen *et al.* [1983])

The study suggests that the deformation pattern may have a significant effect on bond response. The deformation pattern is defined on the basis of the ratio of the rib bearing area (perpendicular to the bar axis) and the bar shear area (area parallel to the bar axis). The presented data indicate that increase in the rib bearing area results in an increase in bond capacity of as much as 70 percent.

The Eligehausen investigation provides data defining the effect of the concrete stress state on bond response (Figures 4.14 and 4.15). The study considers bond response for systems with varying levels of active and passive confining pressure in one direction perpendicular to the anchored reinforcing bar. Here the passive confinement of interest is provided by column longitudinal reinforcement that lies perpendicular to the anchored bar and parallel to the free concrete surface nearest to the anchored bar. Transverse reinforcement lying perpendicular to the anchored bar and parallel to the further free concrete surface likely provides some passive confinement. However, concrete cracking restrained by

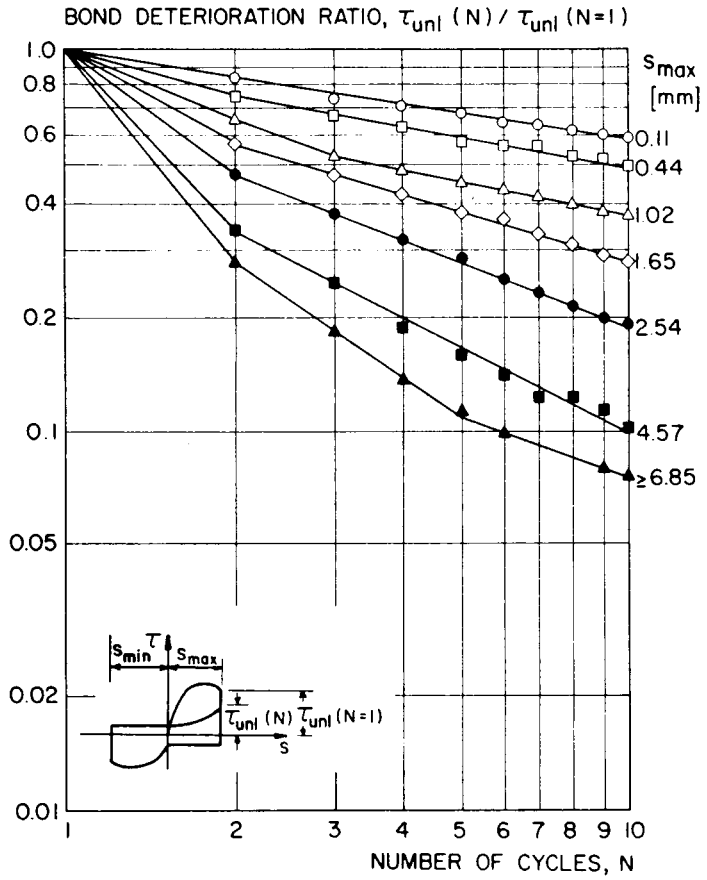

Figure 4.13: Bond Strength Deterioration with Increased Number of Load Cycles (Figure 4.46a from Eligehausen *et al.* [1983])

this reinforcement does not determine bond strength; thus passive confinement provided by this reinforcement is not of interest.

Figure 4.14 shows the bond stress versus slip history for a series of test specimens with variable volumes of longitudinal reinforcement (perpendicular to the embedded reinforcing bar). Specimens with no longitudinal reinforcement exhibit a splitting-type failure under relatively low bond stress demand. Specimens with moderate levels of reinforcement exhibit pull-out failure and achieve relatively high bond strength. With the exception of the specimen with the smallest volume of longitudinal reinforcement, the specimens with variable volumes of reinforcement show minimal variation in response. These results indicate that for all of the specimens except that with the smallest volume of longitudinal

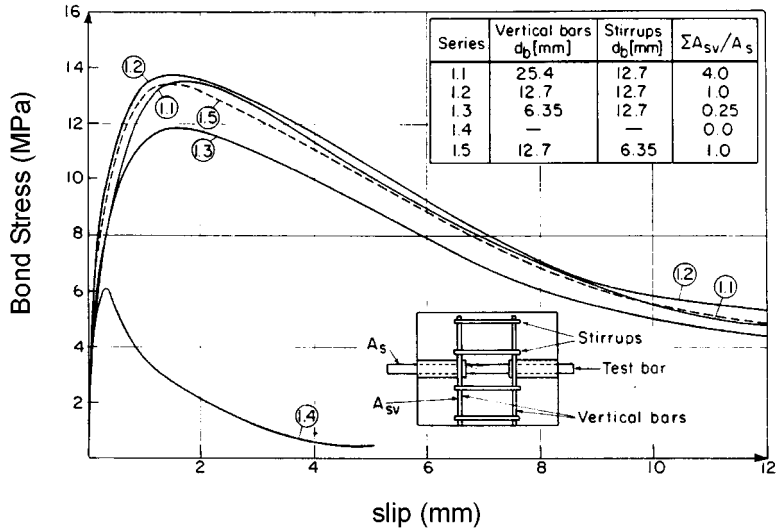

Figure 4.14: Bond Response as a Function of Transverse Reinforcement Volume (Figure 4.18 from Eligehausen *et al.* [1983])

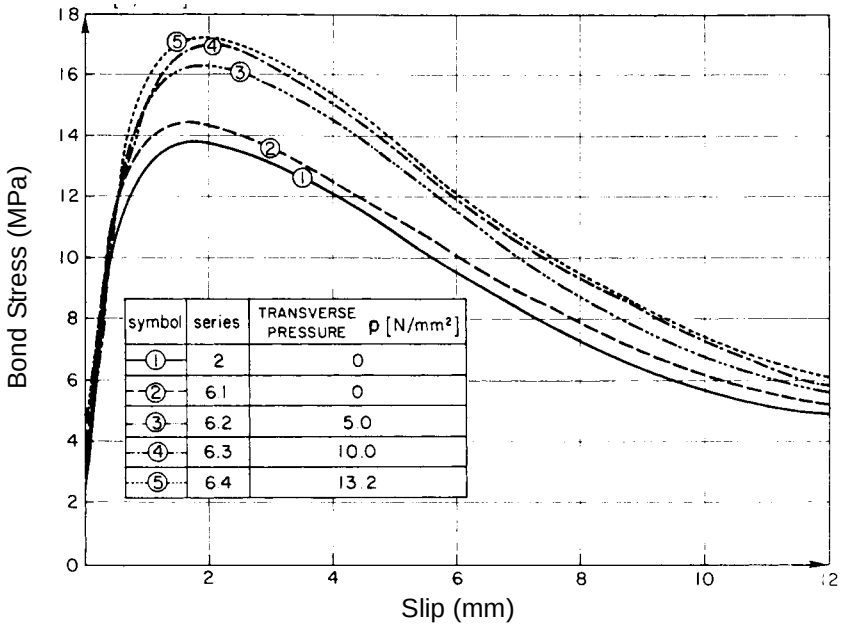

Figure 4.15: Influence of Confining Pressure on Bond Strength (Figure 4.16a from Eligehausen *et al.* [1983])

reinforcement, the volume of reinforcement provided is sufficiently large that yielding of this reinforcement is precluded. Thus, passive confinement provided by longitudinal reinforcement is no larger than that calculated assuming that the yield strength of the four No. 4 (nominal diameter equal to 0.5 inches (12.7 mm)) longitudinal bars is developed. Note

that comparison of data for tests 1.1, 1.2 and 1.5 presented in Figure 4.14 confirm that transverse reinforcement does not determine bond strength.

Figure 4.15 shows the bond response of a series of specimens with variable levels of active confining pressure applied in the direction perpendicular to the axis of the reinforcing bar and parallel to the direction of the longitudinal reinforcement. Longitudinal reinforcement is provided in these specimens. However, it is unlikely that this reinforcement provides significant additional passive confinement since this would require significant crack opening under the applied compression force.

The composite data set provided by the study is presented in Figures 4.16 and 4.17. Here peak bond strength and residual bond strength (developed at large slip levels) are shown as functions of confining pressure perpendicular to the axis of the reinforcing steel. Three *data* in Figure 4.16 represent experimental test specimens with no active confinement, as presented in Figures 4.14 and 4.15. These include a data point for test series 1.4 that is considered to have no confining pressure, a data point for test series 1.3 for which confining pressure is computed on the basis of the nominal yield strength of the No. 2 longitudinal reinforcement (nominal bar diameter equal to 0.25 inches (6.4 mm)), and two intervals that represent the maximum and minimum bond strengths observed in test series 1.1, 1.2, 1.5, 2.0 and 6.1 as well as the range of possible passive confinement. The interval of passive confining pressures is computed on the basis of the possible range of tensile stress developed in the longitudinal reinforcement that is used in test series 1.2 and 1.5 (as discussed previously, maximum confinement corresponds to the four No. 4 longitudinal bars developing nominal tensile strength while minimum confinement is equal to that provided by four No. 2 reinforcing bars at nominal yield strength). For the case of active confinement as presented in Figure 4.15, confining pressure is computed on the basis of the applied load only.

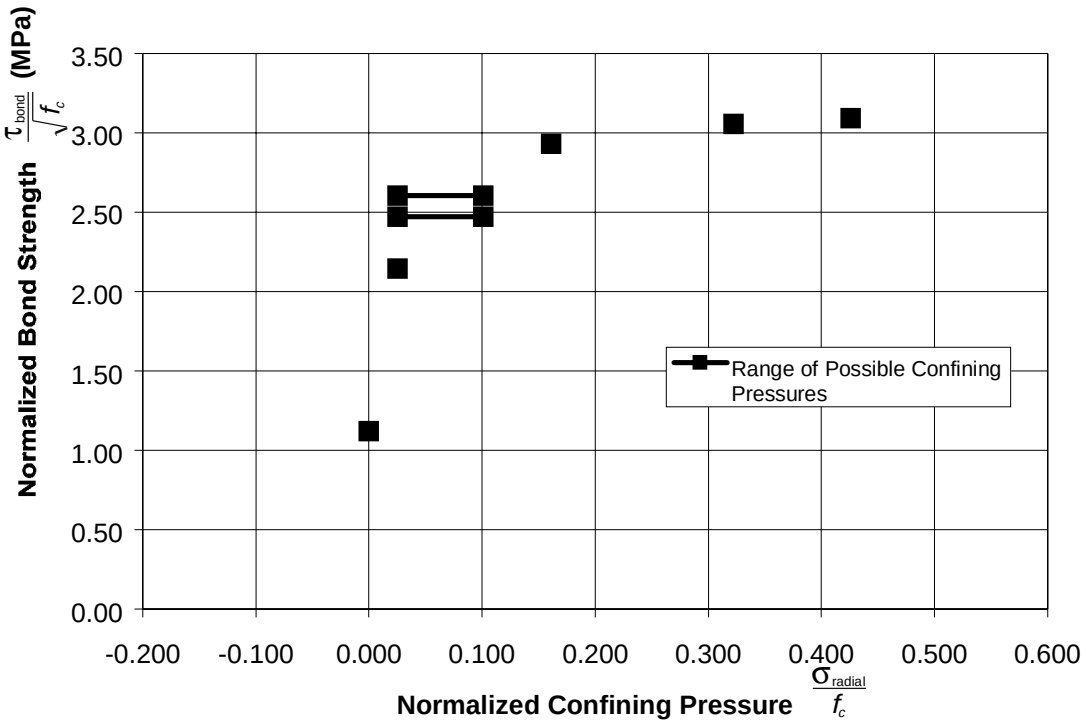

Figure 4.16: Influence of Confining Pressure on Maximum Bond Strength (Data from Eligehausen *et al.* [1983])

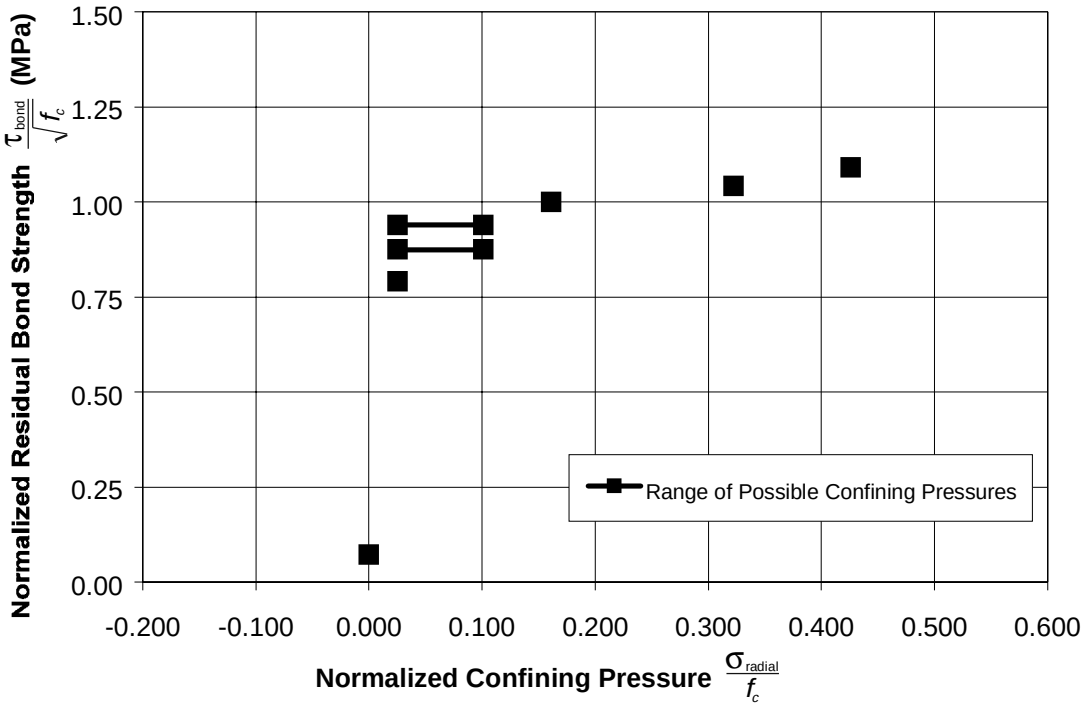

Figure 4.17: Influence of Confining Pressure on Residual Bond Strength (Data from Eligehausen *et al.* [1983])

The Eligehausen study provides extensive data characterizing bond response. Data from this investigation define the monotonic bond stress versus slip response and variation in this response as a function concrete tensile strength, bar size load rate and confinement of the bond zone. Results of this study indicate that confinement of the bond zone determine pull-out versus splitting type bond failure. Data show that these two failure modes have similar bond stress versus slip histories with a pull-out type failure exhibiting significantly more strength and deformation capacity. Additionally, data from this investigation characterize bond stress versus slip histories under cyclic loading. Here data define deterioration of bond strength from the monotonic response as a function of maximum and minimum slip demand and cycle count.

4.2.5.3 Characterization of Cyclic Bond Response

A number of other investigations provide additional data for characterizing the bond-slip response under reversed cyclic loading. Both the Comité Euro-International du Béton (CEB) State of the Art Report on Reinforced Concrete Elements Under Cyclic Loading [1996] and the ACI Committee 408 Bond Under Cyclic Loading, State of the Art Report [1992] provide references and brief discussions of these investigations. Of these additional experimental investigations of cyclic bond-slip response few consider the slip histories characterized by low-cycle loading to large slip levels that are appropriate for analysis of systems subjected to earthquake loading. For example, data presented by Balázs [1991] characterize bond-slip response under high-cycle fatigue loading (with minimal slip demand) and data presented by Morita and Kaku [1973] and Fehlig [1990] define bond-slip response under only moderate slip demands. Singha *et al.* [1964] present bond response for systems subjected to moderately high cycle counts and relatively low slip levels.

Experimental data presented by Hawkins *et al.* [1982] define bond response for systems subjected to load histories that are appropriate for this investigation. The specimens are similar in configuration to those tested by Eligehausen *et al*. [1983] and represent anchorage conditions for beam longitudinal reinforcement anchored in building beam-column connections. However, the specimens used by Hawkins in the cyclic tests have very short anchorage lengths ($< 2d_b$). The investigators report data characterizing the monotonic and cyclic bond-slip response for the prototype specimen. In general, the bond strengths reported in the Hawkins study are much higher than those reported by other researchers. For example, the average bond strength reported by Eligehausen *et al.* [1983] is $2.6\sqrt{f_c}$ MPa (with f_c in MPa, $31\sqrt{f_c}$ psi with f_c in psi); while the average strength reported by Hawkins is $5.0\sqrt{f_c}$ MPa (with f_c in MPa, $61\sqrt{f_c}$ psi with f_c in psi). These high bond strengths likely result from the use of very short anchorage lengths in the Hawkins study. The very short anchorage length puts relatively little demand on the concrete in the vicinity of the bar; thereby limiting concrete damage and increasing apparent bond strength. The results of the Hawkins study may be considered to represent an extreme response developed along the length of the anchorage zone typically used in experimental bond response investigations. While the bond strengths reported in the Hawkins study may not be appropriate for development of a local bond response model, these data do provide insight into relative bond strength degradation under cyclic loading. Figure 4.18 shows observed bond stress versus slip for the case of cyclic and reversed cyclic slip demand with increasing amplitude.

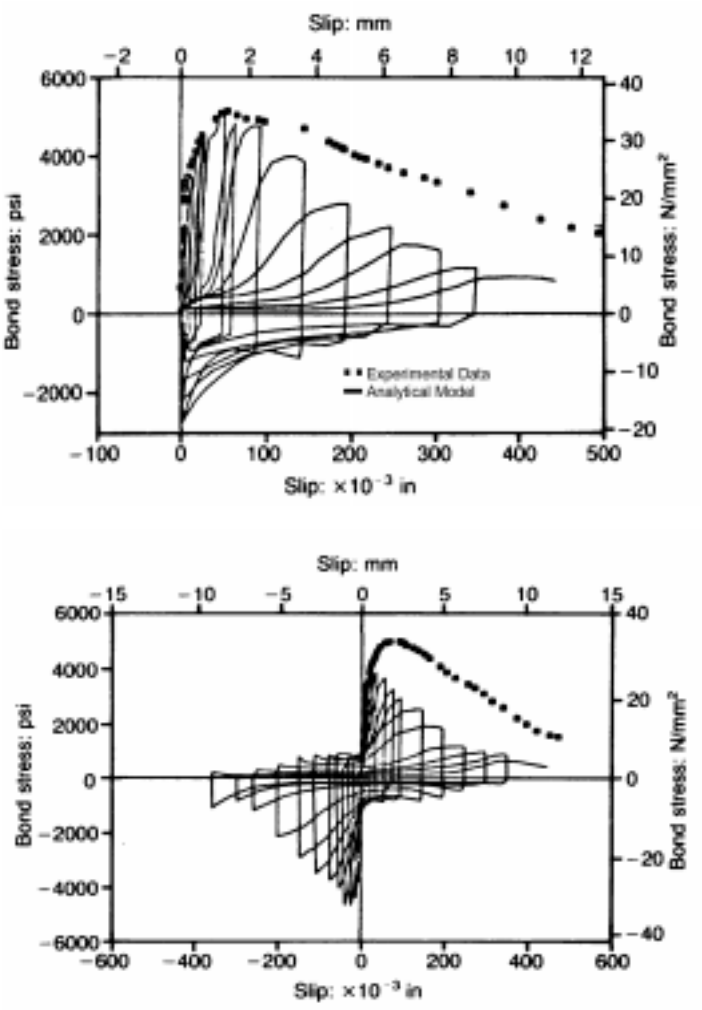

Figure 4.18: Bond Stress Versus Slip for Cyclic and Reversed Cyclic Slip History (Figures 7 and 8 from Hawkins *et al.* [1982])

4.2.6 Investigation of the Radial Stress Developed Through Bond Response and the Effect of Concrete Normal Stress on Bond Response

4.2.6.1 Experimental Studies

The radial component of bond response defines both the radial stresses developed in conjunction with bond stresses and the effect of radial stresses on the bond stress versus slip response. This component of response is addressed directly and completely by few investigations. However, in addition to the previously discussed experimental investigations for which radial bond response is addressed as part of a comprehensive evaluation of

bond (e.g., Tepfers [1979], Viwathanatepa [1979a, 1979c] and Eligehausen *et al*. [1983]), several researchers present independent investigations of radial bond behavior. A study conducted by Untrauer and Henry [1965] investigates the influence of normal pressure on bond strength. Here the prototype specimen consists of a single reinforcing bar, No. 6 or No. 9 (nominal diameters of 0.75 in.(19 mm) or 1.13 in. (28.7 mm)), embedded in a concrete prism. The prism is subjected to constant uniaxial pressure in one direction perpendicular to the reinforcing bar; the protruding end of the reinforcing bar is subjected to monotonically increasing tensile loading that is assumed to be reacted as compression on the face of the prism (this aspect of the test procedure is not discussed). Failure of all specimens is observed when a single splitting crack propagates from the bar-concrete interface toward the two prism surfaces to which the confining pressure is applied. Loading of the test specimen and the observed failure mode likely are not representative of all anchorage zone, since substantial biaxial compression of the bond-zone likely could be developed in some structures. The result of this investigation is an empirical relationship between confining pressure and maximum bond strength for the bar sizes used in the experimental test program. This relationship is defined by the following equations and is shown in Figure 4.16:

For No. 6 bar: $$\frac{\tau_{bond}}{\sqrt{f_c}} = 1.45 + 0.49\sqrt{f_{rad}} \quad (4\text{-}1a)$$

For No. 9 bar: $$\frac{\tau_{bond}}{\sqrt{f_c}} = 1.55 + 0.40\sqrt{f_{rad}} \quad (4\text{-}2a)$$

where τ_{bond} is the bond strength, f_{rad} is the confining pressure and f_c is the concrete compressive strength all defined in MPa. The test specimens and procedure eliminate the possibility of observing residual bond strength.

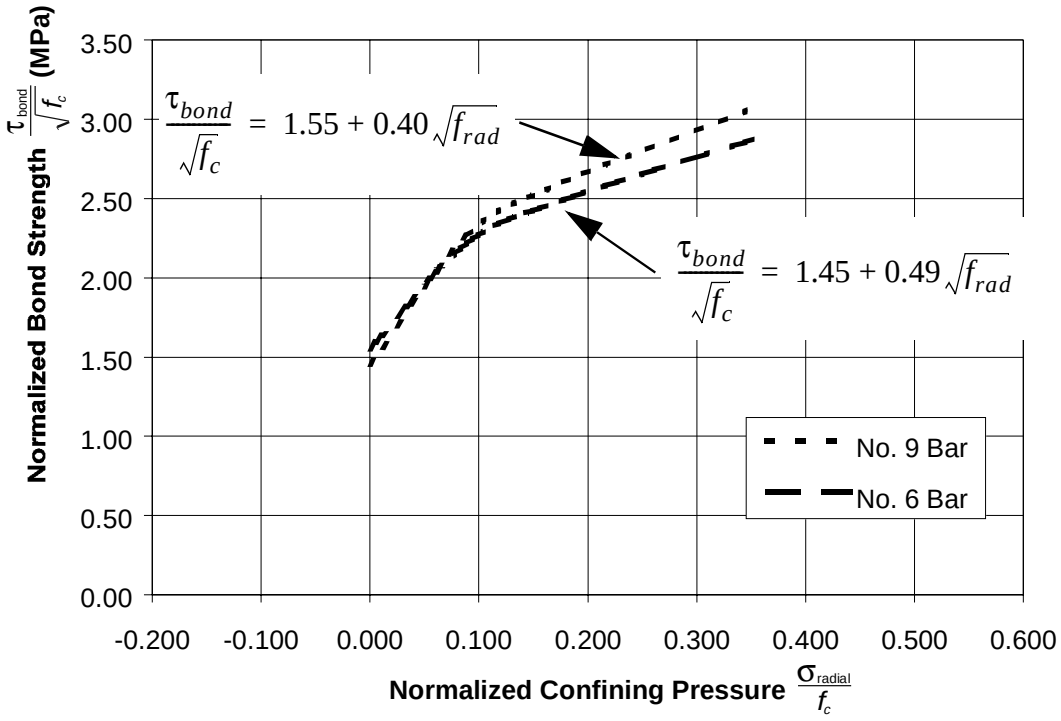

Figure 4.19: Influence of Confining Pressure on Bond Strength (Equations from Untrauer and Henry [1965])

More recently, the radial stress distribution developed as a result of bond-slip response was investigated experimentally by Gambarova *et al.* [1989a, 1889b]. For each specimen in this experimental program, a single reinforcing bar with diameter of 18 mm (0.71 inches) is embedded in a concrete prism with a bonded embedment length of $3d_b$. The concrete prism is pre-cracked on a plane parallel to the bar axis. The opening of this crack is maintained at a prescribed width while tensile load is applied to one end of the reinforcing bar under displacement control. Applied load is reacted through shear on the surfaces of the concrete prism parallel to the crack plane. Slip is measured as the movement of the unloaded bar end with respect to the concrete prism. Figures 4.20 and 4.21 show the observed bond stress versus slip histories and radial stress versus slip histories for one set of specimens tested by Gambarova *et al.* [1989]. Figure 4.22 shows the relationship between normalized bond stress and radial stress. The results of this investigation

also include an empirical relationship between bond strength, τ_{bond}; radial stress, f_{rad}; slip, *slip*, and crack opening width, δ that is represented by the following equations:

$$\frac{(\tau_{bond})_{max}}{f_c} = \frac{a_1}{\frac{\delta}{d_b} + a_2} - a_3 \tag{4-3a}$$

$$\frac{(f_{rad})_{max}}{f_c} = a_4 - \left(a_5 \cdot \frac{\delta}{d_b}\right) \tag{4-3b}$$

$$\frac{\tau_{bond}}{f_c} = \left(\frac{1}{a_6 + a_7\frac{\delta}{d_b}}\right)\frac{\frac{slip}{d_b}}{1 + b_1\left(\frac{\delta}{d_b}\right)\frac{slip}{d_b} + b_2\left(\frac{\delta}{d_b}\right)\left(\frac{slip}{d_b}\right)^2 + b_3\left(\frac{\delta}{d_b}\right)\left(\frac{slip}{d_b}\right)^4} \tag{4-3c}$$

$$\frac{\sigma f_{rad}}{f_c} = \left(a_8 - a_9\frac{\delta}{d_b}\right)\frac{\frac{slip}{d_b}}{1 + c_1\left(\frac{\delta}{d_b}\right)\left(\frac{slip}{d_b}\right) + c_2\left(\frac{\delta}{d_b}\right)\left(\frac{slip}{d_b}\right)^2 + c_3\left(\frac{\delta}{d_b}\right)\left(\frac{slip}{d_b}\right)^4} \tag{4-3d}$$

where a_i, b_i, c_i and d_i are calibration constants. Equation (4-3b) defines the maximum observed confining pressure as a function of crack width opening, not the confining pressure associated with development of the maximum bond strength. Thus, extension of Equations (4-3a) through (4-3d) to define a single independent relationship between bond strength and radial force is not trivial. Data presented in Figure 4.23 show the relationship between concrete confinement and peak bond strength for the crack widths investigated in the Gambarova study. Figure 4.23 also shows the relationship between peak bond strength and peak confining pressure as defined by Equations (4-3a) and (4-3b). This suggests that radial dilation is most significant once the peak bond strength has been achieved and slip levels are relatively large. Equation 4-3c is used to compute a *residual bond strength* defined as the bond strength for a slip of 12 mm (0.47 in.) for the crack width openings investigated in this study. Figure 4.24 shows normalized residual bond strength as a function of normalized confining pressure.

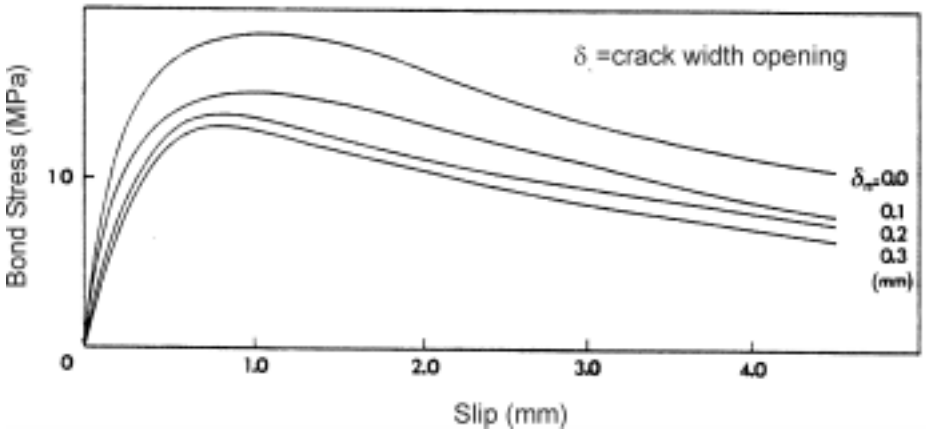

Figure 4.20: Bond Stress Versus Slip for Specimens with Prescribed Splitting Crack Widths (Figure 11a from Gambarova *et al.* [1989a])

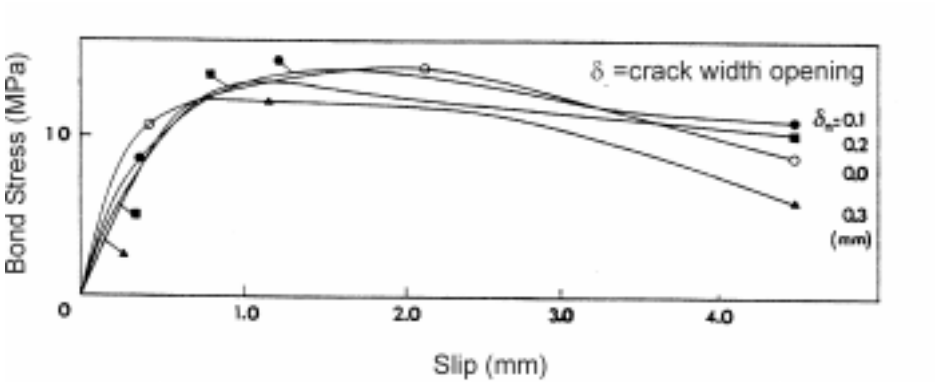

Figure 4.21: Radial Stress Versus Slip for Specimens with Prescribed Splitting Crack Widths (Figure 11b from Gambarova *et al.* [1989a])

Malvar [1992] provides a significant contribution to the characterization of the multi-dimensional bond-slip response under monotonic load conditions. In this experimental investigation the prototype specimen consists of a single reinforcing bar embedded in a concrete cylinder with an anchorage length of $3d_b$. One exposed end of the bar is subjected to load under displacement control while slip is measured as the movement of the unloaded bar end with respect to the concrete cylinder. Here the applied load is reacted as shear on the surface of the concrete cylinder. Additional specimens vary from the prototype by the pressure applied to the exterior of the concrete cylinder. A typical load history consists of applying a monotonically increasing tensile load to the anchored bar while applying a constant, moderate confining pressure to the exterior of the specimen. Once

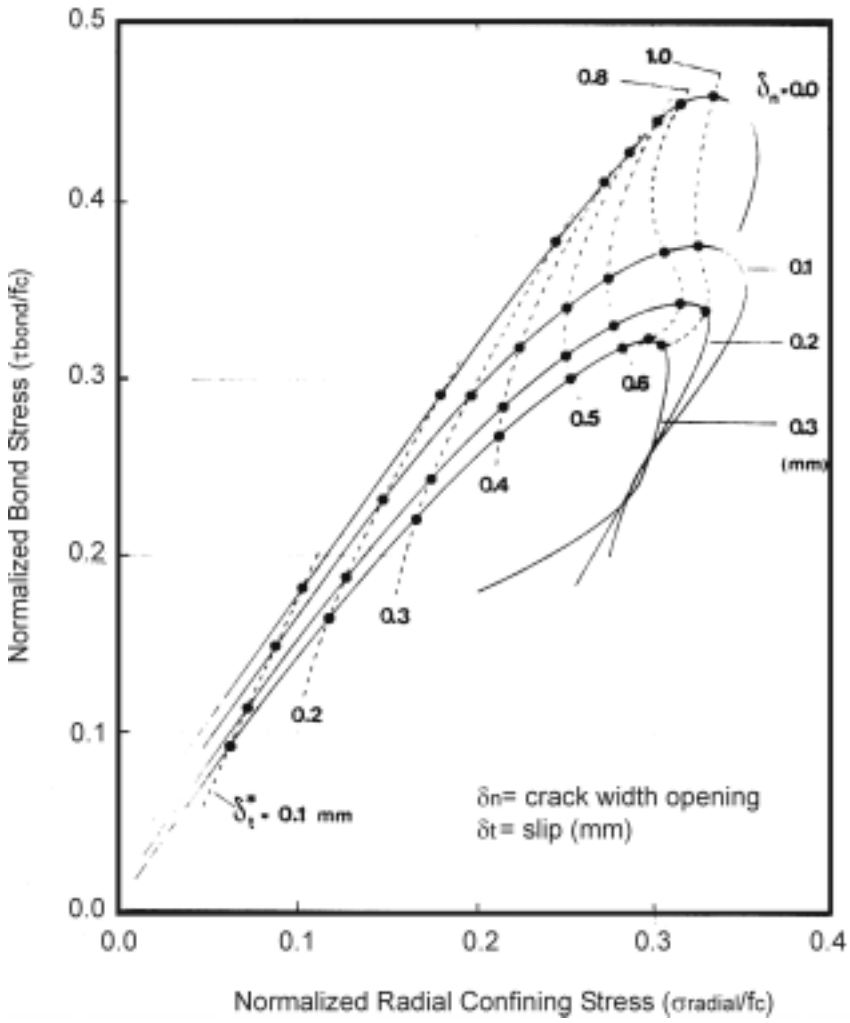

Figure 4.22: Bond Stress Versus Radial Stress for Varying Levels of Crack Width Opening (Figure 12 from Gambarova *et al.* [1989a])

splitting of the concrete cover is observed, the specimen is unloaded, the confining pressure is increased to the prescribed level and the anchored bar is reloaded under monotonically increasing tension. Here it is assumed that the confining pressure is defined by pressure applied to the exterior of the cylinder, which is equal to the average pressure applied to a cross section of the cylinder through the reinforcing bar. Figures 4.25 and 4.26 show bond strength and radial dilation as a function of slip for variable levels of confining pressure. These data show that bond strength increases with confining pressure and that significant confining pressure limits radial dilation. Additionally, the data presented in

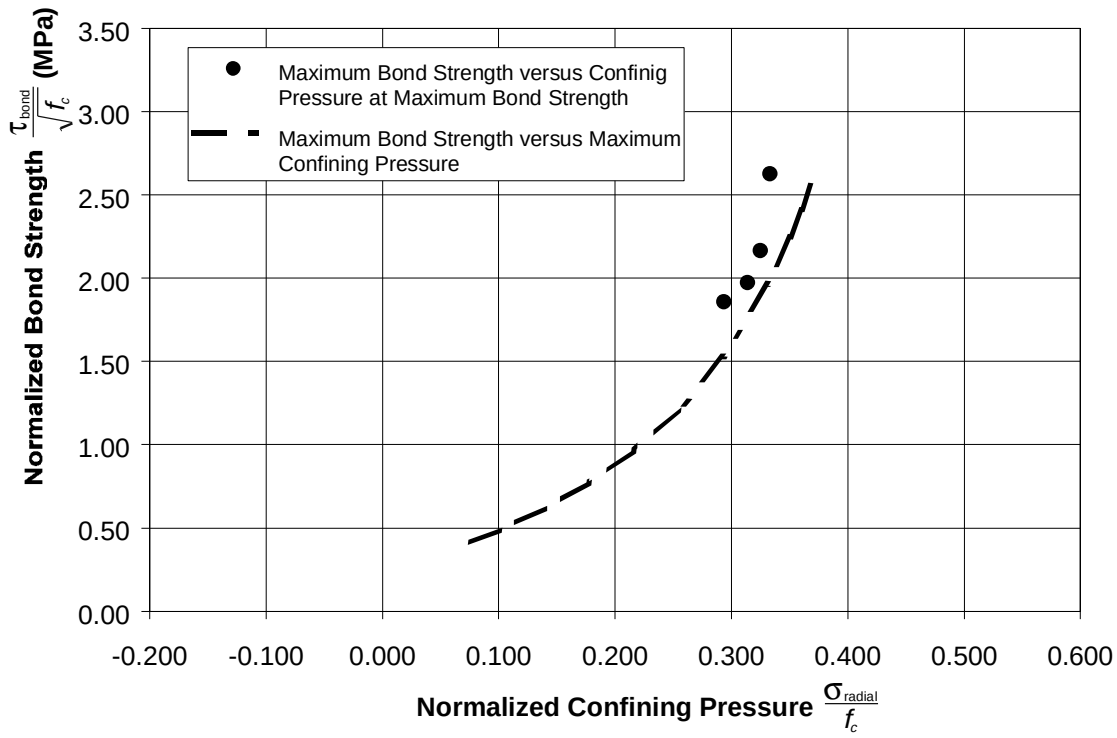

Figure 4.23: Influence of Confining Pressure on Maximum Bond Strength (Data from

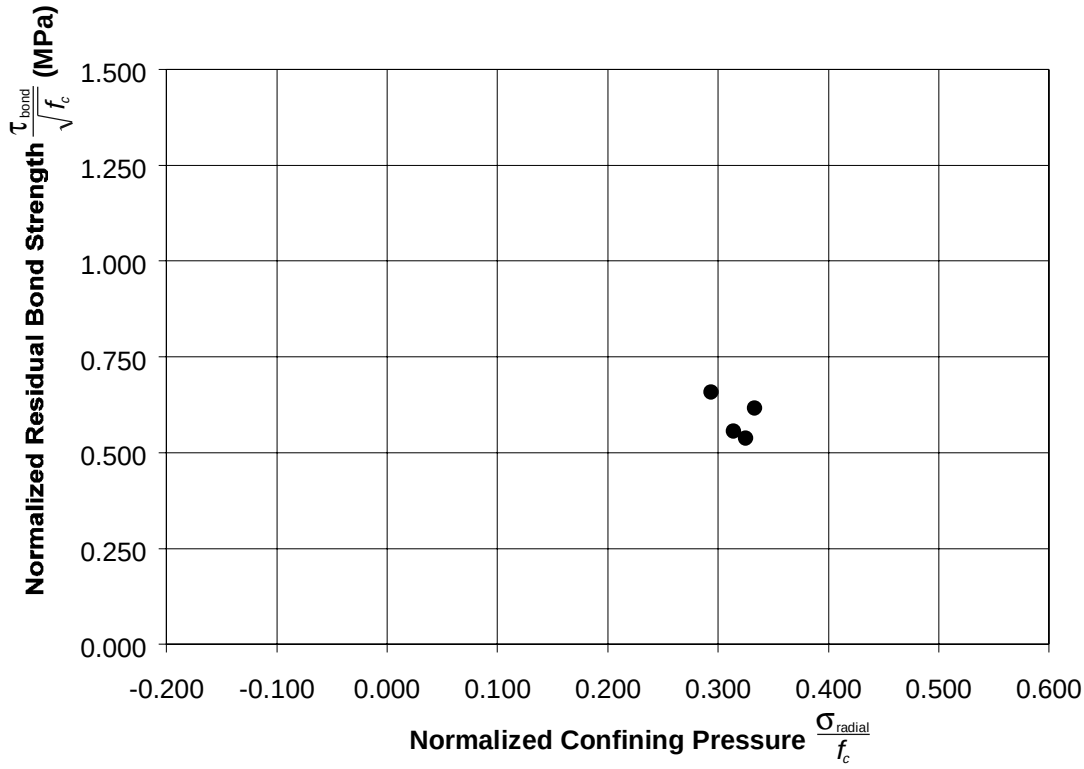

Figure 4.24: Influence of Confining Pressure on Residual Bond Strength (Empirical Relationship from Gambarova *et al.* [1989b])

Figure 4.26 follow the same trend as the data collected in the Gambarova study (Figure 4.22 and Figure 4.23): maximum dilation is observed at slip levels in excess of those corresponding to development of peak bond strength. Figure 4.27 shows the relationship between peak bond strength and confining pressure. For these tests, the application of radial compression could be expected to increase the bond strength more than for previous tests in which pressure is applied on one plane only. However, these tests consider the maximum bond strength of radially cracked concrete cylinders. Thus peak bond strength observed in these tests might be expected to be lower than for previous models in which concrete cracking occurred along a single plane. The net effect of these parameters is unclear, though bond strengths observed in this series of tests are comparable to those observed previously. Figure 4.28 shows the relationship between residual bond strength and confining pressure. Unlike the Gambarova tests, here residual bond strength increases with increasing confining pressure.

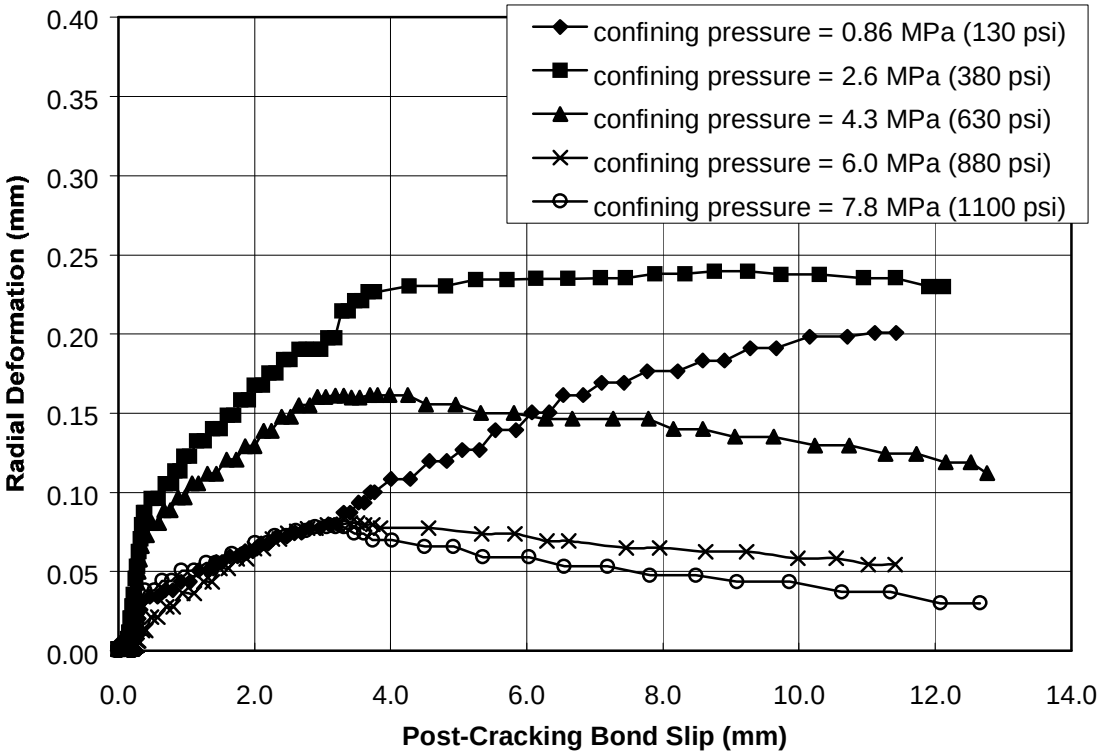

Figure 4.26: Radial Dilation as a Function of Slip for Cylindrical Bond Specimens with Variable Levels of Confining Pressure (Data from Malvar [1991])

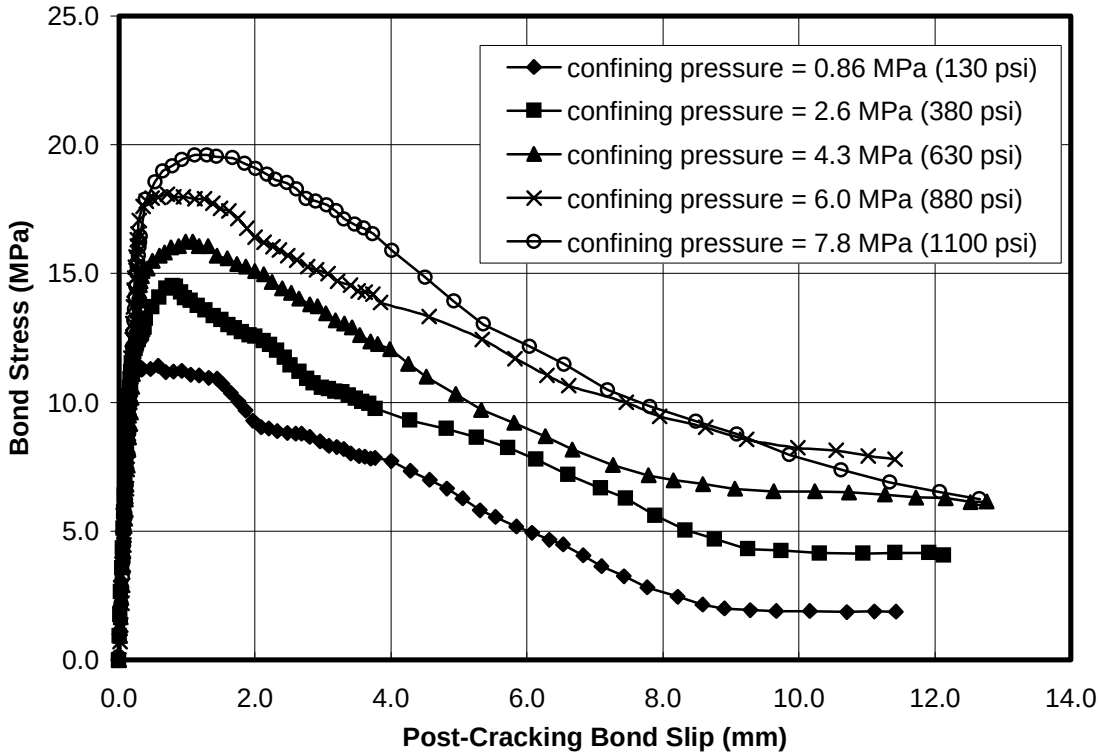

Figure 4.25: Bond Stress - Slip Histories for Pre-Cracked Cylindrical Bond Specimens with Variable Levels of Confining Pressure (Data from Malvar [1991])

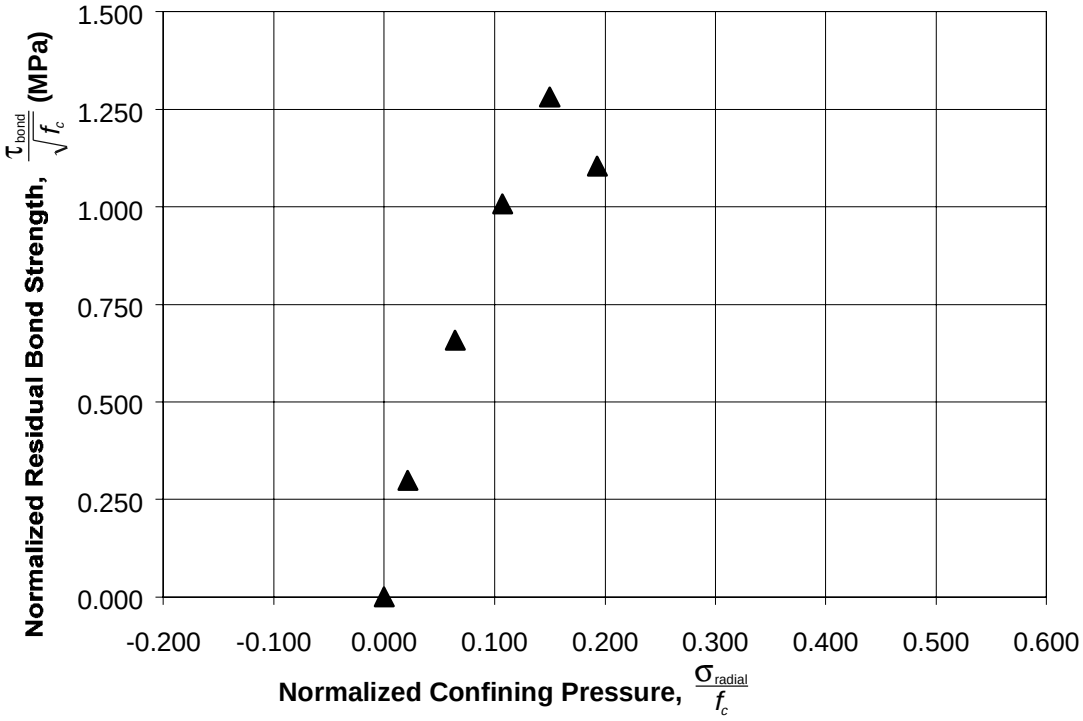

Figure 4.28: Influence of Confining Pressure on Residual Bond Strength (Data from Malvar [1992])

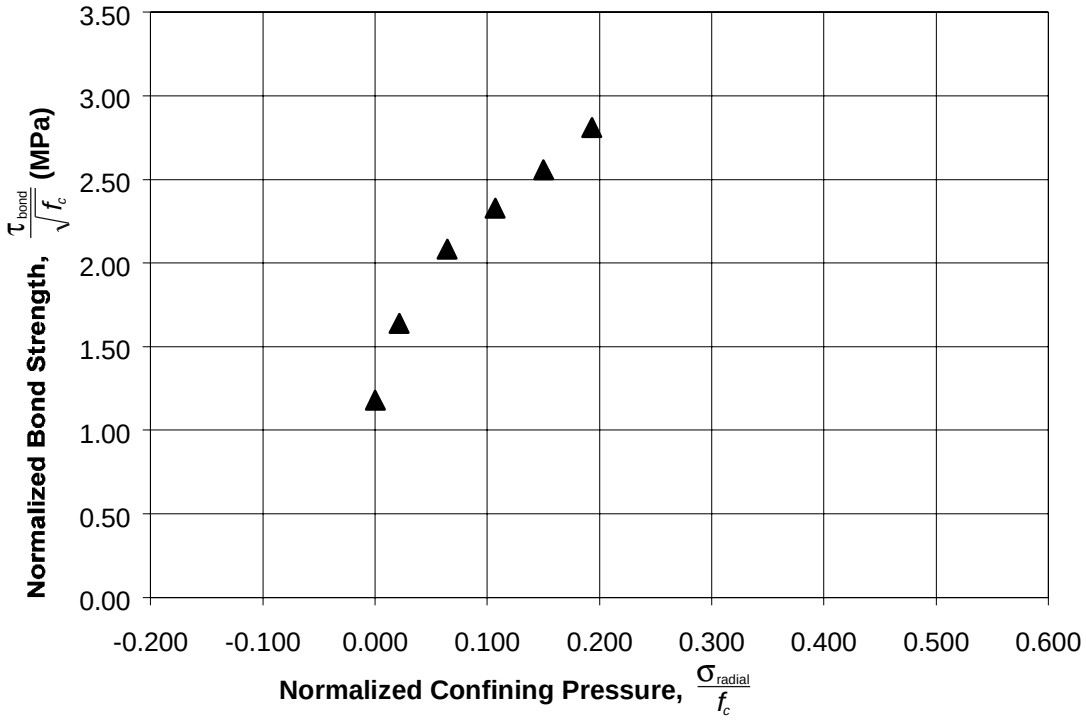

Figure 4.27: Influence of Confining Pressure on Bond Strength (Experimental data from Malvar [1992])

Cairns and Jones [1995a, 1995b, 1996] also investigate the development of radial forces associated with mechanical interaction. Data are collected from an experimental investigation in which equal tensile load is applied to the exposed ends of two lapped bars anchored in a concrete block with a splice length of $20d_b$. Additional data are collected from an analytical study in which a finite element model is used to investigate the distribution of radial stresses developed in a tension lap splice. On the basis of these analytical and experimental investigations as well as investigations conducted by other researchers, the authors propose a non-splitting and a splitting component of bond response, a capacity for the non-splitting component, and a relationship between bond stress, developed parallel to the bar axis, and radial stress, developed perpendicular to the bar axis. The validity of the relationship between bond and radial stress is questionable, since this relationship depends on the results of a linear-elastic finite element model and many researchers have shown

that the response in the vicinity of the reinforcing bar is highly non-linear [Lutz, 1970; Goto, 1971; Eligehausen *et al.*, 1983].

4.2.6.2 Summary of Findings on Radial Bond Response

The results of the investigations that focus on radial bond response combined with results of the previously discussed investigations support a number of conclusions about mechanisms of bond response. All of these studies indicate that concrete compressive stress in the direction perpendicular to the axis of the reinforcing bar increases bond strength. This compressive stress may result from application of active confining pressure, as would be the case for a bar anchored perpendicular to a flexural compressive zone, or from the development of passive confinement, as could be the case if transverse reinforcement is present in the anchorage zone. From the previously discussed mechanisms of bond response it follows that confinement of the bond zone retards longitudinal cracking of the bond zone by limiting tensile hoop stresses that develop in the concrete surrounding an anchored bar. If no confinement is provided by active application of compression to the bond zone, by transverse reinforcement or by substantial cover concrete, then a splitting-type bond failure will result. Data presented by Eligehausen *et al.* [1983] indicate that the most substantial increase in bond strength with confinement is achieved if a pull-out bond failure is promoted over a splitting-type bond failure.

Once a pull-out type failure mechanism is achieved, the experimental data present by Eligehausen also indicate that there is a limit to the level of passive confinement that can be provided by transverse reinforcement (similar conclusion are reached by Orangun *et al.* [1977]). Additionally, the data presented by Eligehausen *et al.* [1983] and by Malvar [1992] appear to suggest that there is a limit to the increase in bond strength that can be achieved for increasing active confinement. If it is assumed that residual bond strength is

primarily due to friction of the reinforcing bar sliding past concrete, then the observed increase in residual bond strength with passive and active confinement is appropriate.

Data presented by Gambarova do not compare to those presented by other researchers. This discrepancy results from the fact that the Gambarova investigation considers systems subjected not to constant pressure in the direction perpendicular to the anchored bar but to constant levels of radial deformation, and therefore variable pressure. Thus, these data are not appropriate for calibrating a model that characterizes bond strength as a function of confining pressure. However, the data are appropriate for verification of the proposed model.

For deformed reinforcement, the development of bond stresses at the concrete-steel interface is accompanied by the development of radial stresses. The Gambarova investigation is the only study that considers radial stress as a function of slip. The results of this study show that peak radial stress is achieved at slip levels slightly in excess of those associated with development of peak bond strength. Because data defining the relationship between radial and bond stress are so limited, model development requires introduction of some assumptions about bond zone behavior to extend these data.

In unrestrained or partially restrained systems, radial stresses that develop at the concrete-steel interface produce significant radial dilation. This dilation is reported for the Malvar investigation. It is important to note that the magnitude of dilation is a function of the experimental bond zone and the level of damage in the concrete surrounding the reinforcing bar. The results of the study presented by Malvar indicate that dilation is maximum at slip levels in excess of that corresponding to development of peak bond strength. However, it is important to note that the accumulation of damage to surrounding concrete also is maximum at these slip levels. For systems with moderate levels of constant confinement, dilation diminishes with increasing slip. However, some dilation is required to

achieve large slip levels. The fact that dilation is determined by concrete material state suggests that this component of response is best represented by the concrete material model.

4.2.7 Investigation of System Parameters that Determine Bond Response

A number of investigations focus on characterizing the effect of particular material, system and load history parameters on bond response. The Comité Euro-International du Béton (CEB) State of the Art Report on Reinforced Concrete Elements Under Cyclic Loading [1996] and the ACI Committee 408 State of the Art Report on Bond Under Cyclic Loads [1992] as well as Bond and Development of Reinforcement [Leon, 1997] provide reference for many of the studies. Parameters of interest to the current investigation include yielding of reinforcing steel, the deformation pattern on the surface of the reinforcement and load rate.

4.2.7.1 Bond Response for Yielding Reinforcement

Experimental testing of reinforced concrete structural elements supports the proposition that local bond strength is reduced for reinforcement that yields in tension and increased for reinforcement that yields in compression. This observed response is explained partly on the basis of the Poisson effect that causes the diameter of the reinforcing bar to shrink once tensile yielding occurs thereby allowing steel to slip past surrounding concrete more easily while causing the diameter of the reinforcing bar to expand once compressive yielding occurs thereby improving the connectivity between the steel and surrounding concrete and increasing bond strength. Additionally, it is proposed that transfer of tensile stress to the surrounding concrete results in more global damage to the surrounding concrete than is the case for transfer of compressive stresses and that this

contributes to reduced bond capacity under tensile loading compared with compressive loading.

While variation in bond strength for steel yielding in compression and tension has been observed during experimental testing of structural systems, this issue has been addressed by few experimental bond studies conducted at the scale of the reinforcing bar. Data from this type of investigation are necessary for model development. Results of the experimental investigation presented by Viwathanatepa [1979a, 1979c] support the previous proposition about bond strength. In the Viwathanatepa study, observed bond strengths are significantly higher for the end of the reinforcement that yields in *compression* than for the end of the reinforcing bar that yields in *tension.* However, the study was not designed so that the effects of steel material state can be isolated from the effects of the concrete stress state, and some variation in bond strength must be attributed to variation in concrete confining pressure. A study completed by Shima *et al.* [1987a, 1987b] is one of the few studies that directly addresses the issue of bond response as a function of reinforcement strain distribution. However, this study only considers steel loaded in tension. For this investigation, the prototype specimen consists of a No. 19M (nominal diameter of 19.5 mm (0.88 in.)) reinforcing bar embedded with an anchorage length of $50d_b$ in a plain concrete cylinder with a diameter of 500 mm (20 in.) and a height of $60d_b$ (Figure 4.29). Note that an unbonded length of $10d_b$ is provided at the loaded end of the bar to eliminate the effect of *end conditions* on bond response. The dimensions of the anchorage block are chosen to provide sufficient concrete cover to preclude a splitting-type bond failure and sufficient anchorage length to ensure yielding of the reinforcing bar. Tensile load is applied to the exposed end of the reinforcing bar and reacted against the adjacent surface of the concrete cylinder at a distance of 17.5 cm from the bar. This is a sufficiently small distance that the reaction likely enhances somewhat the bar anchorage. Bar strain is mea-

sured using foil gages glued to the bar at intervals of $2.5d_b$ and $5d_b$ along the length. It is important to note that no lugs are removed from the reinforcing bar to attach these gages. Slip is computed as the integral of the strain along the length of the bar, assuming that slip of the non-loaded end of the bar is zero and that concrete strain is insignificant. Bond stress is computed based on the derivative of the bar stress distribution along the length of the bar and defined by the measured strains and experimentally observed material stress-stain response. Experimental bond stress is typically computed in this manner; however, it should be noted that the process of taking the difference between observed steel stress/ strain values and dividing by the length compounds any measurement errors.

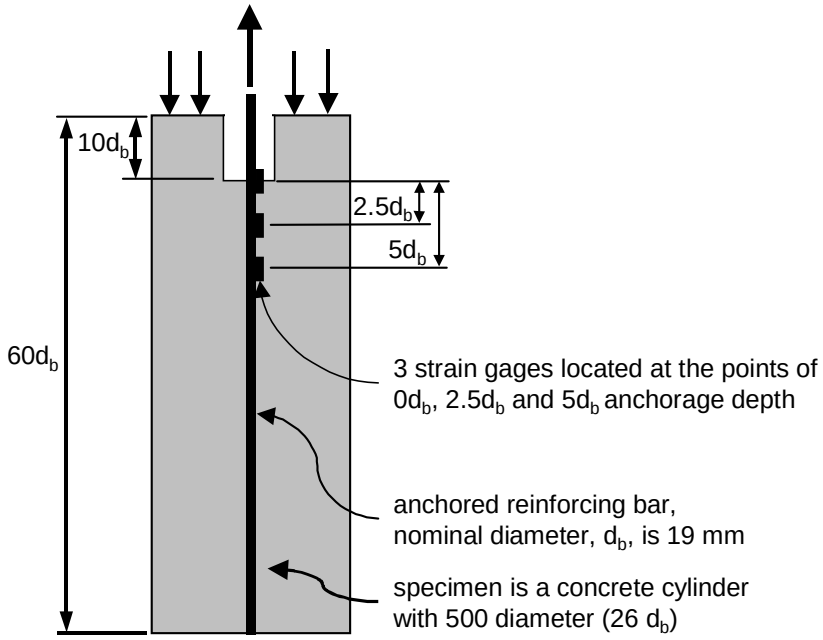

Figure 4.29: Prototype Model for Experimental Test Program by Shima *et al.*, [1987a, 1987b]

The Shima study considers the response of specimens with steel yield strengths of 300, 500 and 700 MPa (40, 70 and 100 ksi). The bond stress versus slip response for these specimens at points within the yielded zone of the bar are shown in Figure 4.30. These data show a significant drop in bond strength once yielding occurs. This loss of strength is

not a function of the additional slip associated with plastic deformation of the reinforcing bar since the increment in slip that determines pre- to post-yield is minimal. Instead, since slip is calculated by integrating strain measurements along the bar length and bond stress is computed from the difference of calculated bar stress at the strain gages, the loss of bond strength is a function of the post-yield modulus of the reinforcing steel. This method of calculating slip and bond strength may result in an over-estimation of loss of bond strength for yielding reinforcement. Note that the variation in the slip level at which each of the specimens exhibits yielding is a result of the additional deformation that can be developed at the concrete-steel interface in the pre-yield phase of response for the specimens with stronger steel.

The data provided by the Viwathanatepa and Shima studies provide a very limited database for model development. Thus, the model developed for this investigation represents only the fundamental rather than the exact characteristics of the observed response. Because the Shima study does not present data for the case of compressive yielding, the data provided by the Viwathanatepa study in combination with a relationship characterizing bond strength as a function of concrete confinement may be used to define the bond strength *increase* associated with compressive yielding. However, because these data define only the increase in bond strength and not associated slip, some assumptions may be required as to the dependence of the strength increase on the steel material state. Data provided by the Shima study can be used to define deterioration in bond strength for reinforcement yielding in tension. Here the data relate bond strength to slip; however, this relationship can be extended to provide the experimentally observed relationship between bond strength and steel strain state as is desired for this investigation.

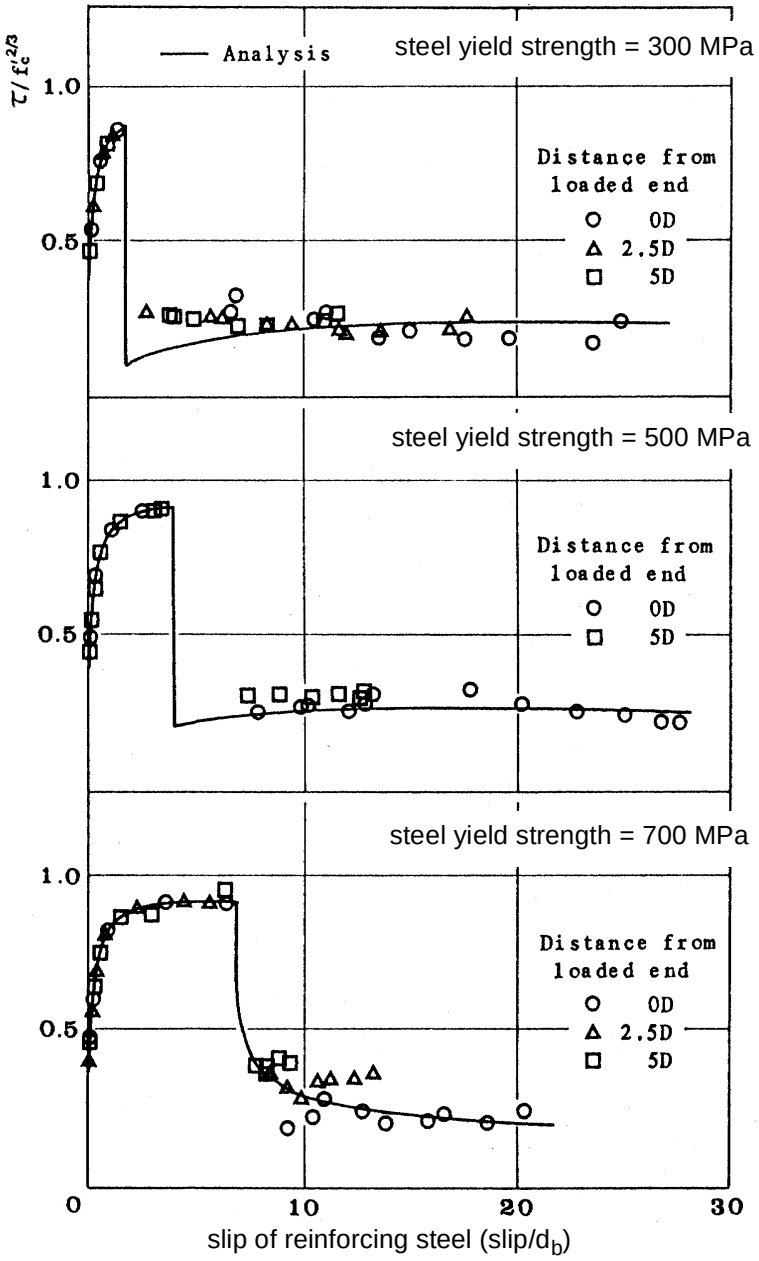

Note: 'Distance from loaded end' refers to embedment depth at which the strain is measured (Figure 4.29)

Figure 4.30: Bond Stress Versus Slip for Systems with Tensile Yielding of Reinforcement (Figure 9 from Shima *et al.* [1987b])

4.2.7.2 Effect of Steel Deformation Patterns on Bond Response

The results of previous experimental investigation indicate that variation in the deformation pattern on a reinforcing bar affects bond response. The deformation pattern on a reinforcing bar is characterized by the lug spacing, height, lug face angle and pattern.

In part these parameters are represented by the relative rib area of the reinforcing bar; relative rib area typically is defined as the rib area perpendicular to the bar axis normalized by the bar surface area between lugs. However, bars with different lug patterns may have approximately the same relative rib area. Results of a study conducted by Darwin and Graham [1993] indicate that increased relative rib area results in increased bond stiffness and increased strength for specimens that do not exhibit a splitting-type bond failure. A study conducted by Hamad [1995] shows similar results though increased bond strength is observed for specimens that exhibit a splitting-type bond failure as well as for those that exhibit a pull-out failure. Cairns and Jones [1995a, 1995b] also report increased bond strength for both pull-out and splitting-type bond failures with increasing relative rib area. Additionally, Hamad concludes that specimens with lug-face angles in excess of 45 degrees exhibit increased strength over bars with lug-face angles less than 45 degrees.

The previous research focusses on modification of the standard deformation patterns to improve bond response. While a few bars with standard deformation patterns are included in the investigations, the data do not represent a comprehensive evaluation of the effected on bond response of variation in deformation pattern for bars with similar relative rib area. Thus the results of these investigations are not necessarily applicable to standard reinforcing steel for which typical deformation patterns have approximately the same relative rib area. Goto [1971] shows significant variation in bond stiffness for several different common deformation patterns. Unfortunately, Goto does not provide relative rib area data for these bars so it is not possible to conclude that the results of this study contradict those of the previously discussed investigations. Thus, for the current investigation it is reasonable to assume that the effect of deformation pattern on bond response is negligible within the limited range of relative rib areas that define standard reinforcing steel.

4.2.7.3 Dynamic Bond Response

Consideration of dynamic bond response is appropriate in development of a model of reinforced concrete structures subjected to earthquake loading. No data are available defining slip rates or bond-stress demand rates for systems subjected to dynamic loads. However, ranges for these rates may be estimated on the basis of computed and experimentally observed stress and strain rates in reinforcing steel and plain concrete. An appropriate maximum slip rate for reinforcing steel bonded to concrete in a bridge structure can be estimated by enforcing equilibrium of an anchored reinforcing bar and assuming that maximum steel strain rates are developed for the case of yielded reinforcing steel. This provides the following relationship between average slip rate and maximum steel strain rate.

$$\dot{\overline{slip}} = \frac{E_{s,\,yield}}{E_{bond}} \frac{d_b}{4 l_b} \dot{\varepsilon} \tag{4-4}$$

where $E_{s,\,yield}$ is the post-yield modulus for the reinforcing steel, E_{bond} is the secant modulus to the bond stress versus slip history, d_b is the diameter of the reinforcing bar, l_b is the anchorage length and $\dot{\varepsilon}$ is the steel strain rate. Assuming $E_{s,\,yield}$ equal to 7000 MPa (1000 ksi), E_{bond} equal to 20 MPa/mm (70 ksi/in.), l_b equal to $40 d_b$, and $\dot{\varepsilon}$ equal to 0.03 per second (the maximum steel strain rate associated with reinforcing steel loaded to a strain in the vicinity of the yield strain, Section 3.2.1) results in an estimated maximum slip rate of 0.08 mm/sec. (0.003 in./sec.). An associated range for average bond stress rate is 1.6 MPa/sec. (0.21 ksi/sec.).

A few investigations consider bond response for load rates that are developed under earthquake loading; most dynamic bond response studies consider the more rapid loading associated with blast loading. Figure 4.31 shows several proposed relationships between peak bond strength and slip rate developed from dynamic bond studies. These relation-

ships are augmented by the data presented in Figure 4.32 that show the data defining the bond stress versus slip rate relationship proposed by Hjorth [1976] and presented in Figure 4.31. The data presented in Figure 4.33 show bond stress as a function of slip for several loading rates [Vos, 1983].

The data suggest that dynamic bond strength increases of less than 5 percent over the observed *static* bond strength for slip and bond stress load rates that may be developed in reinforced concrete bridges subjected to earthquake loading. This increase in strength falls between the predicted strength increase for plain concrete in tension and in compression (Section 2.2.8) and is less than the predicted increase in steel strength (Section 3.2.3). Here is it assumed that variation in bond response as a function of load rate is negligible in comparison with variation in experimental bond response data.

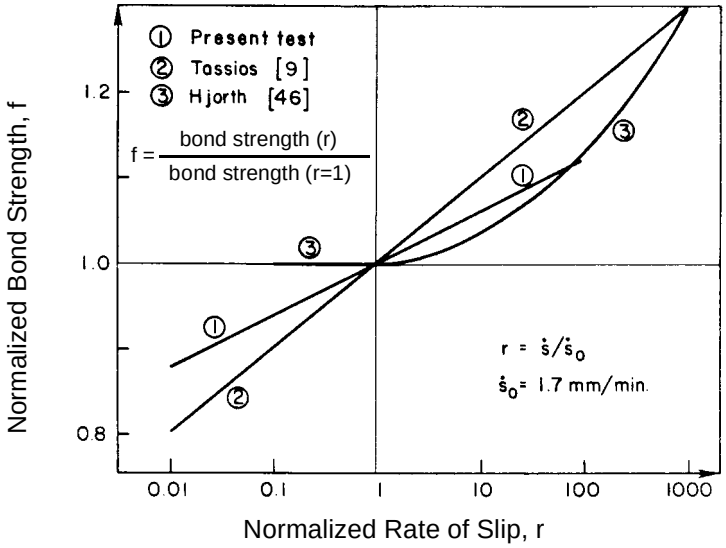

Figure 4.31: Normalized Bond Strength Versus Normalized Rate of Slip (Figure 4.23 from Eligehausen *et al.* [1983])

4.3 Modeling Concrete-to-Steel Bond Behavior

Many models have been proposed for characterization of concrete and steel bond response. These models range in sophistication from one-dimensional zero-length elements that characterize the load-deformation history of the bond-zone material as elastic

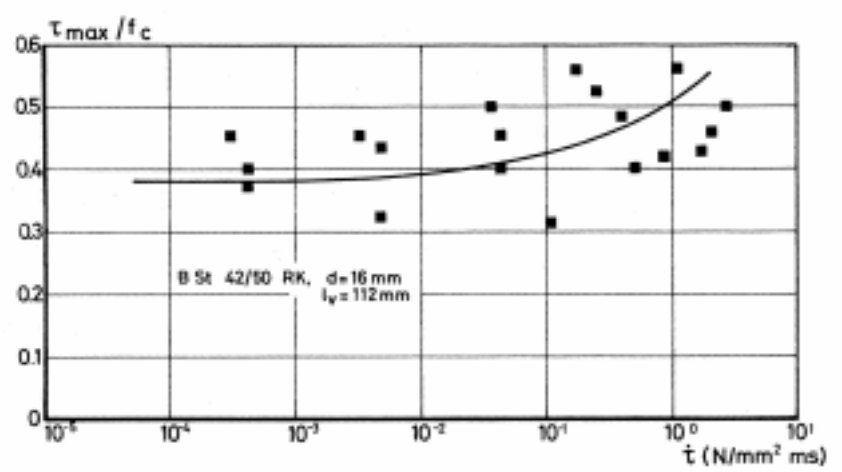

Figure 4.32: Influence of Loading Rate on Bond Strength (Figure 2.1.16 from Hjorth [1976])

to multi-dimensional finite-volume elements that characterize the response of the bond-zone concrete surrounding a reinforcing bar on the basis of continuum mechanics. These models provide insight into the physical mechanisms that determine bond response as well as identify techniques for incorporating bond response into analytical models of reinforced concrete systems.

4.3.1 Bond-Link Models

One of the first bond models is that proposed by Ngo and Scordelis [1967]. Here the global finite element model represents a lightly reinforced concrete beam subjected to monotonically increasing third-point loading and includes elastic plane stress continuum elements to represent the material behavior of plain concrete and reinforcing steel. Concrete damage is represented through the introduction of a set of pre-defined cracks into the system mesh. Connectivity between the concrete and reinforcing steel is achieved through the introduction of a zero-length two-dimensional bond link element that may be idealized as two orthogonal springs. The bond-link element is assumed to have no length and no height. In order to simplify the model, the springs are assumed to have linear elastic force-

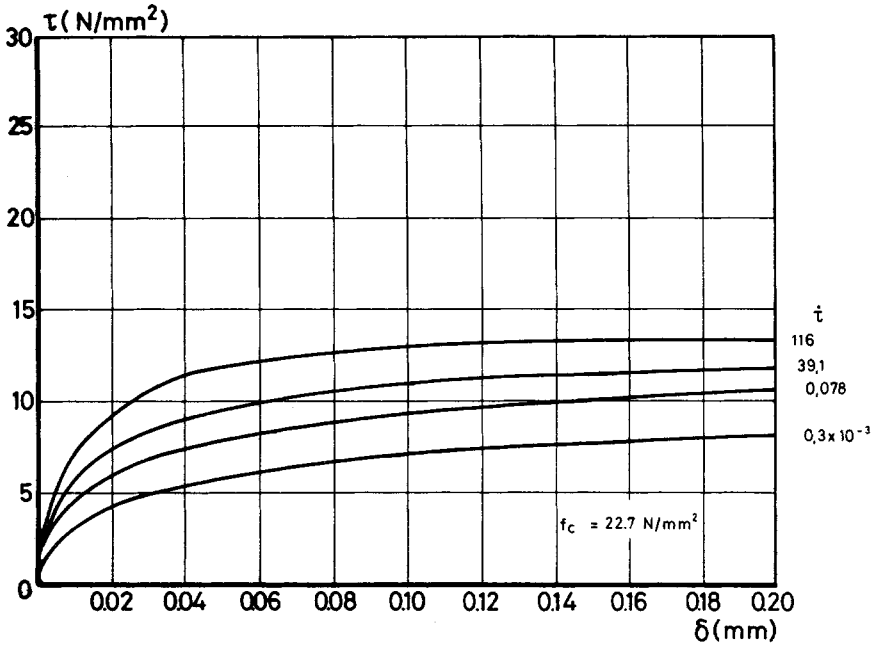

Figure 4.33a: Low Strength Concrete

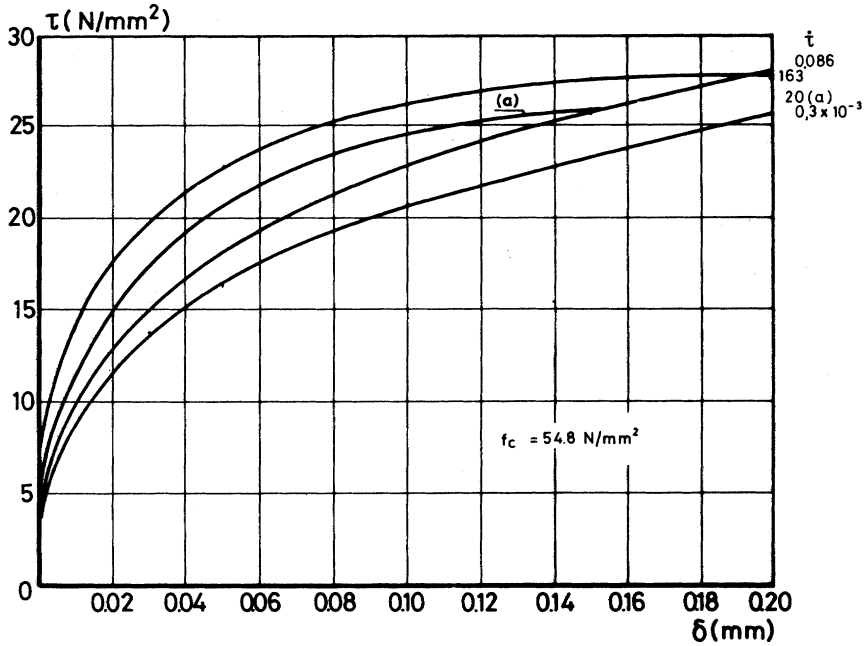

Figure 4.33b: High Strength Concrete

Note: Stress rate is defined as $\dot{\tau} = \frac{N}{mm \cdot msec}$

Figure 4.33: Bond Strength Versus Slip for High and Low Strength Concrete at Various Loading Rates (Figure 4.1.2 and Figure 4.1.3 from Vos [1983])

deformation relationships. Ngo and Scordelis note that if the orientation of the bond-link springs follows that of the reinforcing bar, then the spring aligned parallel to the bar axis represents the relationship between local bond stress and the slip between the concrete and steel. Because the reinforcing steel also is presented as a plane stress element, the orthogonal spring represents the dowel action of reinforcing steel and thus is most important for the case of wide open cracks and significant movement across crack faces. As a simplification they propose a very stiff bond response perpendicular to the axis of the reinforcing steel. The bond force versus slip stiffness is computed from experimental data but is considered to be a problem parameter. The results of a number of analyses indicate that the global deformation of the beam member is proportional to the stiffness of the bond-link element but that the overall variation in deflection is minimal for a 40 percent change in bond stiffness.

The results of the Ngo and Scordelis study do not indicate that modeling imperfect bond between concrete and reinforcing steel has little effect on the predicted behavior of general reinforced concrete systems, only little effect on the predicted response of some systems. The limited effect of explicit bond-zone representation observed by Ngo and Scordelis likely follows from the fact that bond-slip response would not be expected to control the response of the flexural system considered in the study as well as the fact that the subtle effects of imperfect bond are made insignificant by the simplicity of the finite element model used in this investigation. The most significant contributions of the Ngo and study is the development of a simple method for inclusion of bond response in a global finite element model. Additionally, the investigation identifies some of the significant issues associated with representing imperfect bond in a finite element model of a reinforced concrete system, such as evaluation of the effect of bond response on system

response, dowel action as a component of bond response and meshing issues associated with discrete representation of reinforcing steel and bond elements.

Another early representation of bond is that proposed by Nilson [1968]. Here the global model represents a reinforcing bar embedded eccentrically in a concrete prism and subjected to monotonically increasing tensile loading. The finite element model incorporates an elastic steel material model (steel stresses remain within the elastic range) and a hyperelastic, non-linear concrete material model. Additionally, once concrete principal tensile stress exceeds tensile strength, the model is remeshed to introduce an crack into the concrete matrix. The bond-link element has zero length, includes independent force-deformation characteristics in the directions parallel and perpendicular to the axis of the reinforcing bar, and is characterized by a non-linear hyperelastic bond stress versus slip relationship. Additionally, in this investigation, the influence of concrete damage and stress state is incorporated into the bond model by defining bond-link elements in the vicinity of a concrete crack to have a reduced post-peak bond strength in comparison with bond-link elements at a distance from a crack.

Nilson concludes that representation of imperfect bond in part determines the behavior of reinforced concrete systems. This conclusion is not surprising given that Nilson's investigation considers behavior of a bond zone that necessarily will be dominated by concrete-to-steel bond response and that imposed rapid deterioration of bond within the vicinity of a crack provides for large deformation associated with slip. Nilson's identification of the need to define local bond response on the basis of concrete damage is significant because the results of the study show that the assumption of diminished bond strength within the vicinity of a concrete crack leads to development of representative local bond-stress versus slip histories along the length of the reinforcing bar. Additionally, while not incorporating these characteristics into the proposed model, Nilson suggests that an appro-

priate bond model includes bond response associated with the wedging action of reinforcement lugs bearing on surrounding concrete.

4.3.2 Development of Bond Models for Reversed-Cyclic Load Histories

Initial models representing bond-slip response were limited by the available experimental data. Increased interest in earthquake engineering following the 1970 San Fernando Earthquake, lead to experimental investigation of cyclic bond response and experimental data for development and calibration of models to characterize this response. With methods for representing imperfect bond in a global finite element model of a reinforced concrete continuum established, researcher efforts focussed on characterization of the one-dimensional bond stress versus slip response for reinforcement subjected to reversed-cyclic load histories. Typical bond-slip models from this period include those proposed by Morita and Kaku [1973], Shipman and Gerstle [1979] (developed on the basis of experimental data from Singh *et al.* [1964] and Morita and Kaku [1973]), Tassios and Yannopoulos [1981] (developed on the basis of analytical data) and Fehling [1990]. Because the individual models were developed mainly on the basis of unique data sets, the models show some variation in strength and stiffness, though fundamental characteristics of the response are similar. Figure 4.34 shows a schematic of a cyclic bond stress versus slip model including the monotonic envelope and unload-reload curves. This model characterizes the experimentally observed stiff initial unloading curve and the minimal frictional bond resistance achieved upon further slip the unload direction. Individual models vary in the characterization of reload stiffness. The model proposed by Morita and Kaku also accounts for variation in bond capacity under multiple cycles of loading. It is important to note that most of these early cyclic models were developed on the basis of experimental investigation of bond-zone systems subjected to limited slip demand; thus, many of these models define the bond response to be hardening in nature. As a result, these

models are appropriate for analysis of systems subjected only to moderate bond demand. While the authors do not account for deterioration in bond capacity as a result of severe slip demand, they do account for reduced capacity resulting from limited concrete cover (Morita and Kaku) and proximity to concrete cracks (Shipman and Gerstle, and Tassios and Yannopoulos). These cyclic bond models all achieve success in reproducing experimental bond stress versus slip history and vary in levels of success in predicting system response.

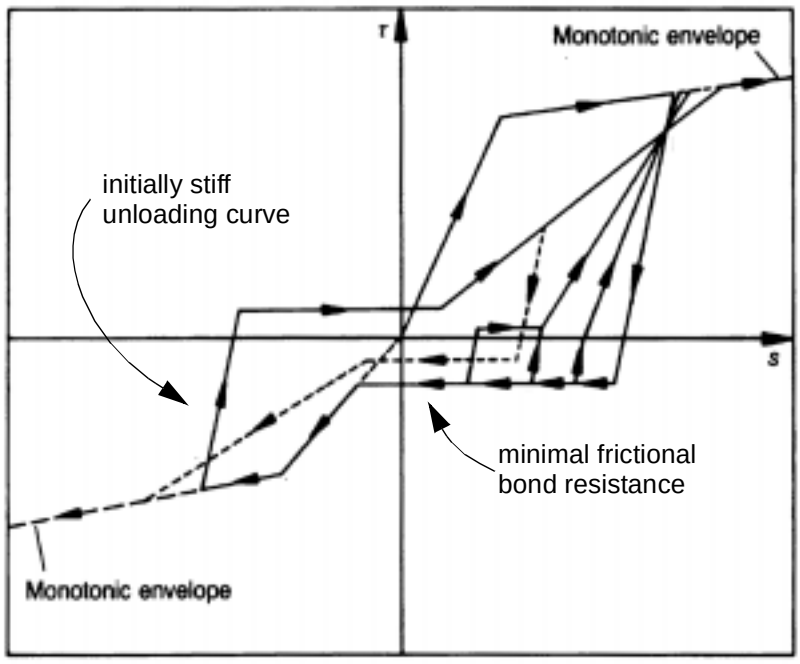

Figure 4.34: Bond Stress versus Slip Response History as Proposed by Morita and Kaku (Figure 77 from CEB, 1996)

Continued experimental investigation of the bond phenomenon [Viwathanatepa, 1979a, 1979c; Cowell, 1982; Hawkins, 1982; Eligehausen *et al*., 1983; Tassios, 1983] supported further refinement on cyclic bond models. A number of similar bond stress versus slip response models were developed on the basis of these data including those proposed by Stanton [1979], Viwathanatepa [1979a, 1797c], Ciampi *et al.* [1982]; Hawkins *et al.*, [1982], Eligehausen *et al.* [1983] and Filippou [1983, 1986]. Figure 4.35 shows the model

proposed by Eligehausen *et al.* that is probably the most general and most explicitly defined of this generation of bond models. These models represent a significant contribution to modeling of bond response because they provide a comprehensive explicit characterization of the bond response. All of these models predict the deterioration of bond capacity under extreme slip demand. Additionally, these models account for deterioration in bond capacity under variable cyclic load histories. In particular the model proposed by Eligehausen *et al.* defines the bond capacity under a variable cyclic slip history as a function of the energy dissipation. Several of these models explicitly account for the influence of the concrete stress and damage state in the vicinity of the reinforcing bar, defining the bond capacity on the basis of concrete confinement, volume of transverse reinforcement and confining pressure perpendicular to the bar. Also, several of these models define the influence on bond response of other system parameters such as concrete compressive strength, bar size, bar deformation pattern, bar spacing, bar stress and bar stress state. These models are verified through comparison of computed and observed behavior for local bond tests (Lin, Hawkins, Eligehausen); distributed bond tests (Viwathanatepa and Ciampi) and reinforced concrete structural elements (Stanton and Filippou).

4.3.3 Multi-Dimensional Bond Response

Multi-dimensional representation of the bond zone provides a framework for integrated characterization of the dependence of the axial and radial bond response. However, this complete representation inevitably leads to the development of highly sophisticated models that are neither easily calibrated nor easily extended to include representation of response under cyclic loading. Typical characterization of multi-dimensional bond zone response follows from the development of a simplified mechanism to represent the response of the concrete volume surrounding a segment of reinforce steel. Such a mecha-

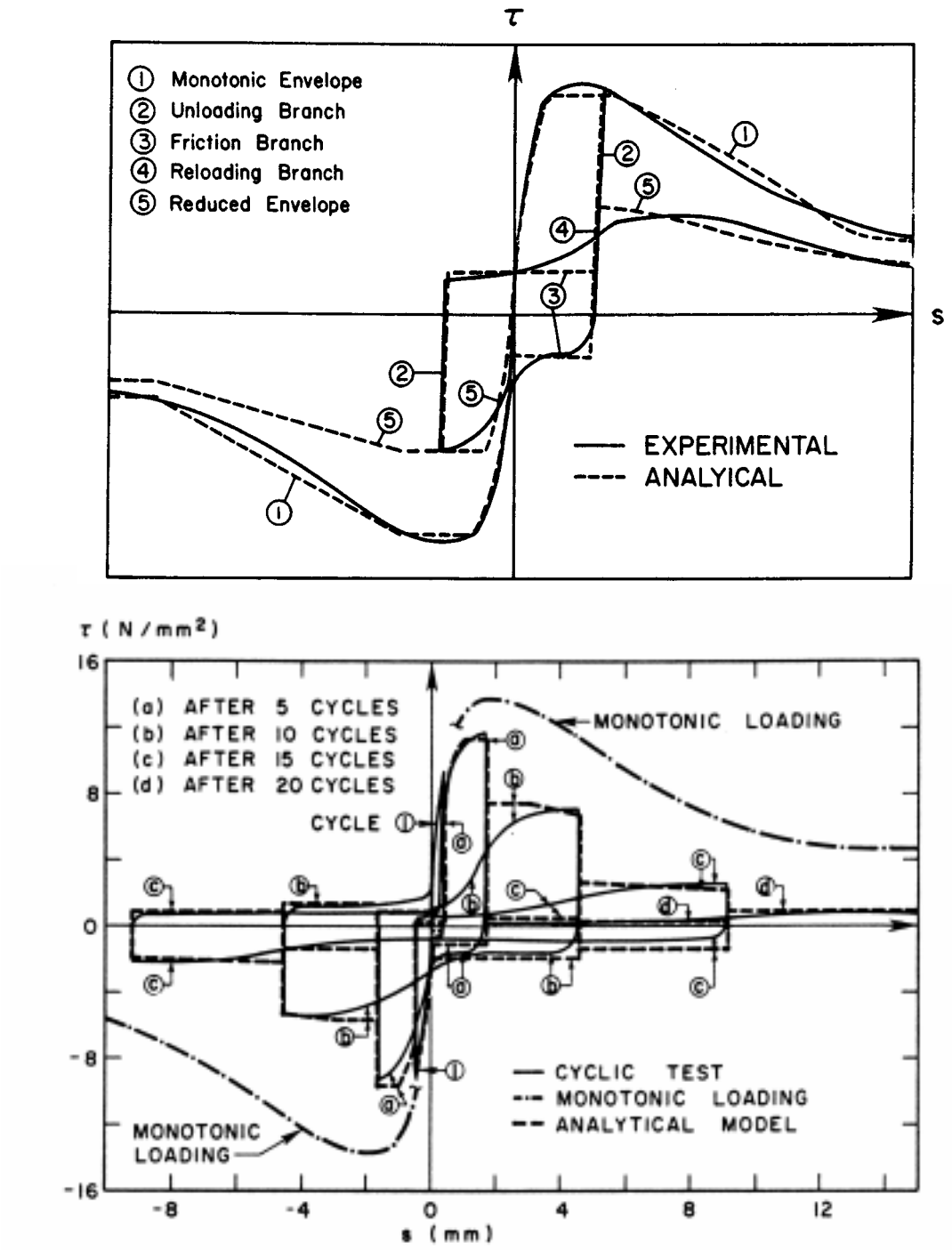

Figure 4.35: Analytical Model for Prediction of Local Bond Stress versus Slip Response (Figures 5.3 and 5.13 from Eligehausen *et al.* [1983])

nisms provides the simplification necessary to support quantitative characterization of the load-deformation response of the bond zone.

4.3.3.1 Concentric Cone Representation of the Bond Zone

Following from the crack patterns observed in the vicinity of an anchored reinforcing bar, de Groot *et al.* [1981] idealize the bond zone as a series of concentric, hollow, frictionless cones centered on the reinforced bar. From the assumption of no interaction between these cones it follows that the cones can carry only axial tension and compression. The angle that these cones form with the surface of the reinforcing bar is defined as a model parameter. To ensure that bond slip results in radial expansion, the orientation of these cones shifts upon load reversal. To complete the representation, a material model representing the steel response as well as an independent friction component of bond response are incorporated into the model. Bond-zone concrete and steel material response are idealized as bilinear, hyperelastic. Concrete *yield strength* is computed on the basis of Mohr-Coulomb yield criteria with tension cut-offs. The material model is implemented within the framework of the finite element method as a 15-node, 45-dof element to achieve compatibility with a 24-node concrete brick element. Some slaving of nodal displacements is introduced to achieve linear representation of slip.

The de Groot *et al.* [1981] investigation provides one of the first finite element models to predict the multi-dimensional characteristics of bond produced by mechanical interaction at the concrete-steel interface. Additionally, the idealization of the bond zone proposed by de Groot *et al.* provides a flexible framework for introducing oriented coupling between axial and radial modes of bond response. Further, because experimental data defining multi-dimensional bond zone response to cyclic loading are limited, this idealization provides a basis for developing a general model in the absence of extensive data. Though the issue is not addressed by the investigators, the proposed model also introduces one of the fundamental problems associated with multi-dimensional bond zone representation, that of unsymmertic coupling between radial and axial bond response. The pro-

posed model has a symmetric tangent matrix; this is numerically pleasing, but implies that while slip produces radial expansion, radial expansion/contraction also produces slip. The proposed model appears to readily support modification to improve the bond zone representation. For example, the symmetric coupling of radial and axial bond response can be eliminated from the model by limiting admissible deformation modes for the concentric cones. Additional improvement in bond response representation likely can be achieved through extension of the model to include more sophisticated material models that more accurately represent the inelastic behavior of steel and bond-zone concrete under cyclic loading.

4.3.3.2 Thick-Walled Cylinder Representation of the Bond Zone

A somewhat similar bond response mechanism is extended to a multi-dimension bond zone representation by den Uijl and Bigaj [1996]. This mechanism follows from the idealization of bond zone behavior introduced by Tepfers [1979] in which the bond zone is represented as a solid steel cylinder surrounded by a thick walled concrete cylinder. Axial load applied to the steel is transferred to the concrete as shear accompanied by radial compression. Radial stresses produces tensile hoop stresses in the concrete and radial cracking of the concrete. den Uijl and Bigaj extend the representation of Tepfers by characterizing the material response of the steel and cracked and uncracked concrete and by introducing a variable angle of orientation between radial deformation and slip at the concrete-steel interface.

The den Uijl and Bigaj model represents uncracked concrete as an elastic material with elastic modulus and tensile strength defined by experimental testing. As suggested in the discussion of Tepfers bond study, cracked concrete is represented as a cohesive material, rather than assuming no capacity for stress transfer across a crack surface. The cracked concrete behavior is defined on the basis of the fictitious crack model proposed by

Hillerborg [1983] and the bilinear softening model proposed by Roelfstra and Whittmann [1986]. The concrete stress-deformation path is calibrated on the basis of the concrete fracture energy and an model-dependent characteristic length. Definition of an appropriate characteristic length relating the volume of damaged concrete to the crack area requires an assumption as to the number of radial cracks that develop in the vicinity of the concrete-steel interface. den Uijl and Bigaj consider this to be a model parameter.

Den Uijl and Bigaj extend the model of Tepfers further by redefining the stages of bond response proposed by Tepfers. Here den Uijl and Bigaj note that partial cracking of the concrete cylinder is representative of a pull-out type bond failure while complete cracking of the bond zone is representative of a splitting-type bond failure. Thus, the type of bond failure is determined by the available concrete cover, and den Uijl and Bigaj identify concrete cover values on the basis of system geometry.

Model development is completed by definition of the angle of orientation between radial deformation and slip at the concrete-steel interface. The ratio of bond stress to radial stress is defined to be unitary and constant. Den Uijl and Bigaj propose that for the case of a splitting-type bond failure, the angle between radial deformation and slip also remains essentially constant with increasing slip. However, for a pull-out failure, additional slip is achieved through development of a slip plane in the vicinity of the concrete-steel interface. Den Uijl and Bigaj propose that the development of this plane and the progressive slip of the bar past the surrounding concrete implies a variation in the angle between radial deformation and slip and a resulting reduction in radial expansion. Also for the case of pull-out bond failure, the authors propose an idealization for use in computing the reduction in radial expansion associated with the Poisson effect. This reduction in the ratio of radial expansion to slip allows for development of significant slip without the significant

increase in radial expansion that would trigger increased radial hoop stress, propagation of concrete cracks to the surface of the concrete cylinder and a delayed splitting-type failure.

The proposed bond response model is verified through comparison with experimental data. While the model represents well the bond response as observed in the test cases, these cases are limited to monotonic loading. Extension of the model to the case of cyclic loading is not trivial. For the case of a pull-out bond failure, model development requires characterization of the relationship between slip and radial deformation on the basis of experimental data. The non-linear relationship between radial deformation and bond stress, defined by the Tepfers' model, adds additional complexity to this calibration process.

A final assessment of the model proposed by den Uijl and Bigaj leads to an additional observation. The proposed model follows from the assumption that for the case of a pull-out failure, radial expansion begins to diminish at slip values less than that corresponding to peak bond strength. Experimental data presented both by Malvar [1992] and Gambarova [1989a, 1989b] indicate that radial expansion increases with slip up to slip levels well in excess of those corresponding to peak bond strength.

4.3.3.3 Characterization of the Bond Zone Continuum

Cox [1994] introduces a two-dimensional axisymmetric monotonic bond model that is defined on the basis of plasticity theory. Definition of a model on the basis of plasticity theory requires identification of a yield surface, the hardening/softening functions that define the evolution of the yield surface, a flow rule that determines the orientation of plastic deformation and a set of internal variables. The author proposes a single internal variable, d, that defines the internal state of the material. This variable is representative of plastic slip and may be associated with total slip in excess of the rib spacing on a reinforcing bar. The author proposes a yield surface that defines bond strength as a function of

confining pressure perpendicular to the axis of the reinforcing bar and the plastic slip. This surface evolves from a power-type criterion, characterized by increasing bond strength, at small plastic slip levels to an exponential criterion, characterized by exponentially decaying bond strength, at larger slip levels. Definition of the bond model is completed by representation of a flow rule. Here a non-associated plastic flow model is required to represent the observed dilatent behavior of the bond zone. The model is calibrated on the basis of experimental data and validated through comparison with additional experimental data. Data from tests conducted by Malvar [1992], Gambarova *et al.* [1989a], Eligehausen *et al.* [1983], Rehm and Eligehausen [1979], Shima *et al.* [1987a] and Tepfers and Olsson [1992] are considered.

The model represents well, within the range of experimental scatter, the above experimental data for systems subjected to monotonic response. Also, the representation of the bond zone continuum provides an ideal coupling of axial and radial response. Calibration of the model on the basis of experimental bond-response data provides for development of the global bond zone model. This eliminates the need to make approximations about the orientation of radial and axial stresses and deformations in the vicinity of the concrete-steel interface. However, it should be noted that the calibration process requires implicit definition of the volume of the bond zone, since the model represents the average response of the volume as defined by the experimental data.

Cox suggests that future research will focus on extension of the model for the case of reversed cyclic loading. Given the complexity of the yield criterion and flow rule calibrated to fit data for monotonic bond response, extension of the model for representation of cyclic bond response will be difficult. Because the original development process does not include identification of a simplified response mechanism, there is no simplified foundation from which to extend flow rules and yield surfaces that are appropriate for the case

of cyclic loading. Extension of this model for representation of cyclic loading likely will require introduction of at least one and likely two additional internal variables to characterize the material state. In particular characterization of the highly pinched bond stress versus slip relationship likely will require multiple internal variable to define plastic slip in each direction as well as accumulated damage due to multiple cycles of loading.

4.3.3.4 Comments on Multi-Dimensional Bond Models

The multi-dimensional bond models discussed here provide conceptual models for coupling of radial and axial bond response. For the de Groot and the den Uijl models that develop from a simplified idealization of the bond zone, quantitative characterization of the idealized representation is straightforward but provides a somewhat limited characterization of the fundamental modes of bond response. Extension of the simplified idealization to provide a complete representation of experimentally-observed bond response complicates the model so much that the original simplified idealization is lost. This fact enhances the desirability of the Cox model that, while equally complex, provides an initial framework that may be used for complete characterization of bond-zone response. Thus, it follows that development of a model to represent cyclic bond response in not a trivial exercise and that there is no one obviously superior framework from which to begin model development. Additionally, evaluation of multi-dimensional models reinforces the fact that there are no data characterizing multi-dimensional bond response under cyclic loading, and that model development requires assuming particular characteristics of the bond response.

4.4 Characterization of Bond Response in the Vicinity of Reinforced Concrete Bridge Beam-Column Joints

Experimental investigation of idealized bond-zone sub-assemblages from reinforced concrete bridges and buildings provides data for identification of material, geometric and load-history parameters that determine bond response. Previously proposed mechanisms of bond-zone response define the fundamental characteristics to be represented in the model. Previously proposed bond zone models provide a framework for model development that facilitates incremental enhancement of the model as well as facilitating implementation within a global finite element model.

4.4.1 Definition of an Appropriate Bond Zone for Analysis of Reinforced Concrete Beam-Column Sub-Assemblages

The bond zone defines the region of material in the vicinity of the anchored reinforcing bar that exhibits localized bond damage and controls bond behavior. Previously proposed bond models have defined this region to have essentially zero volume (e.g., Ngo and Scordelis [1967]), to qualitatively include a volume of concrete and steel in the vicinity of the reinforcing bar (e.g., Viwathanatepa [1979a, 1979b], Filippou [1983]), to explicitly include a volume of concrete in the vicinity of the reinforcing bar (e.g., Cox [1994] and den Uijl and Bigaj [1996]) and to include both concrete and steel in the vicinity of an anchored bar (e.g. de Groot [1981]). The stress and damage state of the concrete-steel composite in the vicinity of the reinforcing bar have a significant effect on the bond response. In a reinforced concrete bridge system subjected to earthquake excitation, these material states show wide spacial and temporal variation. Thus, for this investigation, the bond zone is defined to include the volume of reinforcing steel of interest and a limited volume of concrete in the vicinity of this reinforcing bar. However, since the responses of reinforcing steel and plain concrete as functions of strain demand are defined well by the

previously presented material models (Chapter 2 and Chapter 3), representation of this material response within the bond element introduces unnecessary complexity and redundancy to the global model. For this investigation, the proposed bond model characterizes the response of a fictitious bond zone that is defined to have a finite length but zero radius and exists at the interface of the concrete and reinforcing steel. A non-local modeling technique is employed to incorporate the effect of the stress and damage state of the concrete and steel in the vicinity of this interface in the bond response model.

This definition of the bond zone limits the representation of the radial stress versus deformation relationship. The radial stress versus radial deformation response of the model may be considered to represent the adhesion between the concrete and steel at the concrete-steel interface as well as the response of the composite system loaded in compression perpendicular to the axis of the reinforcing bar. Previous research shows the adhesive strength at the concrete-steel interface to be minimal (maximum strength of 240 psi (1.6 MPa) [Hsu and Slate, 1963]). However, because of the two-dimensional implementation employed in this study, loading of the system in tension induces both tensile response from the continuous concrete zones as well as adhesion, thereby limiting the importance of the reduced adhesive strength. Assessment of the response of a reinforced concrete system loaded perpendicular to the axis of the reinforcement suggests that the system response likely will be controlled entirely by the response of the plain concrete. Thus, it is reasonable to define the bond zone to have a relatively stiff and elastic radial stress versus radial deformation response, and thereby force the response to be controlled by the behavior of the zones of plain concrete.

4.4.2 Mechanisms of Bond Zone Response

Evaluation of experimentally-observed bond response indicates several modes of behavior that must be represented by the proposed model. Gross characterization of these

mechanisms provides the framework for model development. Complete characterization and final calibration of these mechanisms completes model development.

Response mechanisms need only define bond stress and radial stress as a function of slip, since the fictitious bond-zone representation used here does not provide for definition of material deformation in the radial direction. Thus, the proposed bond model comprises three idealized mechanisms of response. These mechanism are designated as a mechanical interaction component, a residual bond component and a virgin friction component. These designations follow from bond studies by Lutz and Gergely [1967] and Yankelevsky *et al.* [1987]. The gross characteristics and the evaluation process followed in defining these mechanisms follows.

4.4.2.1 Mechanical Interaction

The mechanical interaction component of the model represents bearing of the lugs of the reinforcement on the surrounding concrete. Experimental investigation indicates that this mechanism of response contributes to the development of both axial and radial stress.

Consideration of bond-zone response for a system subjected to monotonically increasing slip demand provides insight into the contribution of mechanical interaction to total bond response. For an anchored reinforcing bar subjected to monotonically increasing slip demand, the zone of concrete in the vicinity of the lug exhibits the following progressive damage (Section 4.2.4 discusses in detail experimental observations of bond-zone response). Initially concrete directly in front of the lug is crushed, this is followed by the development of radial cracks that initiate near the top of the lug and propagate at an angle of approximately 60 degrees with respect to the axis of the reinforcing bar. Additional slip is achieved through opening and propagation of these cracks, crushing of concrete in front of the lugs and compaction of crushed concrete. As slip progresses, compacted crushed concrete forms a relatively flat wedge in front of the lug; typically the

effective lug face forms at an angle of approximately 30 degrees with respect to the axis of the reinforcing bar. Loss of mechanical bond capacity is observed when the damage to the concrete reduces the area of the concrete key (concrete that lies between the lugs on the reinforcing bar) to the point that the key shears off completely.

The identified progression of bond-zone response suggests that mechanical interaction contributes significantly to bond zone response. The progressive damage to the system represented by concrete crushing, crack initiation and propagation and shearing-off of concrete keys associated with this response mechanism suggests a bond-slip response history for mechanical interaction that is similar to the typically observed global bond-stress versus slip histories. In the proposed model, the mechanical bond-stress versus slip history follows a typical observed bond stress versus slip relationship.

Characterization of the contribution of mechanical interaction to bond response follows from consideration of bond-zone behavior under reversed cyclic loading. Upon unloading contact between the lug on the reinforcement (or the effective lug) and the surrounding concrete is lost. Thus no force is transferred through bearing. Increasing slip in the reversal direction eventually results in bearing of the opposite lug face on the surrounding concrete and response thereafter is essentially as seen for monotonic loading. When the system is reloaded in the original direction, friction of the lugs moving past the surround concrete initially provides the only resistance to bar slip. Eventually, the lugs on the reinforcing bar bear on the compacted, pulverized concrete, resulting in increased bond strength. The compacted, pulverized concrete may provide greater resistance than undamaged concrete. With increasing slip, the system response return to that observed under monotonic loading, though there may be some additional damage to the concrete keys as a result of previous load cycles in the opposite direction. Such bond-zone response suggests that upon unloading, bond resistance due to mechanical interaction diminishes

rapidly and remains minimal until reloading is achieved in the opposite direction. Upon reloading, bond resistance increases rapidly as the lugs bear against the much stiffer compacted, pulverized concrete. Cyclic loading may diminish bond stress resistance due to mechanical iteration.

The mechanical interaction component of the model contributes to development of the radial-stress versus slip response of the model. However, there are insufficient experimental data to fully support characterization of this response. The experimental study by Gambarova *et al.* [1989a, 1989b] suggests that radial stress peaks at slip levels slightly in excess of those corresponding to peak bond strength and that peak radial stress is slightly larger than that achieved at peak bond strength. The model proposed by den Uijl and Bigaj [1996] defines a constant one-to-one ratio between radial stress and bond stress and a variable ratio of slip to radial deformation. The study by Malvar [1992] shows variation in radial deformation versus slip behavior with constant radial confinement and suggests increased radial stress once bond strength is achieved.

Here it is proposed that the radial stress versus slip response be defined entirely by the mechanical component of response. This component is idealized as the concentric frictionless cones proposed by de Groot (Section 4.3.3.1). However, here the cones are assumed to allow only for deformation in the axial direction. This idealization suggests that the ratio of radial stress to bond stress is constant for all levels of slip and that radial dilation peaks with bond strength. The orientation of these cones defines the angle between bond and radial stresses. Experimental data suggest representative angles vary from less than 45 to 60 degrees (Section 4.2.4.5). This value is considered to be a model parameter and that is considered in future model evaluation.

Figure 4.36 shows the idealized bond stress versus slip response history for the mechanical interaction component of the model. This response follows closely total bond

slip response observed in experimental studies. The response is characterized by reduced stiffness with increasing slip up to a maximum bond resistance that represents a significant portion of the total bond resistance. A plateau at the peak bond resistance approximates actual response histories in this range. Increasing slip demand results in reduced bond-stress resistance to a point of no resistance. Slip reversal is characterized by a rapid loss of bond stress. Resistance to slip in the opposite direction does not develop until slip in this direction exceeds previous slip levels in this direction. Once this is the case, bond resistance rapidly approaches a history that is approximately the monotonic response curve. However, slip history may diminish bond resistance upon unloading or reloading.

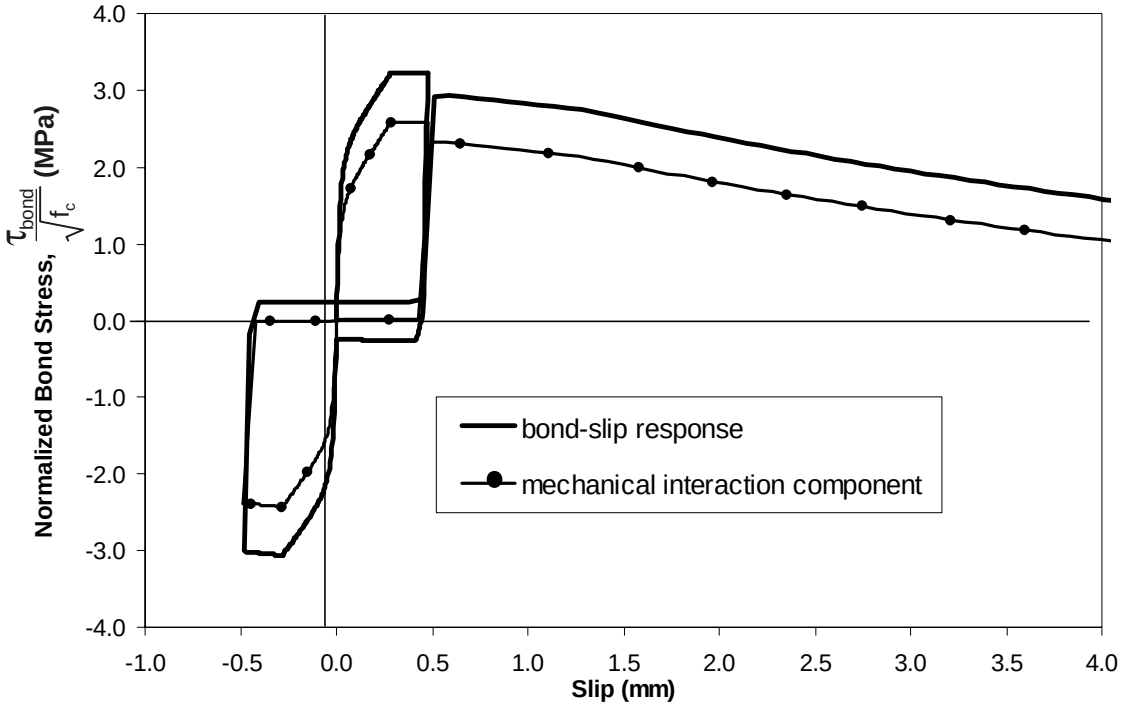

Figure 4.36: Contribution of Mechanical Interaction Component to Total Bond Stress versus Slip Response

4.4.2.2 Residual Friction

The residual friction component of the model characterizes the bond resistance developed through friction as the reinforcing bar slips through a zone of pre-damaged concrete. Following from the previous discussion of bond zone response under monotonic and

cyclic slip demand, residual friction represents the bond resistance that is developed upon slip reversal and that dominates the response until increased bond resistance attributed to reloading of the other components of response is observed. From this idealization of the mechanism, it follows that frictional resistance provides an approximately constant bond resistance to slip in either direction and that slip reversal is accompanied by almost immediate bond resistance in the reversal direction. Additionally, it follows that frictional bond resistance diminishes somewhat with cyclic loading as the slip plane in the vicinity of the reinforcing bar becomes smoother. Figure 4.37 shows an idealization of frictional bond resistance. Residual bond strength is calibrated on the basis of bond strength developed under load reversal.

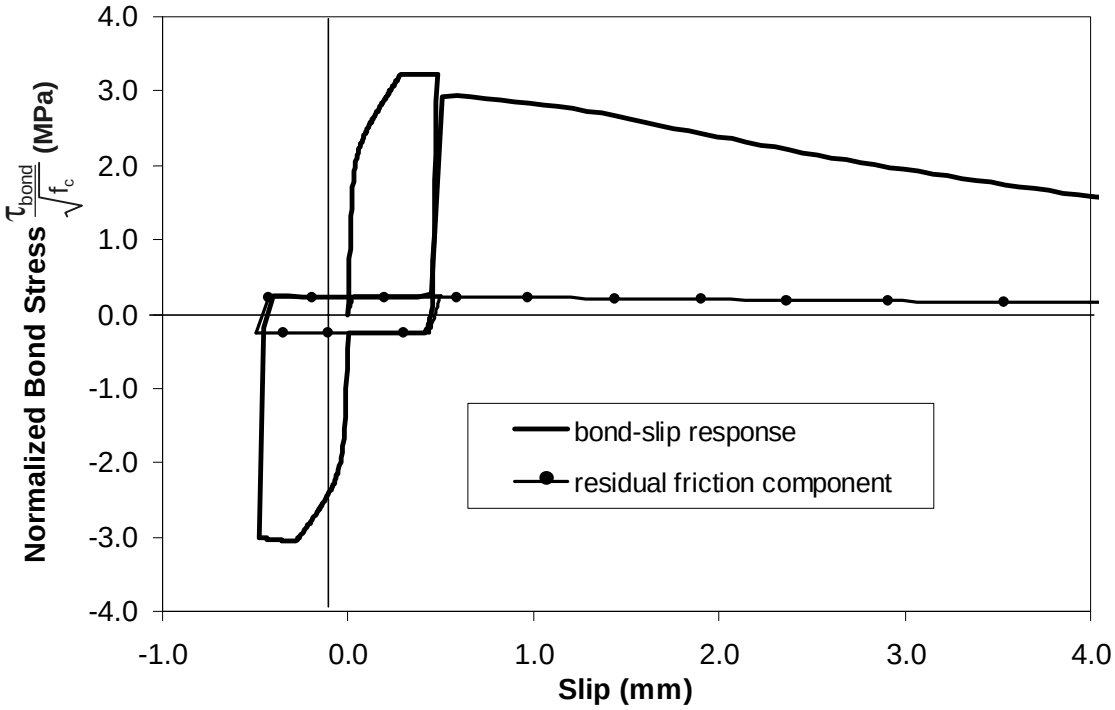

Figure 4.37: Contribution of Residual Friction Component to Total Bond Stress Versus Slip Response

4.4.2.3 Virgin Friction

The virgin friction component of response represents the additional frictional resistance developed as the reinforcing bar slips past previously undamaged concrete. Under cyclic loading, the virgin friction component of response is activated when the current slip approaches the maximum slip in either direction. This definition of the virgin friction component suggests that this mode of response is not affected by cyclic loading since this component of response is only developed during the first cycle of loading to any particular level of slip.

Figure 4.38 shows the contribution of the virgin friction component to the global bond-slip response. This contribution defines a rapid increase in bond resistance under initial slip. Slip reversal is followed by a rapid loss of bond resistance and no additional bond resistance until slip levels are such that the bar slides past undamaged concrete. Virgin friction is calibrated on the basis of bond strength at extreme slip levels for which only frictional components of bond response are active.

4.4.3 Characterization of the Monotonic and Cyclic Bond Response

Representation of monotonic and cyclic bond response requires explicit characterization of the previously identified mechanisms of response. This characterization includes definition of mechanism behavior as a function of system constants as well as definition of an algorithm to compute the response. Previous research indicates that bond response is a function also of system variables, such as the concrete stress state. However, this dependence is included through a non-local modeling technique rather than through explicit representation within the model. Thus, in developing an algorithm to represent bond mechanism response, it is necessary to consider that system variables external to the bond model may contribute to variation in bond strength during the solution process.

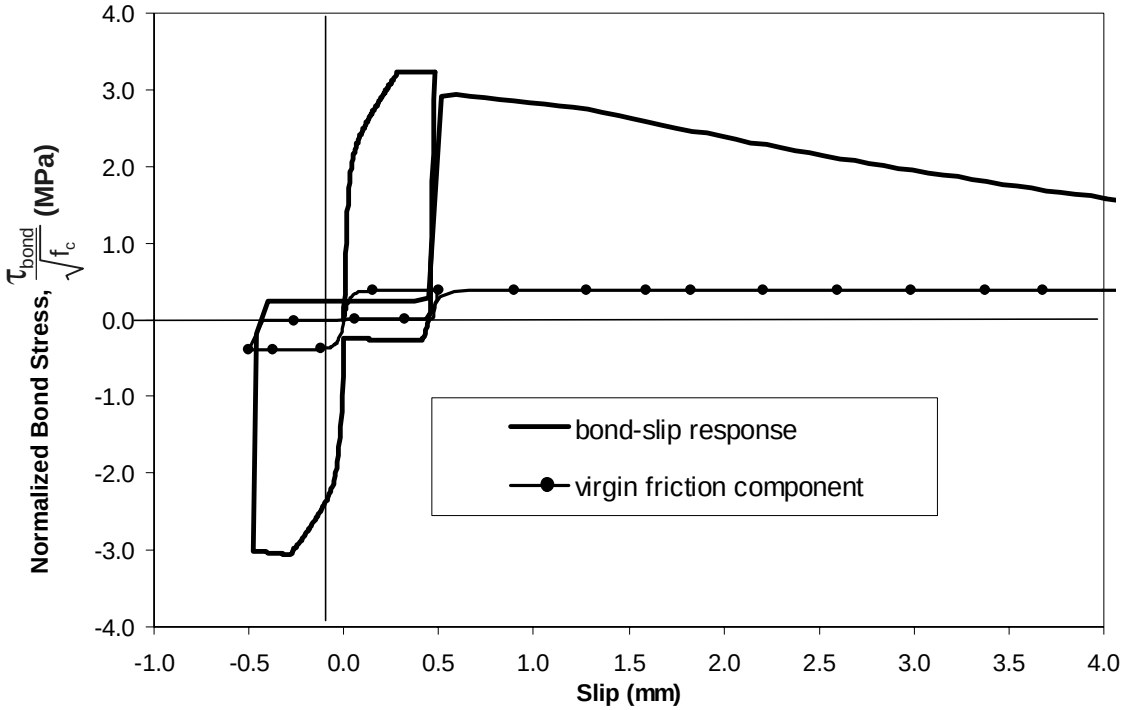

Figure 4.38: Contribution of Virgin Friction Component to Total Bond Stress Versus Slip Response

4.4.3.1 System Parameters that Determine Bond Response

Experimental investigation indicates that a number of system parameters determine bond response. For this investigation, only those parameters that define behavior of typical reinforced concrete beam-column bridge connections are included. Thus, bond response is defined to be a function only of concrete compressive strength and bar size.

Bond strength is determined by damage of concrete at the steel-concrete interface, thus bond strength may be defined to be a function of concrete strength. While localized crushing of the concrete contributes to the deformation, loss of bond strength typically results from the development and opening of localized cracks or from the shearing-off of concrete between the lugs on the reinforcement. Since bond failure is due to tensile cracking or shearing of the concrete, it is reasonable to defined bond strength to be proportional to concrete tensile strength or concrete shear strength. Since both of these quantities typically are approximated as being proportional to the square root of the concrete compres-

sive strength (See Section 2.2.3 on page 28), bond strength also may be defined by the square root of concrete compressive strength. Eligehausen *et al.* [1983] suggest the following relationship:

$$\tau_{bond} \propto (f_c)^{\beta} \qquad \frac{1}{3} \leq \beta < \frac{1}{2} \tag{4-5}$$

while others [Tepfers, 1979; ACI Committee 318, 1979] suggest simply $\beta = \frac{1}{2}$. Here bond strength is normalized with respect to the square root of the concrete compressive strength, $\left(\beta = \frac{1}{2}\right)$.

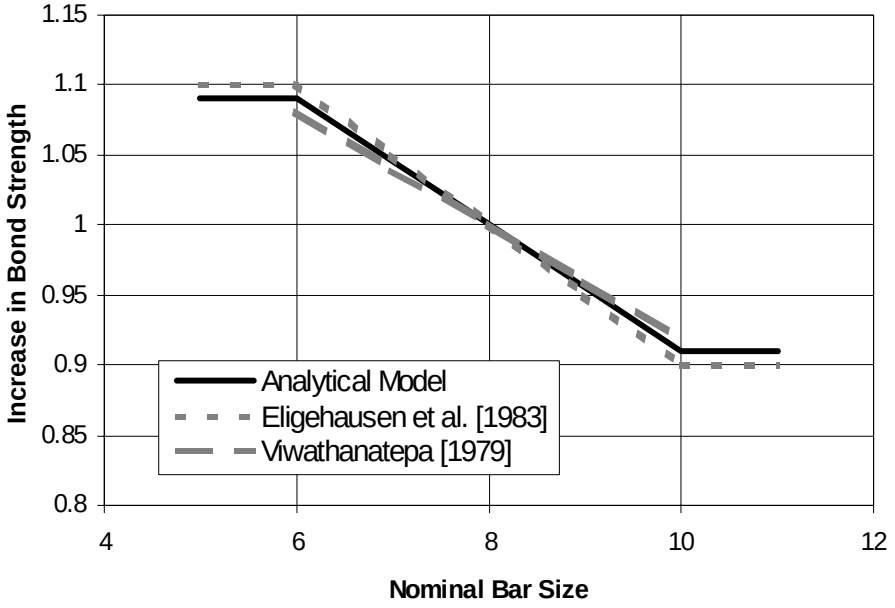

Figure 4.39: Influence of Bar Size on Maximum Bond Strength

Peak bond strength also is defined to be a function of bar diameter. While some suggest sophisticated methods for determining bond strength as a function of bar size [Bazant, and Sener, 1988]. The bar sizes of interest to any single analysis are typically limited to a relatively small range of diameters. Thus a linear approximation is reasonable over the given range of interest to this study. Further, the majority of experimental investigation have considered the response of bars ranging in size from No. 6 to No.10 (nominal bar

diameters of 0.75 in and 1.27 in. (19 mm and 32 mm)) which is the range of sizes of interest to this study. Figure 4.39 shows the relationship between bond strength and bar diameter used in this investigation as well as similar relationships proposed by others to define experimentally observed response. Extension of this model for analysis of significantly larger systems, such No. 11 to No. 18 reinforcement (bar diameters of 1.14 in. and 2.26 in.(36 mm and 57 mm)), likely warrants investigation of experimentally-observed bond strengths for bars of that size

4.4.3.2 Algorithms Defining Monotonic and Cyclic Bond Response

Multiple algorithms are developed to define bond stress as a function of an arbitrary slip history for each mechanism of response. The individual mechanisms are considered to act in parallel and total bond resistance for a given state is simply the sum of individual component resistances. Figures 4.40 and show the contribution by each of the three components to the total bond stress versus slip response.

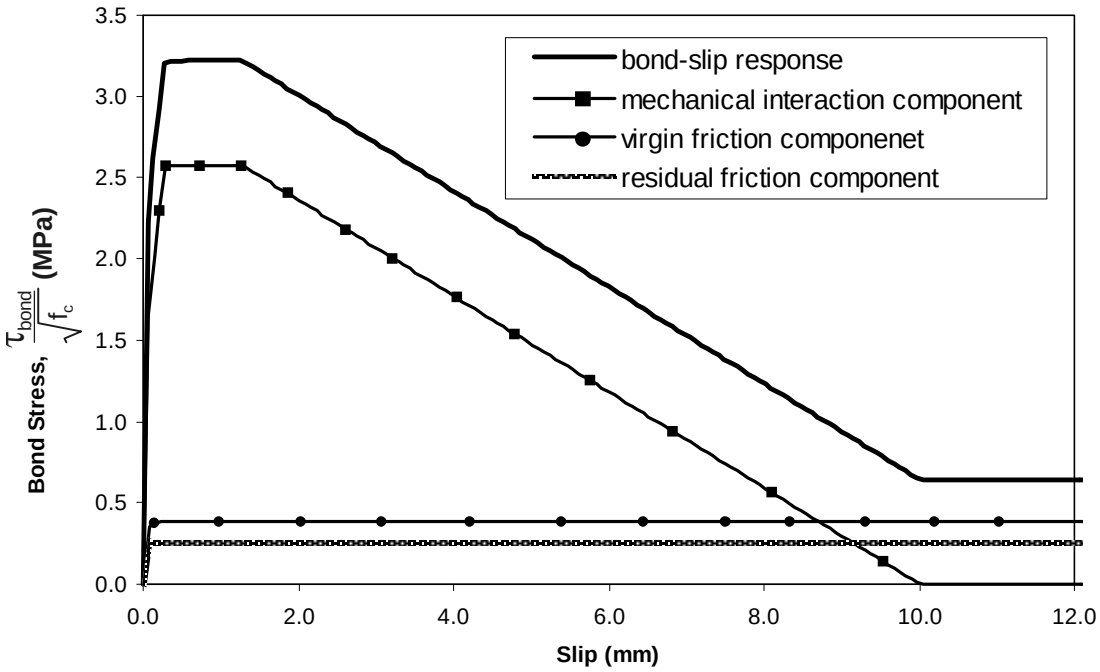

Figure 4.40: Computed Bond Stress versus Slip History and Component Contribution to Global Response for a Monotonic Slip History

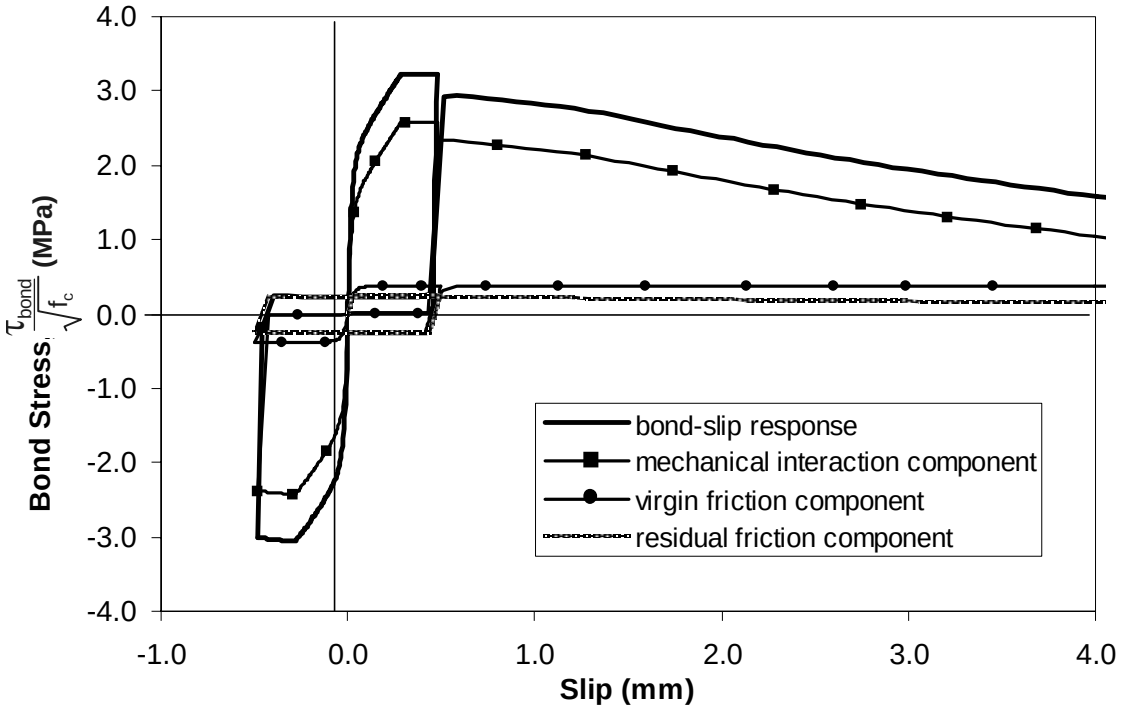

Figure 4.41: Computed Bond Stress versus Slip History and Component Contribution to Global Response for a Cyclic Slip History

The algorithms developed to define bond mechanism response assume a semi-implicit incremental solution algorithm is used to advanced the global solution from a known state of the system at time t^n to a solution at time t^{n+1} given a load increment applied in the interval $\Delta t = t^{n+1} - t^n$. A displacement-based method is used in which the displacement field in the body, while not necessarily the correct displacement field, is considered a known quantity. As was discussed previously in defining the concrete and steel constitutive models, an implicit global solution algorithm requires that given a known *bond-material state* at a previous time, typically at time t^n, and the deformation field at time t^{n+1}, the bond constitutive model define the *state* at time t^{n+1}. Because bond response is defined as a function of the deformation field as well as of several system parameters, an appropriate set of internal variables that contribute to a unique characterization of the *material state* at time t^{n+1} includes response parameters that characterize the material state

at time t^n as well as at the time of the previous slip reversal. It is important to note that these internal variables, the deformation field at time t^{n+1} and appropriate system variables uniquely define the bond material state at time t^{n+1}.

In addition to defining the material state at time t^{n+1}, the global solution algorithm also requires calculation of a material tangent that defines the change in material stress as a function of a change in the material deformation field. Because the bond response is a function of system parameters other than the deformation field, this derivative does not represent a consistent tangent for the element.

Internal variables that contribute to a unique definition of the bond material state follow:

$slip^{n+1}$ = slip at time t^{n+1} (4-6a)

$slip^{n}$ = slip at time t^{n} (4-6b)

$\Delta slip^{n} = slip^{n} - slip^{n-1}$ (4-6c)

$slip_{max}$ = maximum slip (4-6d)

$slip_{min}$ = minimum slip (4-6e)

$slip^{rev}$ = slip at last slip reversal (4-6f)

f_m^{rev} = stress due to mechanical interaction at last slip reversal (4-6g)

f_r^{rev} = stress due to residual friction at last slip reversal (4-6h)

f_v^{rev} = stress due to virgin friction at last slip reversal (4-6i)

n_{cycles} = number of load cycles (4-6j)

Bond response is defined to be a function of the slip history, concrete compressive strength, bar size and appropriate system variables. These system variables include the average concrete pressure in the direction perpendicular to the axis of the reinforcing bar, *p*; the average deterioration of concrete tensile strength that follows from accumulated concrete damage, *d*; and the steel strain state defined by the ratio of the actual steel strain

to the yield strain, *s*. To accommodate variation in bond strength as a function of system parameters external to the bond model, each algorithm defines bond response as a function of peak bond strength.

Bond response is defined in terms of a series of bond response parameters. Some of these parameters are constants that are defined on the basis of experimental observation. Others are defined in terms of the peak bond strength, where peak bond strength is a function of the material state (defined by *p*, *d* and *s*). Bond response parameters are as follows (Figure 4.42):

τ_1, peak mechanical bond strength: $\tau_1 = \tau_1(p = 0, d = 0, s = 0) \cdot \Gamma(p, d, s)$ (4-7a)

τ_3, peak frictional bond strength: $\tau_3 = \tau_3(p = 0, d = 0, s = 0) \cdot \Gamma(p, d, s)$ (4-7b)

τ_v, peak virgin friction bond strength: $\tau_v = \tau_3 \cdot (1 - 0.4)$ (4-7c)

τ_r, peak residual friction bond strength: $\tau_r = \tau_3 \cdot (0.4)$ (4-7d)

k_{secant}, secant to bond response curve between zero slip and peak bond strength and defined on the basis of data presented by Eligehausen: $k_{secant} = 20 \text{MPa/mm}$ (4-7e)

s_1, slip at which peak bond strength is achieved: $s_1 = \dfrac{\tau_1}{k_{secant}}$ (4-7f)

s_2, slip at which bond strength begins to deteriorate: $s_2 = s_1 + 1.0 \text{ mm}$ (4-7g)

s_3, slip at which only mechanical bond resistance is lost: $s_3 = 10.0 \text{ mm}$ (4-7h)

k_1, initial tangent to the bond stress versus slip response curve: (4-7i)

k_2, tangent to the bond stress versus slip response curve at peak bond strength: (4-7j)

k_{unload}, tangent to the bond response curve upon unloading and defined on the basis of data presented by Eligehausen: $k_{unload} = 180 \text{ MPa/mm}$ (4-7k)

$k_{0,}$ small, non-zero tangent to a response curve: $k_0 = 10^{-6} \text{ MPa/mm}$: (4-7l)

k_{1m}, initial tangent (mechanical interaction): $k_{1m} = \left(\dfrac{\tau_1}{\tau_1 + \tau_3}\right) k_{unload}$ (4-7m)

k_{1v}, initial tangent (virgin friction): $k_{1v} = \left(\dfrac{\tau_3}{\tau_1 + \tau_3}\right)(1 - 0.4) k_{unload}$ (4-7n)

k_{1r}, initial tangent (residual friction): $k_{1r} = \left(\frac{\tau_3}{\tau_1 + \tau_3}\right)(0.4)k_{unload}$ (4-7o)

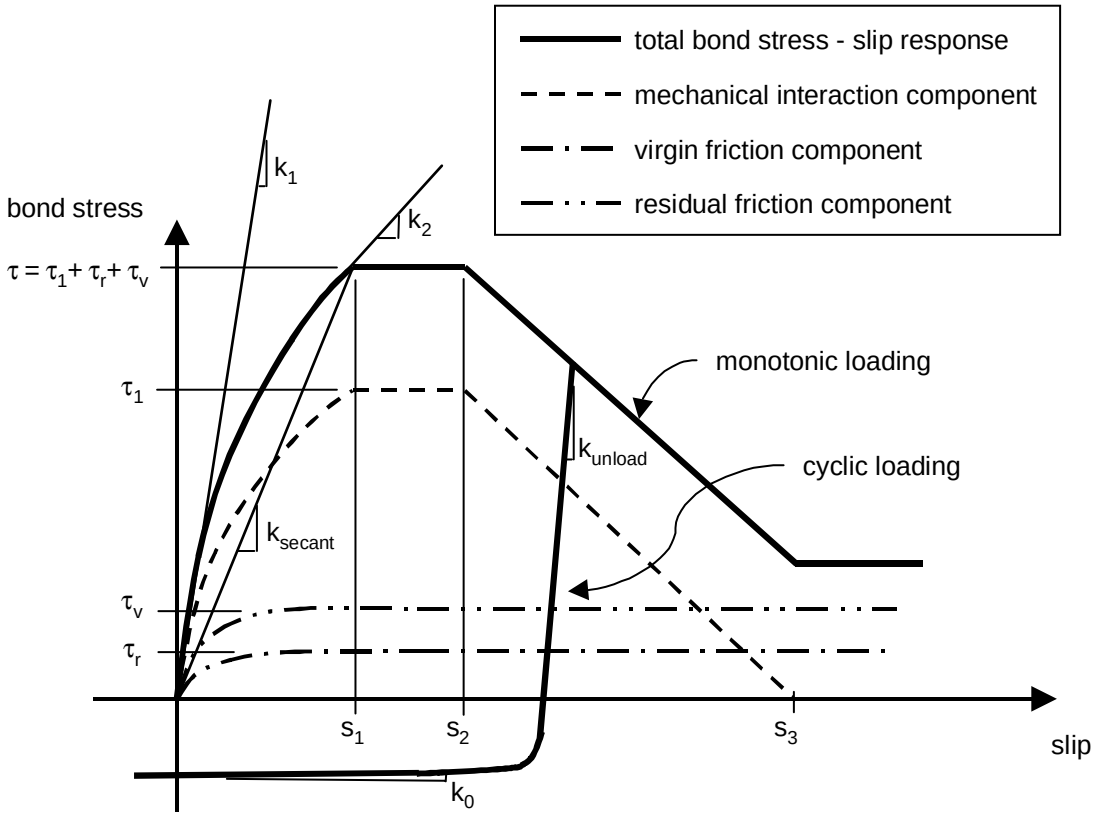

Figure 4.42: Definition of Model Parameters

Note that $\Gamma(p, d, s)$ (Equations 4-7a and 4-7b) defines the effect on bond strength of variation in the composite material state. Note also that value of peak bond strength is calibrated to fit experimental data provided by Eligehausen *et al.* [1983] and Malvar [1992] for the case of a neutral composite material state, defined as $\Gamma(p = 0, d = 0, s = 0) = 1$. While bond strength attributed to frictional mechanisms is calibrated to fit experimental data provided by Eligehausen and Malvar for the case of minimal concrete confinement, defined by $\Gamma(p = 0, d = 0, s = 0) > 1$.

Algorithms for computing the contribution to bond resistance developed by each of the mechanisms follows. These algorithms define the response envelope as a function of

an arbitrary slip history. This envelope is modified through variation in peak bond strength to account for changes in the system parameters and for the actual slip history.

Algorithm 4.1:

mechanical_interaction $\left(\begin{matrix} slip^{n+1}, slip^{n}, \Delta slip, slip_{max}, slip_{min}, slip^{rev} \\ f_m^{rev}, f_v^{rev}, f_r^{rev}, n_{cycles} \end{matrix}, \ldots \right)$

$D = damage(slip^{n}, slip_{max}, slip_{min}, n_{cycles})$

if $(\Delta slip^{n+1} > 0)$ *then*

if $(slip^{n+1} < slip_{max})$ *then*

call ***load_mechanical*** $(slip_{max}, D, f_{mmax}, k_{mmax})$

if $(f_m^{rev} \leq f_{mmax})$ *then*

$dir = 1$

call ***reload_mechanical*** $(slip, slip^{rev}, f_m^{rev}, slip_{max}, f_{mmax}, f_m, k_m)$

else

State at time t^n had smaller slip and higher bond strength due to external system variables, so system is unloading from higher strength state, assume that current state is defined by loading response.

call ***load_mechanical*** $call$ load_mechanical $(slip, D, f_m, k_m)$

end

else

call ***load_mechanical*** $call$ load_mechanical $(slip, D, f_m, k_m)$

end

else

if $(slip^{n+1} > slip_{max})$ *then*

call ***load_mechanical*** $(slip_{min}, D, f_{mmin}, k_{mmin})$

if $(f_m^{rev} \geq f_{mmin})$ *then*

$dir = -1$

call ***reload_mechanical*** $(slip, slip_{min}, f_{mmin}, slip^{rev}, f_m^{rev}, f_m, k_m)$

else

call ***load_mechanical*** $(slip, D, f_m, k_m)$

end

else

call ***load_mechanical*** $(slip, D, f_m, k_m)$

end

end

Algorithm 4.2:

load_mechanical $(slip, D, f_m, k_m)$

This subrountine defines the monotonic bond stress-slip envelope with peak bond strength defined by the damage parameter D *and system parameters* p, d *and* s (Equation 4.5). *The initial portion of this envelope is defined by Menegotto-Pinto curves and final portions are linear.*

$sign = \dfrac{slip}{|slip|}$

$slip = |slip|$

if $(slip < s_1)$ *then*

call ***menegotto pinto curve*** $(0, 0, k_{1m}, s_1, \tau_1, k_2)$

else if $(slip < s_2)$ *then*

$f_m = \tau_1$

$k_m = 0$

else if $(slip < s_3)$ *then*

$f_m = \tau_1\left(1 - \dfrac{slip - s_2}{s_3 - s_2}\right)$

$k_m = -\dfrac{\tau_1}{s_3 - s_2}$

else

$f_m = 0$

$k_m = 0$

end

$slip = sign(slip)$

$f_m = sign(f_m)$

Algorithm 4.3:

reload_mechanical $(slip, slip_{min}, f_{mmin}, slip_{max}, f_{mmax}, f_m, k_m)$

This subroutine defines the unload-reload path from the bond stress-slip point at which load reversal occurred to the bond stress-slip point associated with maximum absolute slip in the unload direction. This 'curve' is defined to be tri-linear with a stiff unload path to zero bond resistance and a stiff reload path to the point of maximum absolute slip in the unload direction.

$s_0 = \dfrac{(f_{mmin} - k_{unload} slip_{min})}{k_0 - k_{unload}}$

$s_1 = \dfrac{(f_{mmax} - k_{unload} slip_{max})}{k_0 - k_{unload}}$

if $(slip < s_0)$ *then*

$f_m = f_{mmin} + k_{unload}(slip - s_{min})$

$k_m = k_{unload}$

else if $(slip < s_1)$ *then*

$f_m = k_0 slip$

$k_m = k_0$

else

$f_m = f_{mmax} + k_{unload}(slip - s_{max})$

$k_m = k_{unload}$

end

Algorithm 4.4:

residual friction $\left(\begin{matrix} slip^{n+1}, slip^n, \Delta slip, slip_{max}, slip_{min}, slip^{rev} \\ f_m^{rev}, f_v^{rev}, f_r^{rev}, n_{cycles} \end{matrix}, \ldots \right)$

if $(\Delta slip \geq 0)$ *then*

$ss_2 = max(s_{max}, s_1)$

call ***menegotto pinto curve*** $(slip^{rev}, f_r^{rev}, k_{1r}, ss_2, \tau_3 + k_0 ss_2, k_0, s, f_r, k_r, 20)$

else

$ss_2 = min(s_{min}, -s_1)$

call ***menegotto pinto curve*** $(slip^{rev}, f_r^{rev}, k_{1r}, ss_2, k_0 ss_2 - \tau_3, k_0, s, f_r, k_r, 20)$

end

Algorithm 4.5:

virgin friction $\left(\begin{matrix} slip^{n+1}, slip^n, \Delta slip, slip_{max}, slip_{min}, slip^{rev} \\ f_m^{rev}, f_v^{rev}, f_r^{rev}, n_{cycles} \end{matrix}, \ldots \right)$

$\Delta slip_{max} = \tau_2 + k_{1v} \frac{k_0}{k_1} slip_{max}$

$\Delta slip_{min} = -\tau_2 + k_{1v} \frac{k_0}{k_1} slip_{min}$

$sslip_{max} = max(slip_{max} - \Delta slip_{max}, 0)$

$sslip_{min} = min(slip_{min} - \Delta slip_{min}, 0)$

if $(\Delta slip \geq 0)$ *then*

if $(slip \geq sslip_{max})$ *then*

if $(slip^{rev} \geq sslip_{max})$ *then*

if $(sslip_{max} = 0)$ *then*

call ***menegotto pinto curve*** $\begin{pmatrix} 0, 0, k_{1v}, s_1, \tau_2 + k_0 s_1, k_0, \dots \\ s, f_v, k_v, 20 \end{pmatrix}$

else

call ***menegotto pinto curve*** $\begin{pmatrix} sslip_{max}, k_{1v} sslip_{max}, k_{1v}, \dots \\ slip_{max}, \tau_2 + k_0 s_{max}, k_0, s, f_v, k_v, 20 \end{pmatrix}$

end

else

$ss_2 = max(s_1, slip_{max})$

call ***menegotto pinto curve*** $\begin{pmatrix} slip^{rev}, f_v^{rev}, k_{1v}, \dots \\ ss_2, \tau_2 + k_0 ss_2, k_0, s, f_v, k_v, 20 \end{pmatrix}$

end

else

call ***menegotto pinto curve*** $\begin{pmatrix} slip^{rev}, f_v^{rev}, k_{1v}, \dots \\ sslip_{max}, \tau_2 + k_0 sslip_{max}, k_0, s, f_v, k_v, 20 \end{pmatrix}$

end

else

if $(slip \leq sslip_{min})$ *then*

if $(slip^{rev} \geq sslip_{min})$ *then*

if $(sslip_{min} = 0)$ *then*

call ***menegotto pinto curve*** $\begin{pmatrix} 0, 0, k_{1v}, -s_1, -(\tau_2 + k_0 s_1), k_0, \dots \\ s, f_v, k_v, 20 \end{pmatrix}$

else

call ***menegotto pinto curve*** $\begin{pmatrix} sslip_{min}, k_{1v} sslip_{min}, k_{1v}, slip_{min}, \dots \\ -\tau_2 + k_0 slip_{min}, k_0, s, f_v, k_v, 20 \end{pmatrix}$

end

else

$ss_2 = min(-s_1, slip_{min})$

call ***menegotto pinto curve*** $\begin{pmatrix} slip^{rev}, f_v^{rev}, k_{1v}, \dots \\ ss_2, -\tau_2 + k_0 ss_2, k_0, s, f_v, k_v, 20 \end{pmatrix}$

end

else

call ***menegotto pinto curve*** $\begin{pmatrix} slip^{rev}, f_v^{rev}, k_{1v}, \dots \\ sslip_{min}, -\tau_2 + k_0 sslip_{min}, k_0, s, f_v, k_v, 20 \end{pmatrix}$

end

Algorithm 4.6:

menegotto pinto curve $(ss_1, ff_1, kk_1, ss_2, ff_2, kk_2, s, f, k, R)$

This algorithm computes the stress, f, and tangent to the stress-slip curve, k for a given slip, s, on curve between Point 1 and Point2. Points 1 and 2 are defined by slip, stress and tangent vectors (ss_1, ff_1, kk_1) *and* (ss_2, ff_2, kk_2).

$$ff_0 = \frac{ff_1 - ff_2\left(\frac{kk_2}{kk_1}\right) + kk_1(ss_2 - ss_1)}{\left(1 - \frac{kk_1}{kk_2}\right)}$$

$$ss_0 = ss_1 - \left(\frac{ff_1 - ff_0}{kk_1}\right)$$

$$s^* = \frac{s - ss_1}{ss_0 - ss_1}$$

$$k^* = \frac{1}{1 + |s^*|^R}$$

$$f^* = \left(\frac{kk_2}{kk_1}\right) + (s^*)\left(1 - \left(\frac{kk_2}{kk_1}\right)\right)(k^*)^{\frac{1}{R}}$$

$$f = (ff_0 - ff_1)f^* + ff_1$$

$$k^* = \frac{kk_2}{kk_1} + \left(1 - \frac{kk_2}{kk_1}\right)(k^*)^{\left(1 + \frac{1}{R}\right)}$$

$$k = \left(\frac{ff_0 - ff_1}{ss_0 - ss_1}\right)k^*$$

4.4.4 Factors that Determine Peak Bond Strength

The numerical implementation of the bond response model developed for use in this investigation is a function of peak bond strength. At any time in the incremental solution history, the peak bond strength is determined by a number of system variables including the cyclic load history, concrete confining pressure, level of concrete damage and steel

strain history. Characterization of the influence of these variables on bond strength follows.

4.4.4.1 Modeling Deterioration of Bond Strength as a Function of Cyclic Slip History

Experimental investigation of concrete-to-steel bond indicates that bond strength deteriorates as the number of load cycles increases. In order to represent this characteristic of response in the proposed bond model, a simple cycle counting algorithm is implemented in the model and a relationship defining the deterioration of bond strength as a function of the number of load cycles is defined to represent the observed response.

Previous research into the response of systems subjected to cyclic loading has lead to the development of a number of algorithms for computing cycle counts. The more notable of these include rain flow cycle counting, range pair counting, peak counting, level crossing counting and range counting methods (Dowling, 1972). However, these methods may require storage of the entire slip history. Additionally, the majority of these algorithms are developed for use in conjunction with fatigue analysis of system loading. In this case, cycle counts are relatively high, individual cycle excursions are relatively small and system response does not vary as a function of a single cycle of loading. While researchers have proposed fatigue analysis for modeling of structures subjected to earthquake loading, the relatively small cycle counts and large excursions observed in structures subjected to earthquake excitation does not support application of standard fatigue-based cycle counting models. Here a more gradual and less discrete cycle counting model is proposed that characterizes the cyclic histories resulting from earthquake excitation of structural systems.

The number of cycles is computed as a function of the slip history, with the slip history defined by the following parameters: the maximum slip, the minimum slip, the cur-

rent slip, the current slip increment since the previous converged solution state and the previous number of cycles. These extreme slip values are defined upon slip reversal so that it is possible to have a system in which the current slip exceeds the maximum slip (*slip* > *smax*) or the current slip is less than the minimum slip (*slip* < *smin*). The algorithm for updating the cycle count on the basis of the slip history variables is shown in Algorithm 4.7:

Algorithm 4.7:

$fsmax = max(smax,slip)$
$fsmin = min(smin,slip)$
if $(smax \cdot smin = 0)$ *then*
  if $(smax > smax)$ *then*
    if $(slip < smax)$ *then*
      $ncycles = 0.25 + \frac{1}{4}\frac{smax - slip}{smax}$
      $ncycles = min(ncycles,0.75)$
    else
      $ncycles = 0.0$
    end
  else if $(smin < 0.0)$ *then*
      if $(slip > smin)$ *then*
        $ncycles = 0.25 - \frac{1}{4}\frac{slip - smin}{smin}$
        $ncycles = min(ncycles,0.75)$
      else
        $ncycles = 0.0$
      end
  else
    $ncycles = 0.25$
  end
else
  $ncycles = ncylces + \left|\frac{dslip}{2(fsmax - fsmin)}\right|$
end

This Algorithm 4.7 is verified through analysis of a series of variable cyclic slip histories. Figure 4.43a shows three different artificially generated cyclic slip histories. Each

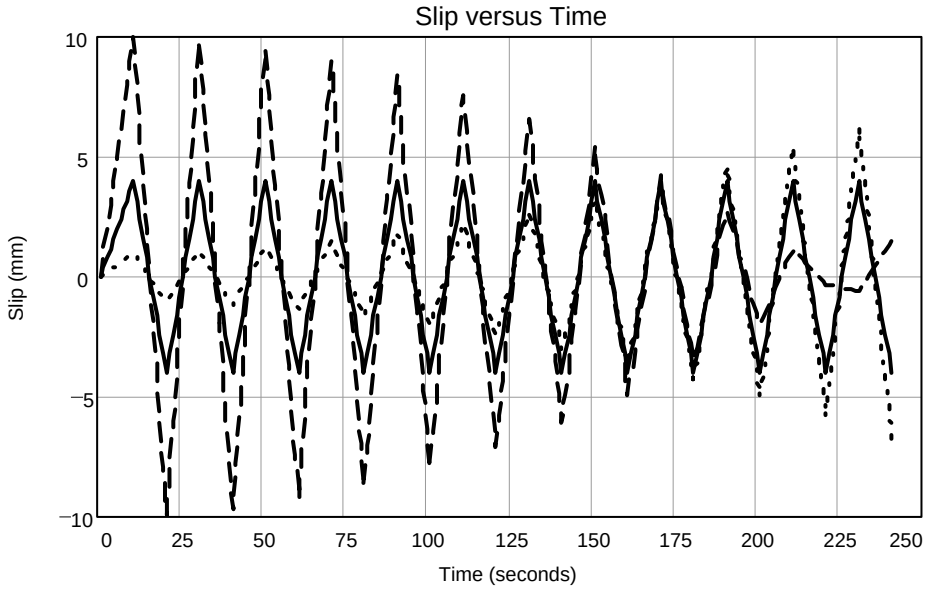

Figure 4.43a: Generated Cyclic Slip Histories

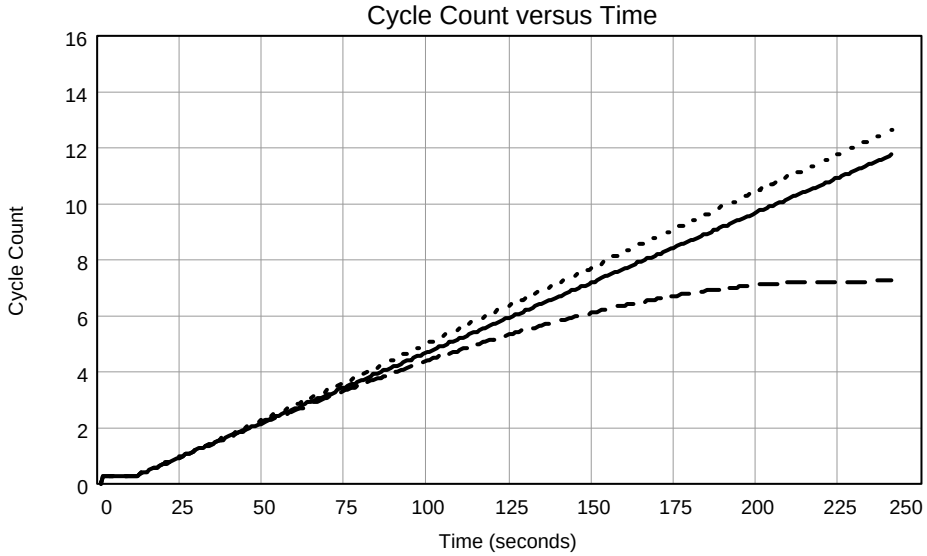

Figure 4.43b: Cycle Counts for Generated Cyclic Slip Histories

of these histories represents slightly more than eleven displacement *cycles* assuming that an individual cycle is not dependent on the absolute value of the excursion. However, these histories represent constant, increasing and decreasing maximum excursion values. As a result, the *number of cycles* counted for these histories varies from approximately seven to approximately thirteen (Figure 4.43b). Figure 4.44a shows a more variable slip

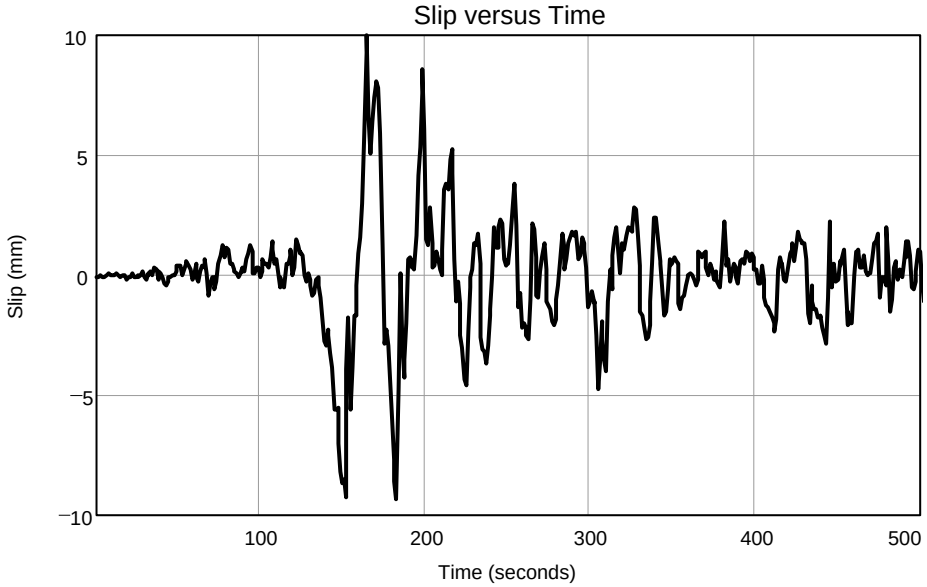

Figure 4.44a: Computed Number of Cycles for Generated Cyclic Slip Histories

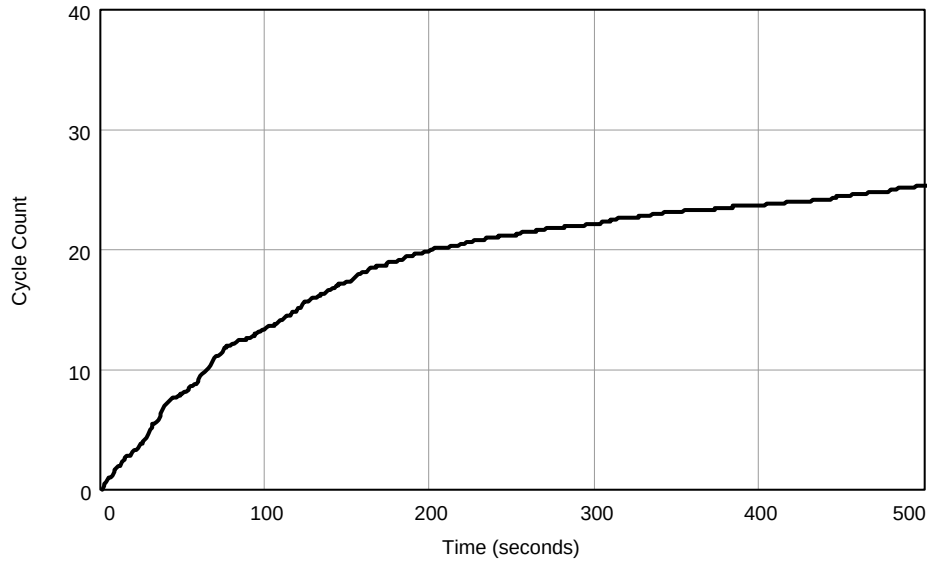

Figure 4.44b: Computed Number of Cycles for Generated Cyclic Slip Histories

history developed on the basis of the ground motion record from the Petrolia record from the Cape Mendecino Earthquake. The cycle count for this record as a function of time is shown in Figure 4.44b.

Following from the cycle counting algorithm, a bond strength deterioration model is developed to characterize the experimental data presented by Eligehausen *et al.* [1983].

Strength deterioration is represented by a damage parameter, δ, defined as the ratio of the maximum bond strength developed under a cyclic slip history versus that developed under a monotonic slip history. Thus, $\delta = 1.0$ represents a state of zero damage due to cyclic loading and $\delta = 0$ represents complete damage due to cyclic loading. The strength deterioration exhibited by the Eligehausen test specimens is defined on by the number of cycles and the absolute maximum slip in both the positive and negative directions (Algorithm 4.8). The plot of the computed deterioration in bond strength for the series of prescribed slip histories used by Eligehausen *et al.* [1983] is shown in Figure 4.45. Here the number of cycles is equal to that computed using Algorithm 4.7 plus one so that the results are comparable with the experimental data presented in Figure 4.46. It is important to note that the bond strength deterioration relationship presented in Figure 4.45, defines deterioration of *maximum* bond strength; while the data in Figure 4.46 show the deterioration of bond strength achieved at a particular maximum slip demand. Figure 4.47 shows a direct comparison between the proposed analytical model and the experimental data. Here deterioration in maximum bond strength is related to absolute maximum slip demand for systems subjected to one and ten cycles of loading.

Algorithm 4.8:

$fsmax = max(smax,slip)$
$fsmin = min(smin,slip)$
if $(ncycles = 0)$ *then*
    $\delta = 1$
else
    $slope = -0.164 - 0.4339(fsmax - fsmin)$

$$\delta = 0.27 + 0.58 \exp\left(\begin{array}{c} (-0.225)(fsmax - fsmin) \cdot \ldots \\ (1 - \exp(-20(ncycles - 0.25))) \cdot \ldots \\ ncycles^{slope} \end{array} \right)$$

    $\delta = min(1.0,\delta)$
end

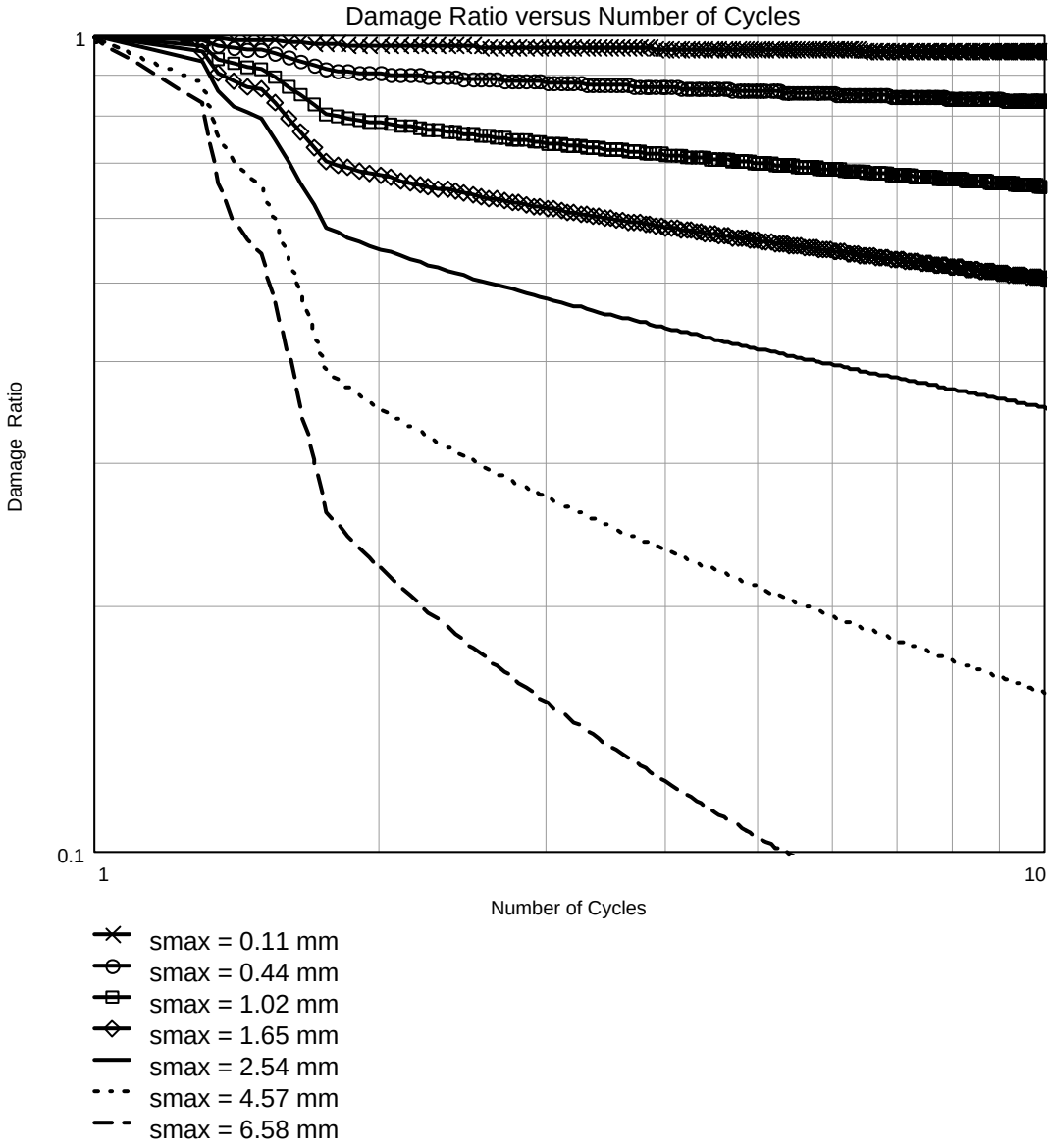

Figure 4.45: Deterioration of Bond Strength with Cyclic Load History (Proposed Analytical Model)

4.4.4.2 Defining Peak Bond Strength as a Function of the Surrounding Concrete Stress and Damage State

Investigation of the bond phenomenon indicates that bond response is a function of the composite material state including the concrete stress and damage state. A non-local modeling procedure is used to incorporate the effect of these composite material parameters on the calculated bond response. Experimental investigation provides data for charac-

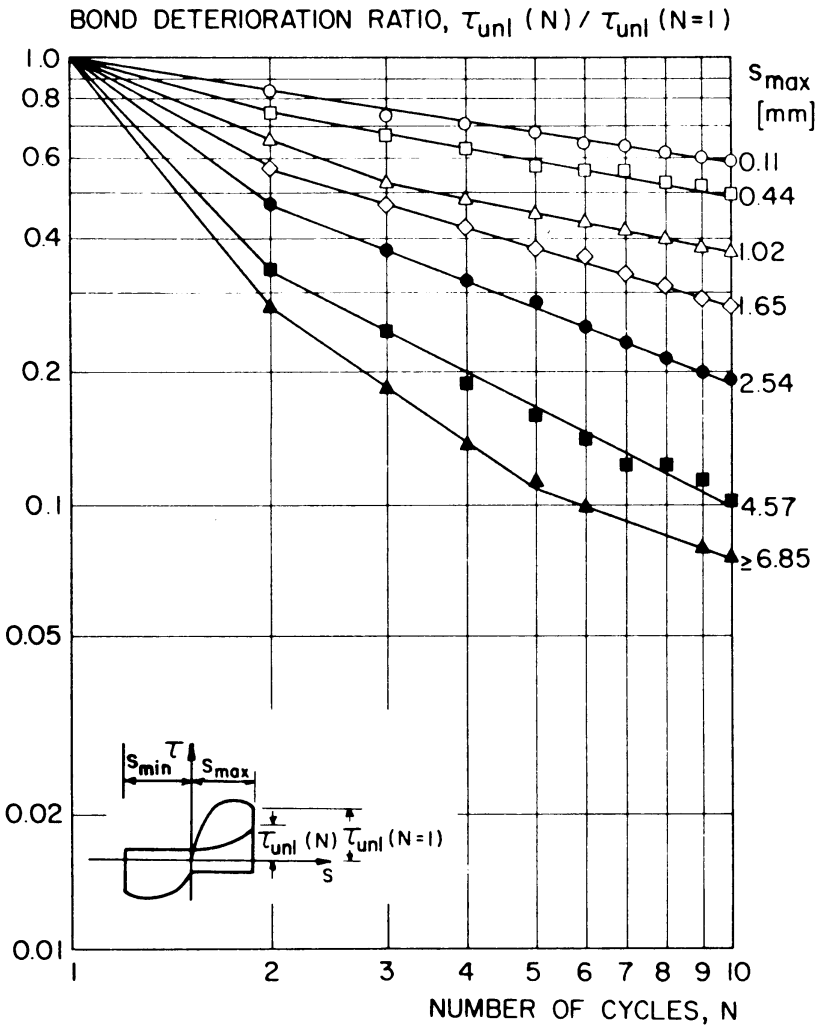

Figure 4.46: Deterioration of Bond Strength with Cyclic Load History (Experimental Data from Eligehausen *et al.* [1983]).

terization of the bond response as a function of concrete stress and damage state. Previously proposed bond represent the effect of the concrete damage in a number of ways including development of different models to represent the different bond response histories observed in different regions of the structure [Viwathanatepa, 1979a and 1979b] and development of bond models that characterize the behavior the multi-dimensional bond zone [de Groot, 1981; den Uijl and Bigaj, 1996; Cox, 1994]. Here the effect of concrete stress state and concrete damage state are considered independently using a non-local modeling technique. The proposed bond response model defines behavior as a function of

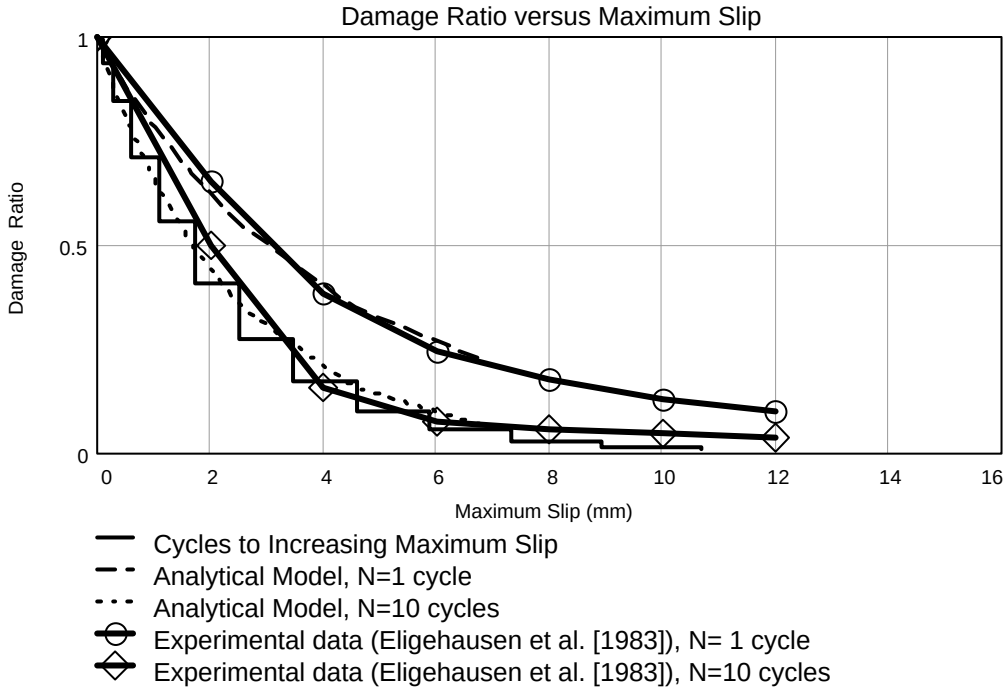

Figure 4.47: Deterioration of Bond Strength after One and Ten Load Cycles as a Function of Maximum Slip Demand

peak bond strength; thus, experimental data are used as a basis for defining relationships between peak bond strength and concrete confining pressure and peak bond strength and concrete damage state.

Experimental investigation provides data for characterization of the bond response as a function of concrete stress state [Eligehausen *et al.*, 1983; Malvar, 1992; Gambarova *et al.*, 1989a; Untraurer and Henry, 1965]. Figure 4.48 shows data from a number of experimental bond studies. Variation in the experimental data can be attributed to several causes, in addition to the unavoidable random nature of experimental observation. First, data are included for experimental investigations in which concrete confining pressure was actively and passively controlled in both one and two planes. The experimental data provided by the Eligehausen study includes both active and passive confinement provided in one direction perpendicular to the axis of the reinforcing bar. Data provided by the Malvar study are for the case of active radial confinement applied to concrete cylinders. Addition-

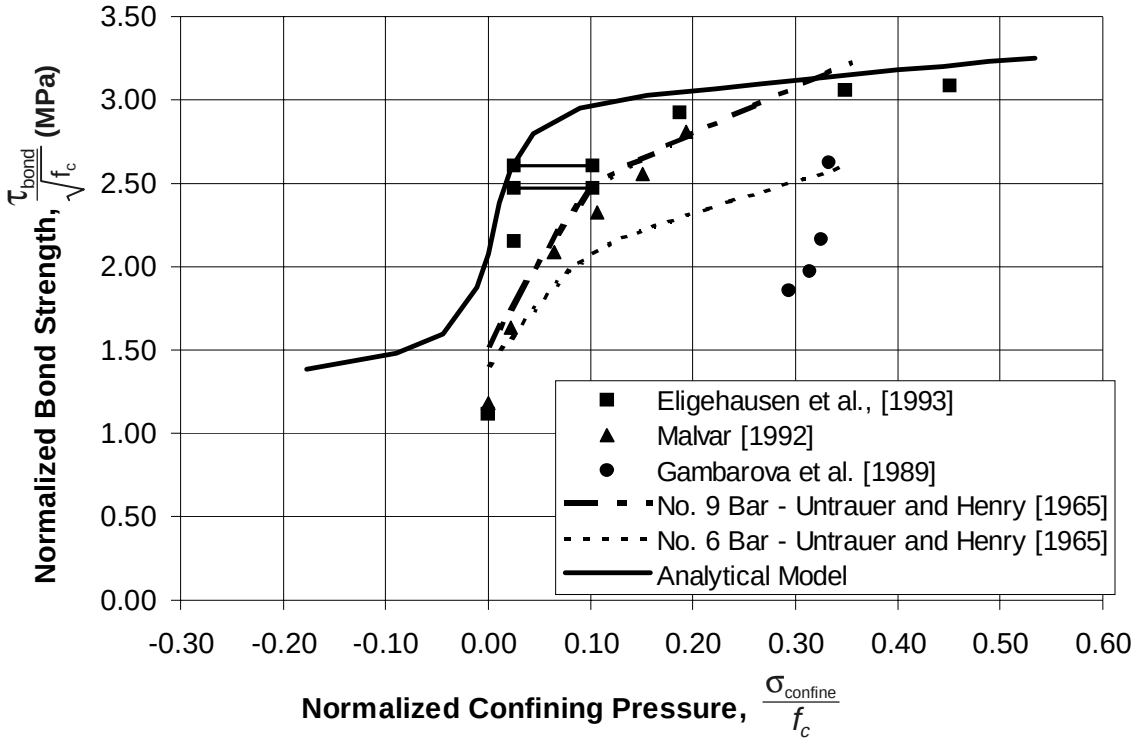

Figure 4.48: Observed and Computed Influence of Confining Pressure on Bond Strength (Experimental Data from Sources Identified in Chart Legend)

ally, data are provided for confining pressure applied to systems that are initially undamaged (e.g., Eligehausen) and for system that are initially damaged (e.g., Malvar and Gambarova). Finally, data are presented for systems that have constant confinement (e.g., Eligehausen, Malvar) and for systems with variable confinement (e.g., Gambarova). These variations in testing procedure undoubtedly contribute to variation in observed peak bond response. A relationship for characterizing the influence of bond strength is shown in Figure 4.48. This relationship does not characterize the average observed response. However, comparison of computed and observed response for reinforced concrete systems indicates that the proposed curve is an appropriate model.

There are essentially no data relating bond strength to concrete damage state. Several studies consider bond behavior for systems that are initially cracked and several investigations provide information on damage patterns resulting from high bond demand, however,

this is essentially qualitative information. If the problem is conceptualized on the basis of the proposed concrete model, then it is reasonable to consider the development of fictitious crack planes that lie parallel and perpendicular to the axis of the reinforcing bar. Damage to the concrete represented by cracking perpendicular to the bar axis (reduced concrete stiffness in the direction parallel to the bar axis) results in reduced bond transfer due to the increased relative flexibility of concrete portion of the system. Thus, this damage need not be explicitly represented by the model. Concrete damage that is represented by the development of crack surfaces parallel to the bar axis does not reduced concrete element stiffness in the direction of applied bond loading and thus does not immediately result in reduced bond strength. However, it is reasonable to propose that bond concrete with wide cracks lying parallel to the axis of an anchored reinforcing bar likely has severely reduced bond strength. Thus, it is necessary to consider deterioration of bond strength as a result of oriented concrete damage. Here it is proposed that the deterioration of bond strength as a function of concrete damage be defined on the basis of the concrete damage surfaces since these surfaces control the deterioration of the plain concrete tensile and shear strength. The ratio of bond strength for damaged concrete to undamaged concrete, ϕ, is defined on the basis of the concrete damage surfaces as follows:

$$\phi = (\Gamma \cdot l)\exp(H_1 \alpha d_1) + (\Gamma \cdot m)\exp(H_2 \alpha d_2) \tag{4-8}$$

where Γ is the rank one tensor that defines the orientation of the axis of the reinforcing bar, l and m are rank one tensors defining the normals to the two fictitious concrete crack planes (Equations 2-33a and 2-33b), and αd (Equation 2-35) and H (Equation 2-43) represent the concrete internal damage variables and damage moduli. With few data to calibrate the proposed relationship, bond response as a function of concrete damage is considered in parametric studies in subsequent chapters.

4.4.4.3 Defining Peak Bond Strength as a Function of the Steel Material State

Critical evaluation of material behavior in the vicinity of the concrete-steel interface suggests that yielding of reinforcing steel affects bond response. Yielding of the reinforcement in tension produces Poisson contraction of the bar that likely reduces bond strength while Poisson dilation of the reinforcement in the compressive post-yield regime likely increases bond strength. This response is observed in several experimental tests programs [Viwathanatepa, 1979a, 1979c]; however, only the data presented by Shima *et al.* [1987b] isolate the influence of tensile yielding on bond capacity. The bond stress versus slip from this test program (Figure 4.30) indicate that bond strength deteriorates by about 75 percent with tensile yielding of the reinforcement. With so few data, the following relationship is proposed as a reasonable method for incorporating the effect of steel yield on behavior.

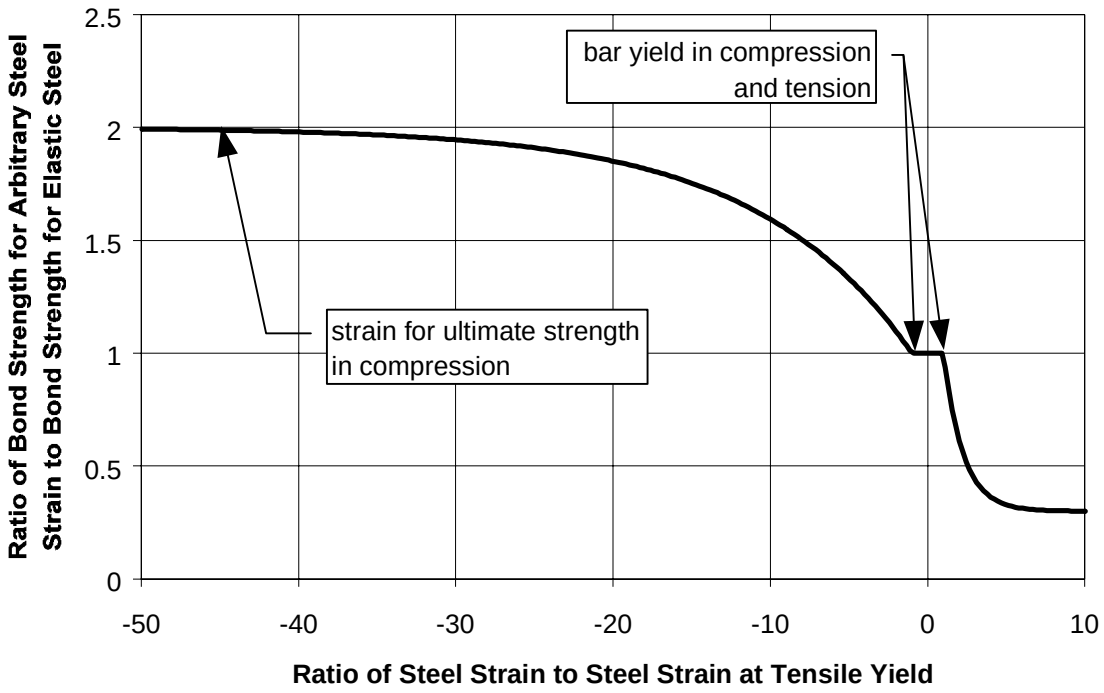

Figure 4.49: Influence of Steel Strain on Bond Strength

4.4.5 Implementation of the Bond Model within the Framework of the Finite Element Method

4.4.5.1 Definition of the Bond Element

A numerical implementation of the bond model is proposed within the framework of the finite element method. Through appropriate representation of the finite deformation field observed within the bond zone, this implementation allows for characterization of the discontinuity associated with bond zone deformation (i.e. slip) without loss of numerical continuity of the global finite element model.

Given the undeformed concrete-steel composite, points X and $\tilde{X}$ are at the same location on the concrete-steel interface, but with point X defining a location on the steel surface and point $\tilde{X}$ defining a location on the concrete surface. Once the system is loaded and there is deformation along the concrete-steel interface, points X and $\tilde{X}$ are no longer at the same location. Slip, *slip*, is defined as the movement between these two points in the direction parallel to the bar axis and radial deformation, *rad*, is defined as the movement of these two points in the direction perpendicular to the axis of the bar (Figure 4.50):

$$slip = U - \tilde{U}$$

$$rad = V - \tilde{V}$$

Figure 4.50 shows an finite element idealization of the vicinity of the bond zone. In order to facilitate the discussion, the bond element is depicted as having a finite width (depth in the direction perpendicular to the axis of the reinforcing bar). In order to maintain C_0 continuity along the element boundaries of the bond element and thereby force the entirety of the slip and radial deformation discontinuity to be represented by the bond element, it is necessary that the numerical approximation of the displacement field along these boundaries be of the same order as those used to approximate the displacement field in the surrounding concrete and steel elements. Thus, the element is defined to have four

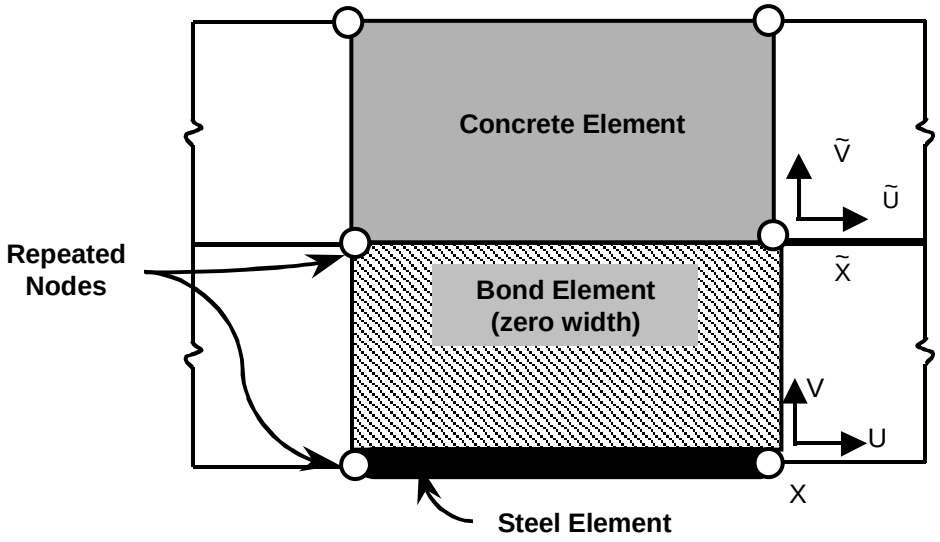

Figure 4.50: Finite Element Mesh and Nodal Displacements in the Vicinity of the Concrete-Steel Interface

nodes and the displacement field along the bond-concrete element boundary and the bond-steel element boundary are approximated using the same shape functions as used for the other elements. Since action in the directions perpendicular to the bar axis does not affect response in the parallel direction and since action in the perpendicular direction is determined entirely by bond element response, continuity restrictions on the deformation approximation in this direction depend entirely on maintaining finite energy for modes of response defined by the bond model. The proposed model represents radial response as a function of relative radial displacement, thus the only requirement is that the shape functions be finite. Here the bond element is represented as a four note element; nodes a_1 through a_4 define the boundary of the bond element and maintain connectivity with concrete and steel elements that compose the remainder of the model. Linear shape functions are used to approximate the displacement fields.

Bond response is defined by deformation in the directions parallel and perpendicular to the axis of the reinforcement. Given the element and approximations defined above, the continuous deformation modes are defined as follows:

$$\begin{bmatrix} slip \\ rad \end{bmatrix} = \begin{bmatrix} u_{concrete} - u_{steel} \\ v_{concrete} - v_{steel} \end{bmatrix} \tag{4-9a}$$

$$\begin{bmatrix} slip(\xi) \\ rad(\xi) \end{bmatrix} = A \cdot B(\xi) \cdot U \tag{4-10a}$$

where

$$A = \begin{bmatrix} -1 & 0 & 1 & 0 \\ 0 & -1 & 0 & 1 \end{bmatrix} \tag{4-10b}$$

$$B(\xi) = \begin{bmatrix} N_1(\xi) & 0 & N_2(\xi) & 0 & 0 & 0 & 0 & 0 \\ 0 & N_1(\xi) & 0 & N_2(\xi) & 0 & 0 & 0 & 0 \\ 0 & 0 & 0 & 0 & N_2(\xi) & 0 & N_1(\xi) & 0 \\ 0 & 0 & 0 & 0 & 0 & N_2(\xi) & 0 & N_1(\xi) \end{bmatrix} \tag{4-10c}$$

$$U = \begin{bmatrix} u_1 & v_1 & u_2 & v_2 & u_3 & v_3 & u_4 & v_4 \end{bmatrix}^T \tag{4-10d}$$

$$N_1(\xi) = 1 - \xi \qquad N_2(\xi) = 1 + \xi \tag{4-10e}$$

Given the approximate deformation field within the element, the bond stress and radial stress field are defined by the previously presented relationships. Using the principle of virtual work as the basis for equating the virtual work done by the external reactions with the internal work done by the element deformations and distributed stress fields results in the following:

$$\delta U^T R = \int_L \begin{bmatrix} \delta slip(x) & \delta rad(x) \end{bmatrix}^T \begin{bmatrix} bond\ stress(x) \\ radial\ stress(x) \end{bmatrix} dx \tag{4-11}$$

Assuming a numerical integration scheme with appropriate integration points, *l*, weight function, *w*(*l*) and Jacobian, *j*(*l*). This is extended as follows:

$$\delta U^T R = \sum_{l=1}^{lint} \delta U^T B(\xi_l)^T A^T \begin{bmatrix} bond\ stress(\xi_l) \\ radial\ stress(\xi_l) \end{bmatrix} w(l) j(l) \tag{4-12}$$

Given that the internal and external virtual work must be equal for any arbitrary displacement field, this provides the following definition for the element nodal reactions:

$$R = \sum_{l=1}^{lint} B(\xi_l)^T A^T \begin{bmatrix} bond\ stress(\xi_l) \\ radial\ stress(\xi_l) \end{bmatrix} w(l) j(l) \tag{4-13}$$

4.4.5.2 Implementation of the Non-Local Bond Model

Computation of bond stress and radial stress requires knowledge of the composite material state as well as the local element deformation modes, slip and radial deformation. Within the framework of displacement-based finite element methods, simplified methods for stress field recovery can result in an unrealistic and possibly dicontinuous stress distribution when the true stress field must be bounded and smooth. Here the projection process (Zeinkiewicz and Taylor, 1994) is used to provide a means of more accurately computing the material stress field. The projected nodal stresses are computed and then averaged for each bond element. A similar procedure is used to computer an average concrete damage parameter and the average steel stress.

4.4.5.3 Solution Algorithm in the Presence of the Non-Local Element Model

Introduction of the non-local bond element into the finite element model requires implementation of a non-standard global solution algorithm. Typical algorithms implemented for solution of non-linear systems include the Newton-Raphson iteration:

$$U_{j+1}^{k+1} = U_j + K(U_{j+1}^k)^{-1}[R(U_{j+1}^k, Q_j)] \tag{4-14}$$

Here subscripts j and j+1 refer respectively to the converged solution states at times j and j+1, assuming an incrementally increasing solution algorithm, and superscripts k and k+1 refer to system variables at intermediate unconverged solution states on the solution path

to the converged solution state at any time j+1. Here progression towards a converged solution state requires updating the unbalanced residual, $R(U^k_{j+1}, Q_j)$, and updating and *inverting*[1] the tangent, $K(U^k_{j+1})$, for each k+1 iteration. Computational demand is reduced by implementation of a second common solution algorithm, the Quasi-Newton initial tangent iteration method:

$$U^{k+1}_{j+1} = U_j + K(U^1_{j+1})^{-1}[R(U^k_{j+1}, Q_j)] \tag{4-15}$$

Here the tangent is updated and the system solved only once for each time step on the global solution path.

Implementation of the non-local bond element requires modification of these algorithms to account for the bond element dependence on the global solution parameters. This modification can be achieved in two ways; however, each of these modified methods requires some compromise of typical solution algorithms. The guarantee of a quadratic rate of convergence for the Newton-Raphson iteration algorithm can be maintained by assuming that the bond element response at time j+1 may be approximated as depending on global model parameters as computed at time j rather than j+1. This eliminates the implicit dependence of the bond element behavior at time j+1 on the global model parameters at time j+1 and allows for computation of a consistent tangent at time j+1. Following this approach, the solution algorithm is defined as follows:

$k = 1 \qquad U^k_{j+1} = U_j \qquad Q_{j+1} = Q_j$

loop until a converged solution state is achieved

$U^{k+1}_{j+1} = U_j + K(U^k_{j+1})^{-1}[R(U^k_{j+1}, Q_{j+1})]$

$k = k + 1$

Depending on how large is the interval between times j and j+1, this method may intro-

1. Typically solution of the linearized system is achieved using algorithms in which the inverse of the tangent is not explicitly computed.

duce undesirable and incalculable error into the solution. A second method is to compute the bond element response at time j+1 as a function of global model parameters at time j+1. This maintains the accuracy of the solution but compromises the guaranteed quadratic rate of convergence. Additionally, this method may require modification of the time step in order to achieve a converged solution at time j+1. This method is defined as follows:

$k = 1 \qquad U_{j+1}^{k} = U_j \qquad Q_{j+1}^{k} = Q_j$

loop until a converged solution state is achieved

$U_{j+1}^{k+1} = U_j + K(U_{j+1}^{k})^{-1}[R(U_{j+1}^{k}, Q_{j+1}^{k})]$

compute composite material parameters, Q_{j+1}^{k+1}, using stress projection method

$k = k + 1$

The second method provides the most accurate results and, for this reason, is used in all analyses presented as part of this investigation.

4.5 Comparison of Bond Model with Experimental Data

The proposed bond model is compared with experimental data provided by several researchers defining the bond stress versus slip response for reinforcement with a variety of anchorage conditions and subjected to monotonic and cyclic slip histories.

For the case of monotonically increasing slip demand, the bond stress versus slip response is determined by the concrete compressive strength, the diameter of the reinforcing bar, the concrete stress state in the vicinity of the bar and the steel stress state. Other parameters contribute in a minor way to the response. Figure 4.51 shows the monotonic bond stress versus slip history as reported by a several researchers compared with that computed using the proposed model for an concrete compressive strength of 30 MPa (4350 psi) and an assumed confining pressure of $0.2f_c$. Figure 4.52 shows the monotonic bond stress versus slip history as observed by Eligehausen *et al.* [1983] and as computed using the proposed model. Bond strength is normalized with respect to $\sqrt{f_c}$ and data are

provided for one case in which concrete confining pressure is lost as soon as splitting cracks developed (splitting-type bond failure), two cases in which concrete confining pressure is provided by transverse reinforcement (passive confinement) and for three cases in which concrete compressive stress in one direction perpendicular to the bar is actively maintained as a prescribed level. Figure 4.53 shows the monotonic bond stress versus slip response as observed by Malvar [1992]. Here data are shown for five levels of concrete confining pressure provided in the radial direction perpendicular to the axis of the reinforcing bar. The data provided by Eligehausen and Malvar are for specimens with short anchorage lengths and as a result steel stresses are low. Figure 4.54 shows computed and observed bond stress versus slip response for specimens tested by Shima *et al.* [1987b] in which anchorage lengths are sufficiently long to allow for tensile yielding of the reinforcing steel. The data presented in these figures show good correlation between computed and observed bond strength for a relatively wide range of bond-zone systems. The most important source of discrepancy between computed and observed response for individual specimens likely is variation in the temporal and spatial distribution of confining pressure developed at the perimeter of the bond zone during laboratory testing.

Figure 4.55 shows bond response for a system subjected to cyclic slip demand with increasing amplitude in one direction only and nominally zero slip demand in the other direction. As previously discussed, the bond study completed by Hawkins *et al*. [1982] used very short anchorage lengths. As a result the presented data appropriately are considered to be the most extreme response exhibited along a bond zone length that is typical for most experimental investigations. Figure 4.56 shows the computed bond stress versus slip response for a system subjected to a cyclic slip demand comparable to that used in the Hawkins study. Given that the data presented by Hawkins represent extreme bond zone response, the response presented in Figure 4.56, in which no deterioration of bond strength

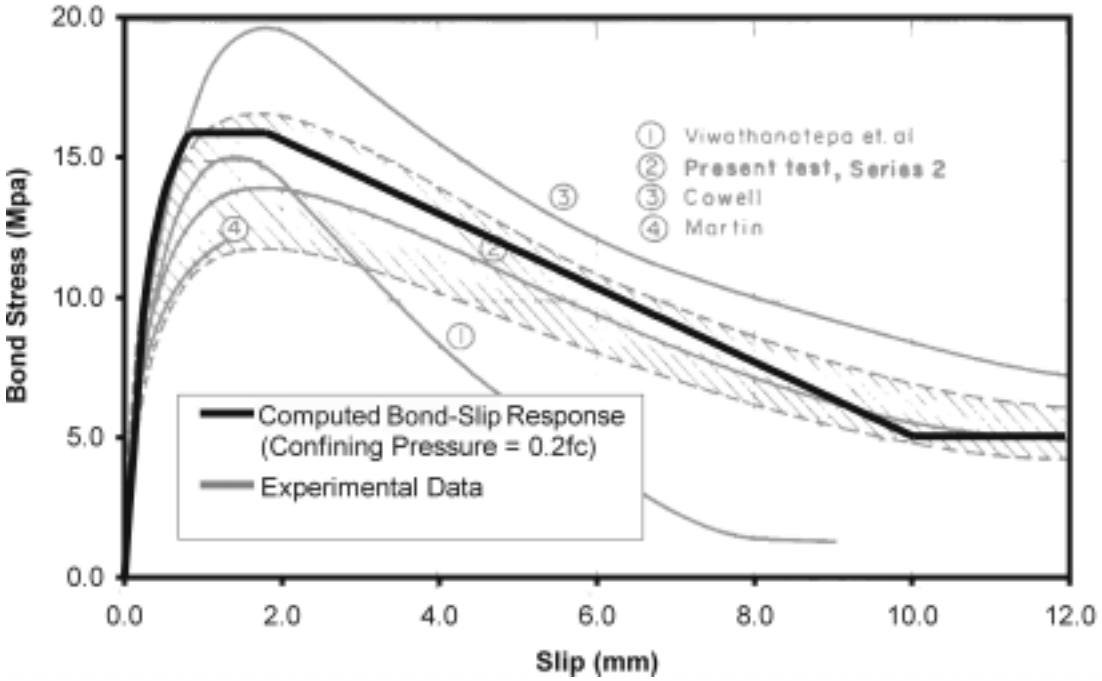

Figure 4.51: Computed and Observed Bond Stress Versus Slip Response (Figure 4.21 from Eligehausen *et al.* [1983])

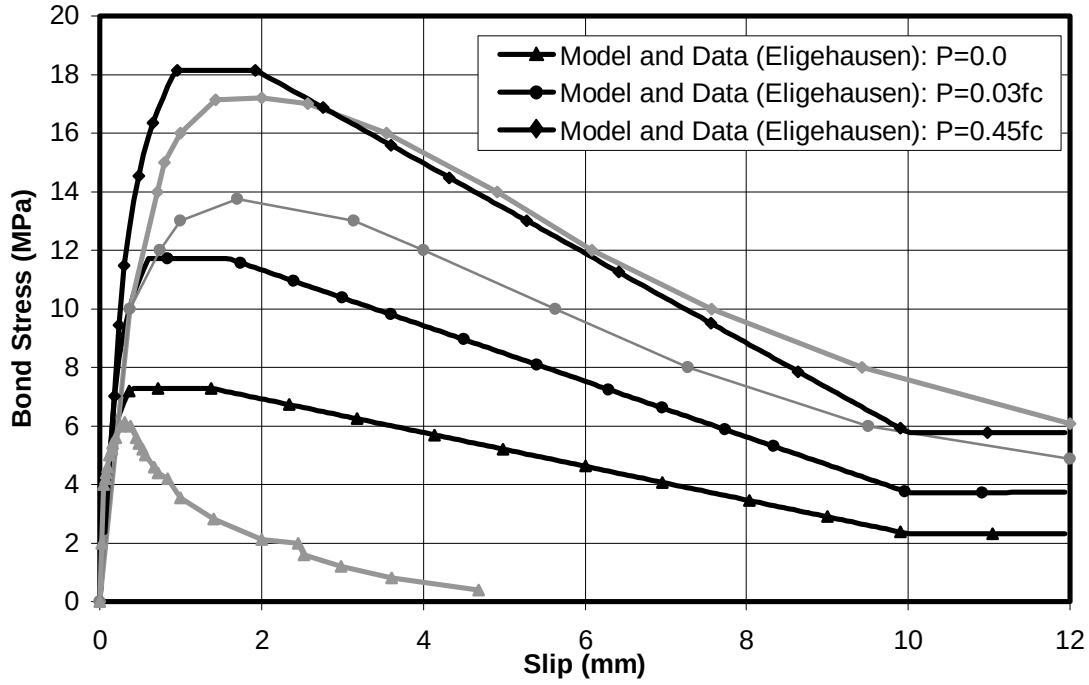

Figure 4.52: Computed and Observed Bond Stress Versus Slip Response for Concrete with Compressive Strength of 31 MPa (Experimental Data, Shown in Grey, are from Eligehausen *et al.* [1983])

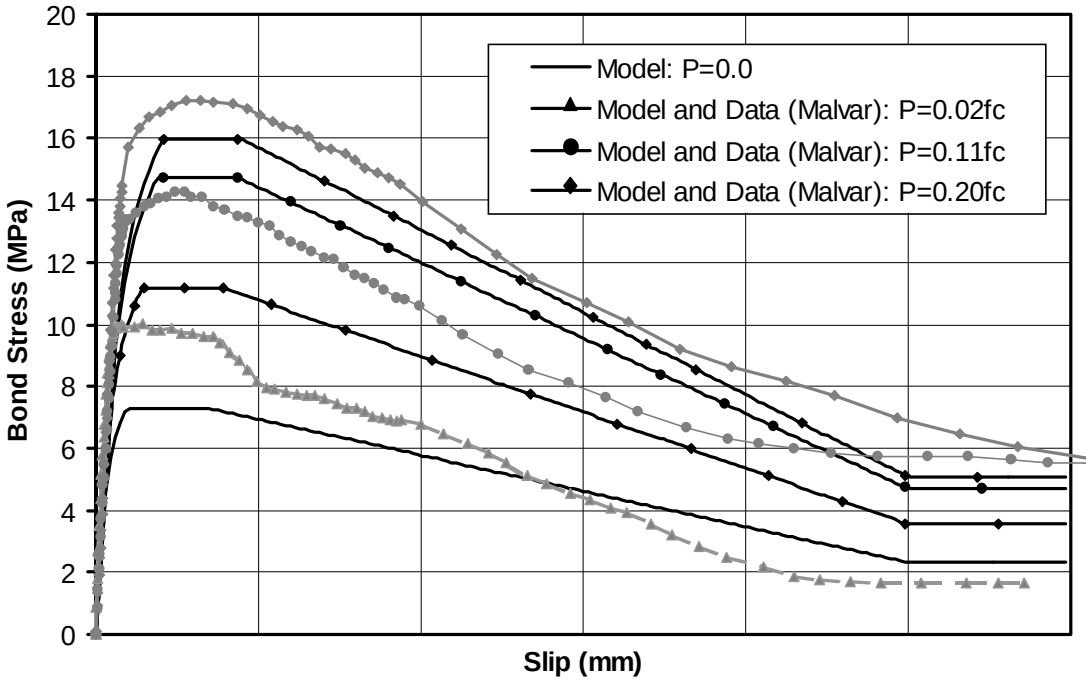

Figure 4.53: Computed and Observed Bond Stress Versus Slip Response for concrete with compressive strength of 30 MPa (Experimental Data, Shown in Grey, are from Malvar [1991])

is indicated by the model, likely is an appropriate representation of the response. Figure 4.57 shows the computed bond stress versus slip response for a system subjected to cyclic slip demand with increasing amplitude in one direction and a minimal fixed amplitude in the opposite direction. Here response is characterized by deterioration of bond strength with progressive loading. These data presented in Figures 4.56 and 4.57 identify the limitation of the cycle counting algorithm and bond strength deterioration model developed for this investigation. However, the computed response bounds that observed by Hawkins and others (e.g., Eligehausen *et al.* [1983]) and thus is considered a plausible model of the physical system.

For the case of reversed cyclic loading, in addition to the previously identified parameters, bond response is determined by the slip history. Figures 4.58 and 4.59 show bond stress versus slip history for systems subjected to reversed cyclic slip histories as

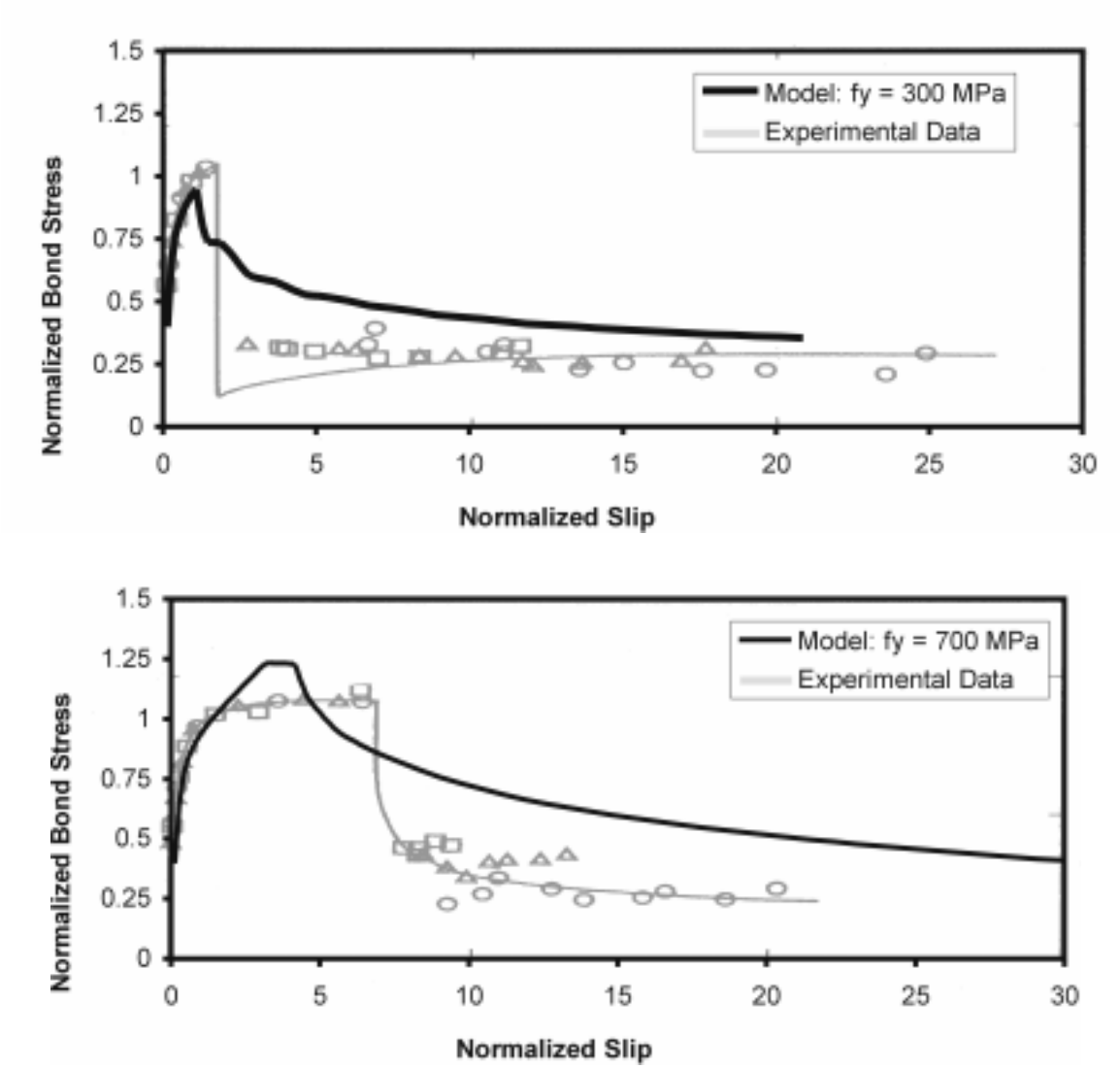

Figure 4.54: Computed and Observed Bond Stress Versus Slip Response (Data from Shima *et al.* [1991])

computed using the proposed model and as observed by Eligehausen *et al.* [1983]. Figure 4.58 shows the response of a system subjected to ten cycles to a maximum slip level that is less than that at which maximum bond strength is developed. Data indicated that maximum bond strength is approximately equal to that achieved under monotonic loading. Figure 4.59 shows the response of a system subjected to cyclic loading to a maximum slip level that is approximately equal to that at which maximum bond strength is achieved. For

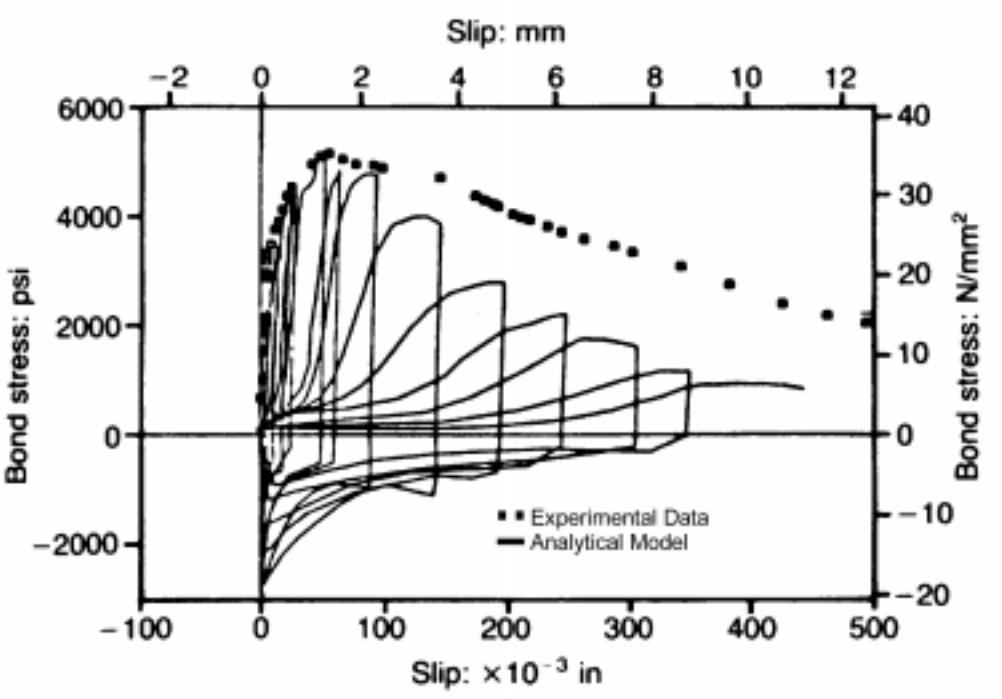

Figure 4.55: Observed Bond Stress Versus Slip Response for Cyclic Slip Demand (Figure 11a from Hawkins *et al.* [1983])

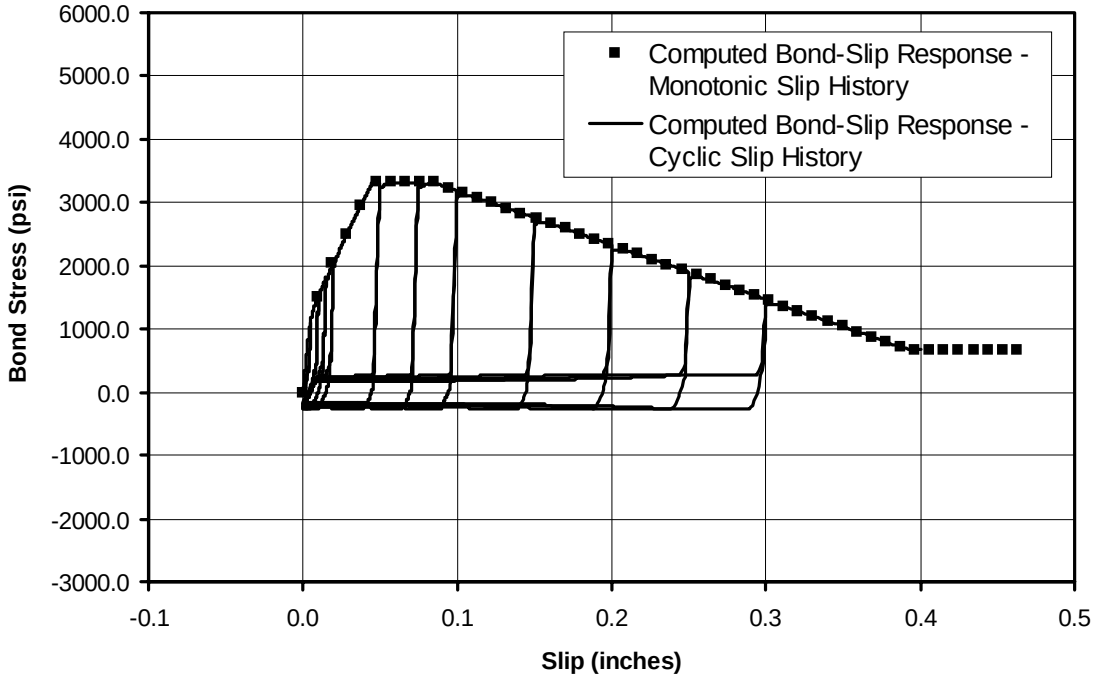

Figure 4.56: Computed Bond Stress Versus Slip Response for Cyclic Slip History Comparable to that of Hawkins *et al.* [1983]

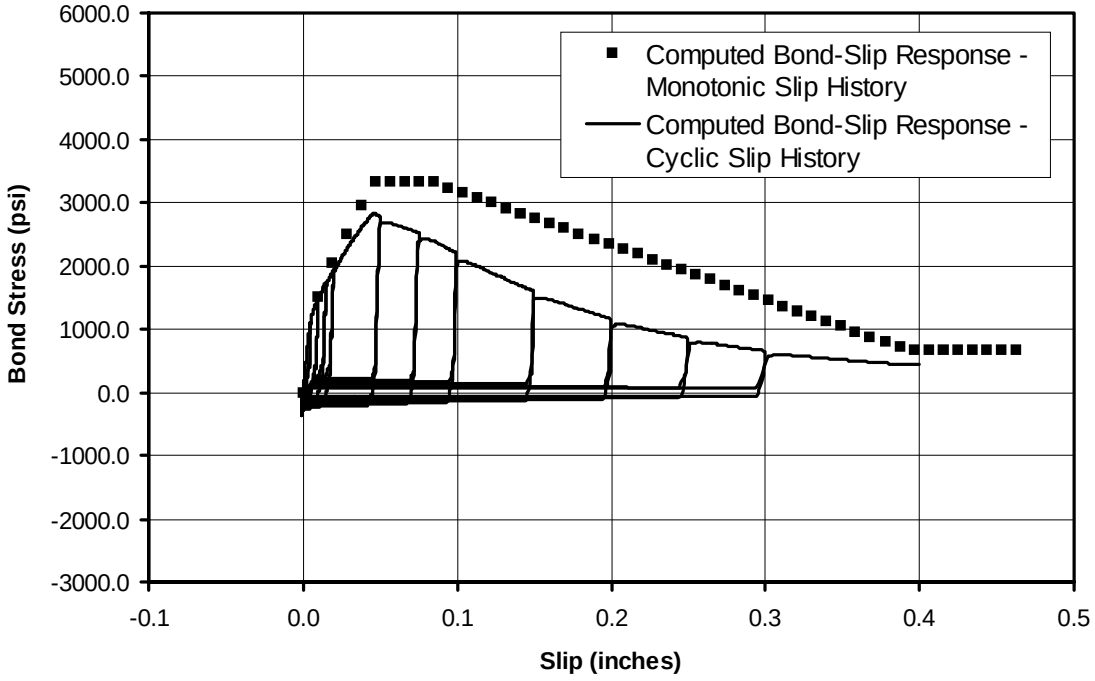

Figure 4.57: Computed Bond Stress Versus Slip Response for a Slip History Comparable to Hawkins *et al.* [1983] with Minimal Slip Demand in the Non-Load Direction

this slip history bond strength at more extreme slip levels is significantly less than that observed under monotonic loading.

The current investigation indicates that radial stress developed in association with bond stress can determine the bond strength of a system. Figures 4.60 and 4.61 show the bond stress versus slip history and the radial stress versus slip history as observed by Gambarova *et al.* [1989a]. These data show stress versus slip histories for several levels of splitting crack width. The current proposed model defines bond strength on the basis of confining pressure rather than crack width opening, thus these data are compared with the computed response for a system with confining pressure equal to the average confining pressure developed during the test.

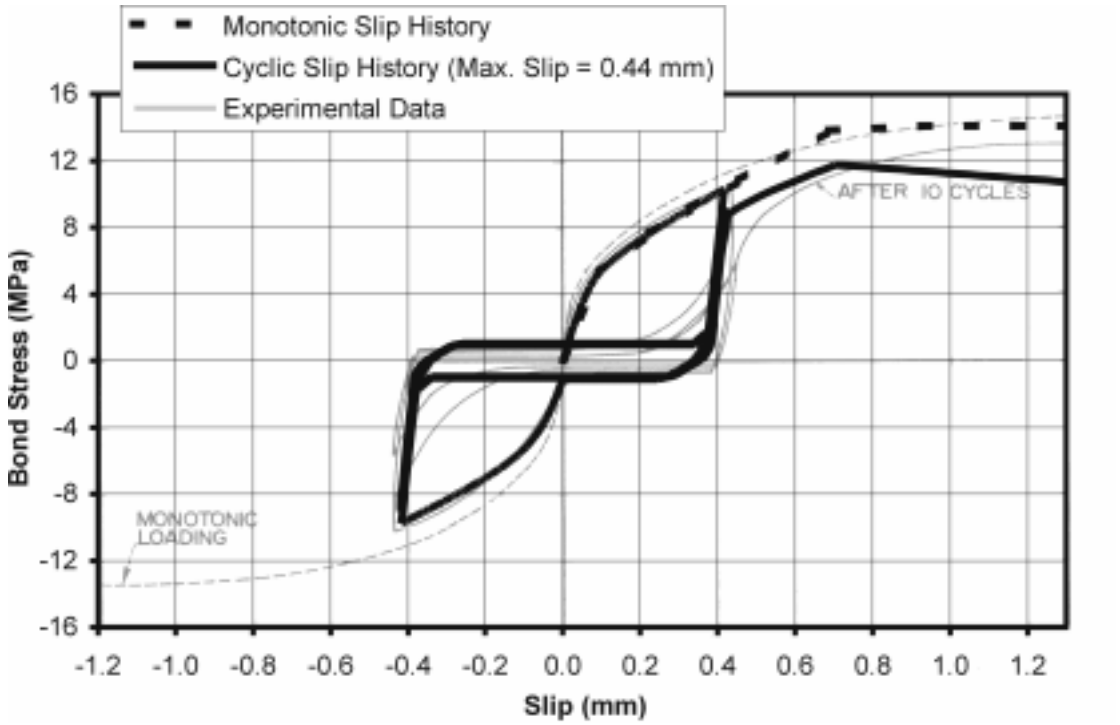

Figure 4.58: Computed and Observed Bond Stress Versus Slip Response for Reversed-Cyclic Slip Demand of 0.44 mm (Data from Eligehausen *et al.* [1983])

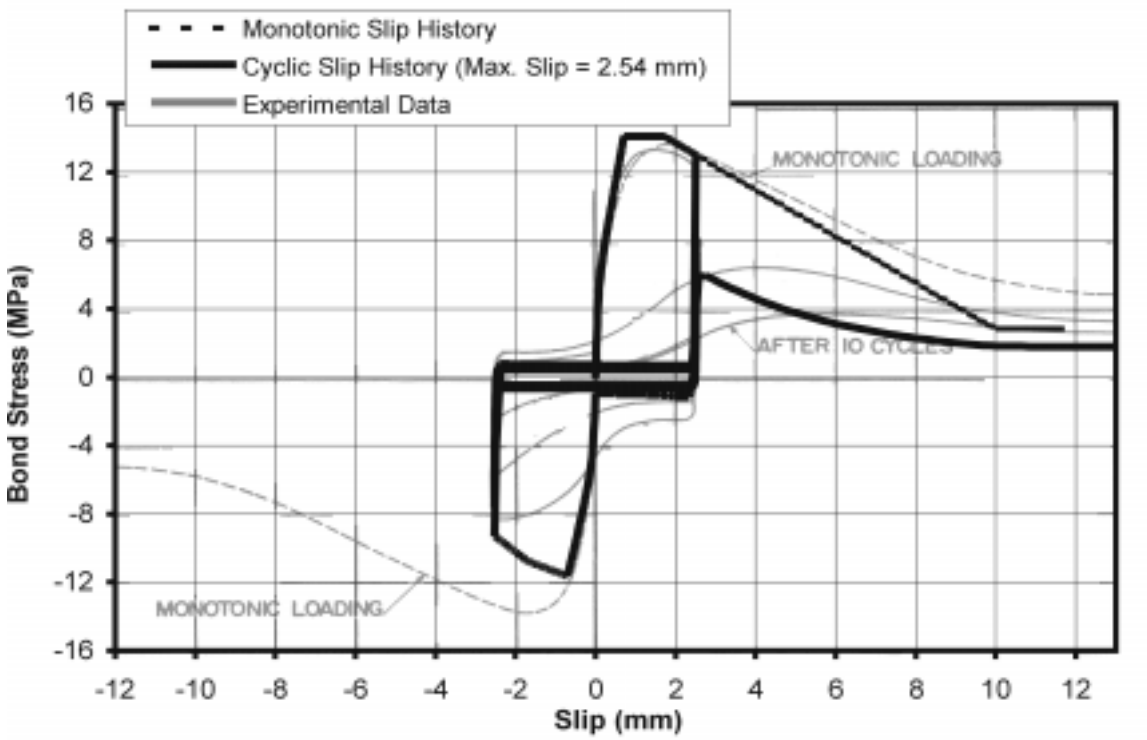

Figure 4.59: Computed and Observed Bond Stress Versus Slip Response for Reversed-Cyclic Slip Demand of mm (Data from Eligehausen *et al.* [1983])

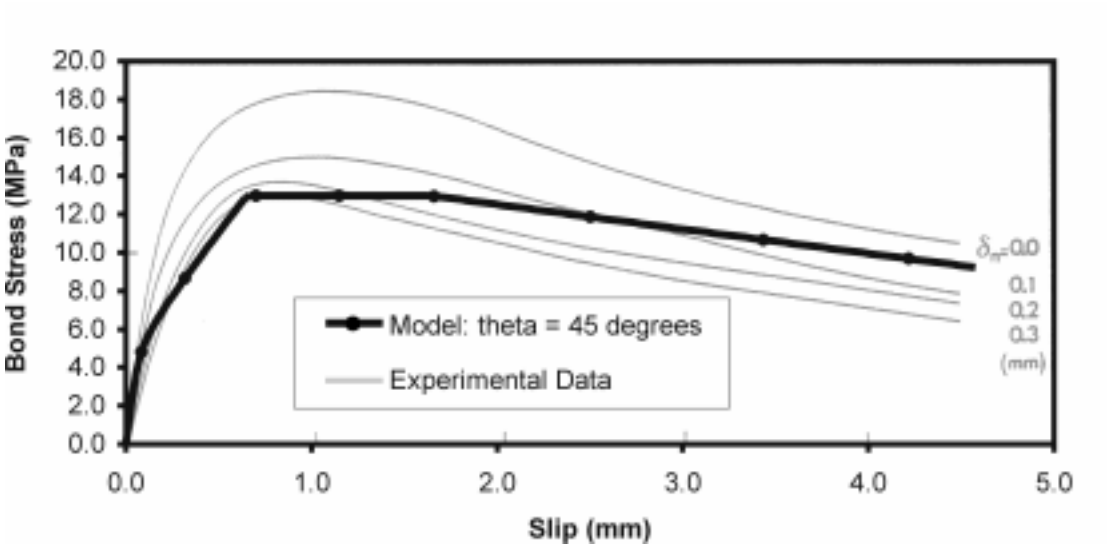

Figure 4.60: Computed and Observed Bond Stress Versus Slip Response (Data from Gambarova *et al.* [1983])

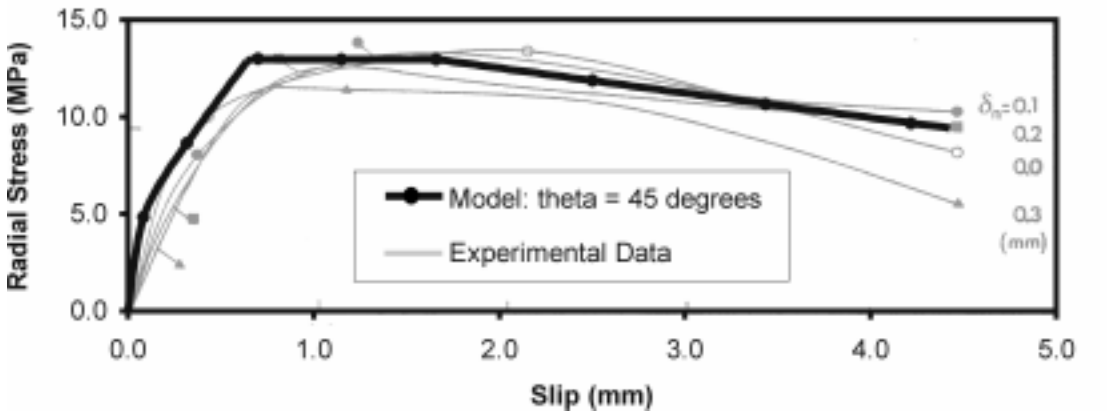

Figure 4.61: Computed and Observed Radial Stress Versus Slip Response (Data from Gambarova *et al.* [1983])

4.6 Conclusions

Previous experimental investigations provide data for development, calibration and verification of a model to represent load transfer between reinforcing steel and concrete. The results of previous analytical investigations provide insight into model development and implementation within the framework of the finite element method.

The results of previous bond studies indicate that load transfer between concrete and reinforcing steel may be idealized as occurring through friction and through mechanical

interaction between the lugs on the reinforcing bar and the surrounding concrete. Mechanical interaction describes the bearing on surrounding concrete of steel lugs or effective lugs composed of crushed concrete that becomes wedged in front of the lugs. Mechanical interaction is the dominant mechanism of load transfer at small to moderate slip levels and results in load transfer in the direction both parallel and perpendicular to the bar axis. Friction is the dominant mode of load transfer at extreme slip levels and immediately upon load reversal. Identification of these mechanisms supports calibration, description and implementation of a model that defines general bond response.

The results of previous experimental bond investigations indicate that bond response is determined by a number of parameters. These parameters include characteristics of the component design and construction such as material properties, steel ratios and the thickness of cover concrete over anchored reinforcing bars. For the current study, system parameters that are considered to determine bond response include concrete compressive strength and reinforcing bar diameter. System parameters that are considered to have minimal effect on bond response include bar deformation pattern, bar spacing and the volume of reinforcement transverse to the anchored bar. Previous research indicates that bond response is determined by characteristics of the load history including the rate of loading, the stress and damage state of the concrete and reinforcing steel, the slip history. Load history parameters that determine response in the currently proposed bond zone model include the concrete and steel material state in the vicinity of the anchorage zone and the slip history of the reinforcing bar. Rate of loading is not included in the current model.

Previous investigation of bond zone modeling suggests a number of plausible bond zone idealizations. Bond zone response may be modeled at several scales. For the current investigation bond response is represented at the scale of the reinforcing bar. This modeling scale appears to provide both a representation of bond zone response that is sufficient

for accurate representation of structural component behavior as well as a global model that can be analyzed and solved using a typical finite element program and computer. The physical bond zone may be represented by one-, two- and three-dimensional elements. Additionally, bond response may be characterized as a one-, two- or three- dimensional phenomenon. Here the bond zone is defined to include the concrete and reinforcing steel in the vicinity of the reinforcing bar, since material response of concrete and reinforcing steel determined bond response. However, the bond zone is represented using a two-dimensional element with finite length and zero width that provides continuity between individual reinforcing bars and surrounding concrete. Bond zone response is considered to include the bond stress versus slip behavior and radial stress versus slip behavior. Additionally modes of bond element response (radial stress versus radial deformation) simply provide continuity of the global model. This idealization of the bond zone and bond response allows for representation of only bond response within the bond element, representation of the effect of concrete and steel material behavior on bond response and representation of concrete and steel material response using the previously defined material models.

Implementation of the bond model within the framework of the finite element method requires definition of a number of algorithms for characterizing response, defining the load history and achieving solution of the global system. The Menegotto-Pinto formula is used extensively to define segments of the response curves. Use of this formula facilitates characterization of observed response. Bond response is defined to be a function of slip history. An algorithm is developed for counting cycles that is applicable for earthquake loading of systems in which cycle counts are relatively low and that requires storage of relatively few variables defining the previous loading history. Finally, a global

solution algorithm and a method of manipulation output from a typical finite element program is introduced to enable non-local modeling.

The proposed bond zone model is verified through comparison with experimental data. The bond stress versus slip history as computed using the proposed model and as observed are compared for a series of specimens tested by a number of different researchers. The results of these comparisons indicate that the proposed model represents well bond zone behavior for a variety of slip histories, concrete and steel stress states and bond zone configurations. Additionally, comparison of bond response as computed and observed indicates that the proposed model represents reasonably well radial stress developed in conjunction with bond stress.